METABOLIC SUBSTRATES EXHIBIT DIFFERENTIAL EFFECTS ON FUNCTIONAL PARAMETERS OF MOUSE SPERM CAPACITATION

Summer Gail Goodson

A dissertation submitted to the faculty of the University of North Carolina at Chapel Hill in partial fulfillment of the requirements for the degree of Doctor of Philosophy in the Department of Cell and Developmental Biology

Chapel Hill
2011

Approved by:

Deborah A. O'Brien, Ph.D.

Keith Burridge, Ph.D.

Mohanish Deshmukh, Ph.D.

Thomas M. O'Connell, Ph.D.

Michael G. O'Rand, Ph.D.

ABSTRACT

SUMMER G. GOODSON: Metabolic Substrates Exhibit Differential Effects on Functional Parameters of Mouse Sperm Capacitation
(Under the direction of Deborah A. O'Brien, Ph.D)

Sperm are capable of fertilization only after undergoing physiological changes in the female reproductive tract. These changes, known as capacitation, include the onset of a form of sperm motility called hyperactivation. Capacitation requires glycolysis, and sperm deficient in glycolytic enzymes are infertile due to defects in ATP levels and motility. Despite evidence of the importance of glycolysis in fertilization, several substrates not metabolized by this pathway have been shown to support sperm motility. To investigate the effects of substrate utilization on sperm functional changes required for fertilization, we first developed a method to evaluate patterns of mouse sperm motility. This tool, called CASAnova, is based on a multiclass support vector machines (SVM) model incorporating kinematic parameters of sperm motion generated by computer-assisted sperm analysis (CASA). Over 2,000 tracks were visually classified into five patterns of motility, and CASA parameters associated with these tracks were incorporated into established SVM algorithms to generate four equations. These equations, integrated into a decision tree, sequentially sort tracks into progressive, intermediate, hyperactivated, slow, or weakly motile groups. CASAnova incorporates these equations into a program for the automatic classification of sperm motility profiles. Comparisons of motility profiles of capacitating versus non-capacitating sperm confirmed the ability of

CASAnova to distinguish hyperactivated motility. Furthermore, CASAnova accurately classified sperm with severe motility defects and revealed differences in motility profiles of sperm from genetically diverse inbred strains. Our analyses indicate that CASAnova provides rapid and reproducible measurements of sperm motility.

We utilized CASAnova in conjunction with other measurements of sperm function to investigate the metabolic requirements of mouse sperm during in vitro capacitation. Our results demonstrate that mouse sperm maintained comparable ATP levels and percent motility when metabolizing either glycolytic or nonglycolytic substrates. However, only glucose and mannose supported the full spectrum of events associated with capacitation. Analyses of sperm incubated with metabolic inhibitors indicate that sperm utilizing fructose are capable of hyperactivation if oxidative phosphorylation is uncoupled. Metabolomic analyses of sperm incubated with glucose or fructose revealed alterations in antioxidant metabolites, suggesting that changes in redox state may contribute to the differential abilities of these substrates to support hyperactivation.

ACKNOWLEDGEMENTS

"Come on. Chill. You can do this."

The road to completing my Ph.D. has been a long one, with a detour or two along the way. I would like to thank my advisor, Debbie O'Brien, for her guidance and support throughout this process, and for helping me rediscover a love for science that I thought I had lost. I would also like to thank my committee members for their support, helpful ideas, and encouragement. I am most indebted to my parents, Barron and Sharon Goodson, my sister, Sunni Goodson, and my grandparents, J.W. and Dorothy Ragan, for their continuous love and support throughout the entire journey.

TABLE OF CONTENTS

LIST OF TABLES

TABLE

LIST OF FIGURES

FIGURE

LIST OF ABBREVIATIONS

129	Mouse strain 129S1/SvImJ
ACE	Angiotensin converting enzyme
ACH	Alpha-chlorohydrin
AKAP	A-kinase anchoring protein
ALH	Amplitude of lateral head displacement
ANOVA	Analysis of variance
ATP	Adenosine triphosphate
BCF	Beat cross frequency
BL6	Mouse strain C57BL/6J
BSA	Bovine serum albumin
BSTFA	Bis(Trimethylsilyl)-Trifluoroacetamide
Ca^{2+}	Calcium
$CaCl_2$	Calcium chloride
cAMP	Cyclic adenosine monophosphate
CASA	Computer-assisted sperm analysis
CCCP	Carbonyl cyanide 3-chlorophenylhydrazone
CO_2	Carbon dioxide
CYCT	Testis-specific cytochrome c
DBT	Database text file
DHAP	Dihydroxyacetone phosphate
DHB	D-(β)-hydroxybutyrate

DLD	Dihydrolipoamide dehydrogenase
DMSO	Dimethyl sulfoxide
DNA	Deoxyribonucleic acid
EDTA	Ethylenediaminetetraacetic acid
ES-	Negative electrospray ionization
ES+	Positive electrospray ionization
ESI	Electrospray ionization
GAPDHS	Sperm-specific glyceraldehyde phosphate dehydrogenase
GC	Gas chromatography
GC-TOFMS	Gas chromatography- time of flight mass spectrometry
GC/MS	Gas chromatography- mass spectrometry
HCl	Hydrochloric acid
HEPES	4-(2-hydroxyethyl)-1-piperazineethanesulfonic acid
HK-S	Sperm hexokinase
HPLC	High performance liquid chromatography
HTF	Human Tubal Fluid medium
IVF	In vitro fertilization
KCl	Potassium chloride
KH_2PO_4	Potassium phosphate
LC	Liquid chromatography
LC/MS	Liquid chromatography-mass spectrometry
LDH	Lactate dehydrogenase

LIN	Linearity
$MgSO_4 \bullet 7\ H_2O$	Magnesium sulfate heptahydrate
MS	Mass spectrometry
NaCl	Sodium chloride
NAD+	Nicotinamide adenine dinucleotide
NADH	Nicotinamide adenine dinucleotide, reduced
NADPH	Nicotinamide adenine dinucleotide phosphate, reduced
$NaH_2PO_4 \bullet 7\ H_2O$	Sodium phosphate dibasic heptahydrate
$NaHCO_3$	Sodium bicarbonate
ODF	Outer dense fibers
PBS	Phosphate-buffered saline
PBST	Phosphate-buffered saline + 0.1% Tween
PDH	Pyruvate dehydrogenase
PFK	Phosphofructokinase
PGK2	Phosphoglycerate kinase 2
PK	Pyruvate kinase
PKA	Protein kinase A
PMCA4	Plasma membrane Ca^{2+} ATPase 4
PWK	Mouse strain PWK /PhJ
ROS	Reactive oxygen species
sAC	Soluble adenylyl cyclase
SDS	Sodium dodecyl sulfate
SDS-PAGE	Sodium dodecyl sulfate- polyacrylamide gel electrophoresis

SEM	Standard error of the mean
SER/THR	Serine/Threonine
SORD	Sorbitol dehydrogenase
STR	Straightness
SVM	Support Vector Machine
TCEP	Tris(2-carboxyethyl)phosphine
TMCS	Trimethylchlorosilane
TOFMS	Time of flight mass spectrometry
Tris	Tris(hydroxymethyl)aminomethane
VAP	Average path velocity
VCL	Curvilinear velocity
VDAC	Voltage-dependent anion channel
VSL	Straight-line velocity

CHAPTER I

INTRODUCTION

In order to achieve fertilization, mammalian sperm undergo a complex series of physiological alterations designed to allow them to navigate the female reproductive tract, reach the egg, and penetrate the surrounding vestments [1]. These include changes in membrane structure and fluidity, differential protein tyrosine phosphorylation, acquisition of the ability of undergoing a zona-induced acrosome reaction, and development of hyperactivated motility. Multiple, integrated signaling pathways exist to ensure that sperm complete these steps at the time and location necessary for fertilization to occur [2, 3]. Recent gene targeting studies demonstrate that sperm metabolism is an important regulator of the signaling pathways that control sperm motility and fertility [4-7].

Sperm structural organization

Mammalian sperm have a highly organized, compartmentalized structure (Figure 1). The sperm head contains a condensed nucleus and overlying acrosome, which releases hydrolytic enzymes needed to penetrate the investments surrounding the egg. The flagellum, which provides motility to deliver the DNA to the egg, comprises over 90% of the length of this extremely polarized cell [8]. Although this general architecture is maintained, sperm length and head shape vary between species [9]. For example, mouse

sperm are approximately 120 μm in length, twice the length of human sperm [8]. The flagellum itself is a highly ordered structure, consisting of the connecting piece, the mitochondria-containing midpiece, the principal piece, and the end piece [10]. Like typical eukaryotic cilia and flagella, the sperm flagellum contains a central 9+2 axoneme that extends throughout its entire length [10]. Dynein ATPases are associated with the outer microtubules and proved the force for driving flagellar motility [11]. Mammalian sperm have additional accessory structures surrounding the axoneme. The outer dense fibers (ODFs) are cytoskeletal structures associated with each of the outer doublets of the axoneme, beginning at the connecting piece at the anterior end of the sperm tail and ending at different points along the principal piece [10, 12]. The fibrous sheath is another cytoskeletal structure that defines the limits of the principal piece, surrounding the axoneme and ODFs [13]. It consists of two longitudinal columns connected by circumferential ribs [10]. Major constituents of this highly insoluble, disulfide-crosslinked structure are cyclic AMP (cAMP)-dependent A-kinase anchoring proteins (AKAPs) [13]. AKAPs act as scaffolds to bring together signaling complexes and were originally identified based on their ability to bind protein kinase A (PKA) through the PKA regulatory subunit [14, 15]. Disruption of PKA-AKAP binding results in disruption of sperm motility in bull sperm [16]. In mouse PKA activity is responsible for driving events needed for sperm to fertilize the egg, and sperm lacking the PKA catalytic subunit are infertile [17, 18]. In addition to providing an anchoring point for PKA signaling and providing structural support for the flagellum, the fibrous sheath serves as a scaffold for glycolytic enzymes and protein signaling complexes [19]. Rho-signaling pathway

proteins and calcium-binding proteins have all been associated with the fibrous sheath [20-22].

Sperm physiological changes required for fertilization

After spermatogenesis is complete, sperm must undergo maturation during transit through the epididymis, which occurs over approximately five and half days in both mouse and human [23]. During transport to the site of sperm storage in the cauda epididymis, sperm acquire the capacity to achieve progressive motility and to bind the zona pellucida [1]. These changes are acquired as a result of interaction with the epididymal environment, resulting in alterations in the sperm plasma membrane and protein modifications including disulfide crosslinking [1, 24]. Sperm are only capable of fertilization after they have resided in the oviduct or in media mimicking the oviductal environment for a period of time. During this time, sperm undergo additional physiological changes culminating in the ability to fertilize the egg. This process, termed capacitation, includes the activation of pathways that render sperm capable of achieving hyperactivated motility and undergoing the acrosome reaction following interaction with the zona pellucida surrounding the egg [2, 3].

Sperm isolated from the cauda epididymis display progressive motility characterized by high velocities with low amplitude, symmetrical flagellar bends [25]. Sperm recovered from the oviducts of mice, or sperm incubated in defined media, display vigorous non-progressive motility with asymmetric, high amplitude flagellar bending [26]. This particular type of movement, known as hyperactivation, is required for

fertilization [1, 27, 28]. Hyperactivated motility is necessary for sperm penetration of the zona pellucida and may facilitate detaching from oviductal epithelia and navigating the cryptic environment of the oviduct. [29].

While many of the signaling pathways involved in sperm capacitation have not been fully characterized, the efflux of cholesterol from the sperm plasma membrane is required for sperm to initiate capacitation (Figure 2) [30]. This is believed to account for the changes in membrane composition and fluidity that take place during capacitation [2]. In addition to cholesterol efflux, capacitation events require the presence of specific ions. Both bicarbonate and calcium are important for capacitation-associated tyrosine phosphorylation as well as hyperactivated motility [1, 27, 31-35].

At the initiation of capacitation, the influx of bicarbonate stimulates the activity of a soluble adenylyl cyclase (sAC) (Figure 2) [36]. Activation of sAC leads to an increase in the production of cyclic AMP (cAMP) and activation of PKA. The upregulation of PKA-directed serine/threonine phosphorylation leads to a downstream increase in tyrosine phosphorylation of key residues on a number of proteins [18]. A significant portion of these tyrosine phosphorylated proteins are localized to the sperm flagellum [37]. The exact mechanism of how PKA induces an increase in tyrosine phosphorylation has not been fully elucidated. Initial reports suggested that activation of Src kinase was directly responsible for the upregulation of tyrosine phosphorylation during capacitation in both human and mouse [38-41]. However, a recent paper suggests that the increase in tyrosine phosphorylation may involve alterations in the activities of sperm phosphatases directed by the Src family of kinases [42]. The significance of both sAC and PKA is demonstrated by deletion of either the sAC gene or the PKA catalytic subunit from the

male germline. Both of these knockout models exhibit defects in male fertility due to abnormal sperm motility [17, 43].

While the requirement for calcium to support tyrosine phosphorylation varies among be species [31, 44, 45], its role in supporting hyperactivation is well established [46-49]. Deletion of any one of the four subunits of the CatSper channel leads to the loss of hyperactivated motility and infertility [28, 32, 50, 51]. Other studies suggest that a store of intracellular calcium is present in the sperm and can trigger hyperactivated motility upon release [52]. Hyperactivated motility is also inhibited when bicarbonate is omitted from fertilization media [33-35], and some reports suggest that cAMP is involved in the regulation of hyperactivity [48, 53, 54]. In both mouse and human, capacitation is modulated by the levels of reactive oxygen species (ROS), although it has not been established that ROS is absolutely required for capacitation [55-60]. In addition, both hyperactivated motility and tyrosine phosphorylation require metabolism of substrates via the glycolytic pathway [27, 37, 61-64].

Energy metabolism in sperm

Energy metabolism in sperm possesses several features that distinguish it from canonical metabolism in somatic cells. Like other cells, sperm utilize both mitochondrial oxidative phosphorylation and glycolysis to produce ATP. In somatic cells, glucose is metabolized to pyruvate through glycolysis in the cytoplasm, followed by conversion of pyruvate to acetyl-CoA, which serves as a substrate for the citric acid cycle in the mitochondria. Mitochondrial ATP production is capable of producing 34-36 ATP per

molecule of glucose, while glycolysis alone results in the net production of 2 ATP per molecule of glucose. The first distinguishing feature of these pathways in sperm is their distinct compartmentalization in separate parts of the flagellum (Figure 1). Mitochondria are sequestered in the midpiece of the flagellum, while the glycolytic machinery is localized in the principal piece. Several glycolytic enzymes are tightly associated with the fibrous sheath in the principal piece, including sperm-specific glyceraldehyde phosphate dehydrogenase (GAPDHS), lactate dehydrogenase A (LDHA), aldolase A, and pyruvate kinase (PK) [20]. As a result of the distinct localization of glycolysis, a large portion of the pyruvate produced from glucose is converted to lactate by LDH and exported out of the cell (Figure 3) [65].

In addition to the compartmentalization of metabolic pathways, sperm metabolism features both glycolytic and oxidative enzymes with unique properties. With respect to mitochondrial enzymes, both cytochrome c (CYCT) and succinyl-CoA transferase are encoded by genes expressed only during spermatogenesis [66, 67]. Several sperm glycolytic enzymes are germ line-specific isoforms [68-78]. GAPDHS, PGK2, and LDHC are transcribed from distinct genes only expressed during spermatogenesis or in oocytes, while HK-S is the result of alternative splicing [67, 68, 71, 73, 74, 79, 80]. Three unique isoforms of aldolase A are expressed in mature sperm, arising from both independent retrogenes and alternative splicing [70, 81]. Many of the sperm-specific glycolytic isozymes possess distinctive functional or structural properties. For example, the sperm-specific isoform of HK lacks the porin-binding domain normally found in somatic cells [69, 72]. GAPDHS and two of the aldolase A isozymes in sperm possess

N-terminal extensions that appear to be important for binding to the fibrous sheath [69, 72].

Even though mitochondria are localized to the midpiece in sperm, some mitochondrial enzymes have been detected in other compartments of the sperm flagellum. In hamster sperm, multiple proteins in the pyruvate dehydrogenase complex (PDH) have been localized to the principal piece of the flagellum, including PDHA2, dihydrolipoamide dehydrogenase, and PDH subunit E1β, which undergo capacitation-dependent tyrosine phosphorylation [82-85]. The voltage-dependent anion channels (VDAC) 2 and 3 have also been detected in association with outer dense fibers in bull sperm [86]. The extramitochondrial localization of these enzymes, coupled with the unique structural and functional properties of glycolytic enzymes, suggests that novel metabolic pathways may exist in sperm.

Sperm from a variety of species have been reported to metabolize substrates utilized by both glycolysis and the citric acid cycle, although the relative efficiencies of these pathways differ among species [87-95]. For example, bull sperm exhibits high rates of mitochondrial respiration, while mouse sperm display intermediate levels of mitochondrial function [96]. Human sperm are similar to mouse with regards to the importance of glycolysis in generating ATP [90, 91, 95]. Both the metabolic similarity between human and mouse sperm and the ability to genetically manipulate the mouse genome make the mouse an excellent model system for studying the interaction between sperm metabolism and function.

The deletion of several sperm-specific enzymes by gene targeting has provided insight into the roles of metabolism in sperm motility and fertilization. Mice deficient in CYCT display slight defects in sperm function yet remain fertile [6]. By contrast, mice deficient in any one of three sperm-specific glycolytic enzymes (GAPDHS, LDHC, or PGK2) display severe defects in male fertility due to abnormal sperm motility [4, 5, 7]. In addition, sperm motility is also negatively affected by inhibitors of sperm glycolysis [97, 98]. Taken together, this evidence argues that energy production via glycolysis rather than oxidative phosphorylation is the most important metabolic pathway for sperm function in multiple mammalian species.

The role of glycolysis in sperm capacitation and hyperactivation

Studies in multiple species provide evidence that glycolysis plays an integral role in ensuring proper sperm function. Early studies showed that glucose is sufficient as the sole substrate to support in vitro fertilization (IVF) [61, 62] and that omission of glucose reduces fertilization rates in human IVF [99]. Additional studies have highlighted the capacitation steps that are influenced by glucose metabolism. Experiments analyzing the effect of various substrates on sperm motility demonstrated that glucose is required for high levels of hyperactivation [27], while other studies showed that other glycolysable sugars such as mannose [61] or sorbitol [100] supported hyperactived motility in addition to glucose. Substrates metabolized by the mitochondria, such as lactate and pyruvate, cannot support hyperactivation, although they maintain the percentage of motile sperm [27, 61].

The dependence of capacitation-associated tyrosine phosphorylation on glycolysis has also been demonstrated in mouse sperm, since glucose was shown to be required for an increase in tyrosine phosphorylation to occur [37, 64]. Moreover, Travis et al. [64] demonstrated that neither lactate nor pyruvate is sufficient to support tyrosine phosphorylation.

While the importance of glucose in sperm capacitation has been well described, not all glycolysable sugars are capable of supporting these functional parameters. The most notable example is fructose. When compared to other metabolic substrates, sperm incubated in fructose are not capable of supporting hyperactivated motility [27, 61, 101]. While the exact reason for the difference between glucose and fructose is not known, the inability of fructose to support hyperactivation may arise from an alternative metabolic pathway known as the Hers' pathway, whereby fructose is converted to fructose-1-phosphate by fructokinase. Fructose-1-phosphate is then metabolized further to glyceraldehyde-3-phosphate, thus entering the glycolytic pathway at the GAPDHS step and bypassing signaling that is initiated by the top half of glycolysis [102]. The difference between consequences of glucose versus fructose utilization in sperm may have physiological relevance, as these sugars show differential abundance in the male and female reproductive tracts. Fructose is present in millimolar concentrations in mammalian seminal fluid, while glucose is more abundant in the oviduct than in seminal fluid [103-106]. As sperm must undergo hyperactivation in a time-dependent manner in order to fertilize in vivo [107], the inability of fructose to support hyperactivation may serve to ensure that sufficient quantities of sperm are capable of navigating the female

reproductive tract, encountering glucose, and then hyperactivating in the time and manner required for fertilization.

Methods of analyzing sperm motility and hyperactivation

Sperm freshly isolated from the cauda epididymis display progressive motility due to symmetrical flagellar beating [25]. In contrast, sperm isolated from the oviduct display hyperactivated motility characterized by asymmetric flagellar beating, resulting in non-linear, high velocity motility [26]. Several approaches to quantitatively measuring changes in sperm motility have been developed, including Minimum Bounding Square Ratios and lineal equations [108, 109]. However, the two most commonly used methods are flagellar waveform analysis and computer-assisted sperm analysis (CASA) [110-113].

Hyperactivated motility is an event characterized by changes in flagellar dynamics. Flagellar waveform analysis carefully analyses the movement of the flagellum in response to various treatments or conditions. Typically, sperm are incubated on a glass slide and a portion of the sperm population will adhere to the slide by the head. Sperm with heads attached to the slide still display flagellar beating. Videomicrography is performed, traces of flagellar bends are generated and overlaid, and various parameters can be calculated from these analyses [110, 112]. Waveform analysis allows for extremely detailed investigation of flagellar dynamics. However, the disadvantage is that this approach is highly labor intensive and so is only typically performed on 10-15 sperm per condition. In addition, the level of expertise required to accurately perform flagellar waveform analysis is such that the technique is not widely used in the field [110, 112].

CASA is an automated method developed to assess the motility of all sperm within a sample [114]. This approach tracks the movement of the sperm head over a defined period of time, generates sperm motility tracks, and calculates measurements of velocities and other kinematic parameters for individual sperm. This allows the rapid assessment of changes in total motility, including averages for kinematic parameters, in response to various treatments or perturbations. While the percentage of motile sperm is an important consideration, the onset of hyperactivation can occur without a change in total motility. In addition, reports suggest that calculating the averages for CASA parameters is not sufficient to reflect changes in sperm motility, especially hyperactivation [115].

To distinguish hyperactivated motility in sperm samples, CASA parameter gates are often used following CASA [7, 35, 50, 116-118]. In this approach, sperm displaying hyperactivated motility are identified visually and the CASA parameters from hyperactivated sperm are compared with nonhyperactivated tracks. The CASA parameters most changed between these groups are identified, and then thresholds are set based on combinations of these parameters. While CASA gates have been validated and recommended for human and rat sperm studies, no consensus CASA thresholds have been described in mouse [113, 114, 119]. Moreover, few hyperactivation gates have been validated in mouse, and the inability of these CASA parameters to reflect visual assessment of hyperactivation in the literature has been explicitly described [50]. However, due to the importance of hyperactivated motility in sperm function, the use of CASA-based thresholds has been adopted as a relative, albeit inaccurate, method of determining hyperactivation.

Research presented in this dissertation

Various studies have demonstrated that nonglycolysable substrates are capable of maintaining sperm motility in vitro. However, these studies did not uniformly address the role of non-glycolysable substrates in supporting functional parameters of sperm capacitation. Moreover, the methods used to detect changes in sperm motility, namely hyperactivation, do not accurately reflect visual assessments of shifts in motility patterns.

Chapter 2 of this dissertation focuses on the development of a novel approach to classify hyperactivated sperm as well as four other patterns of sperm motility. This technique utilizes multiple support vector machines (SVM), a commonly used approach in supervised machine learning, to mathematically identify sperm motility patterns based on CASA-derived measurements of velocity and head movement. This model, named CASAnova, is rapid, accurate, and reproducible, and requires minimal training for the user. CASAnova is capable of detecting changes in sperm motility patterns under both capacitating and non-capacitating conditions, and is also able to detect large-scale changes in motility patterns in sperm with defects in motility. Furthermore, it accurately reflects differences in motility patterns in sperm from multiple strains of mice, including those routinely used to generate genetically altered mouse lines. The use of CASAnova in investigating sperm motility promises to be a useful method for studies of biochemical, pharmaceutical, or genetic effects on sperm motility.

Chapter 3 of this dissertation describes the utilization of this model in studies of substrate metabolism during sperm capacitation and their effects on functional sperm

parameters. Analyses of sperm incubated in the presence of various energy substrates indicate that both glycolysable and non-glycolysable substrates maintain similar percentages of sperm motility and ATP levels throughout a 2 h in vitro capacitation period. Use of CASAnova demonstrates that sperm incubated with non-glycolysable substrates exhibit higher levels of non-vigorous motility and do not undergo hyperactivation. Among glycolysable substrates, only glucose and mannose support hyperactivation in the manner required for proper sperm function. Examination of capacitation-associated tyrosine phosphorylation suggests that there are differences between the pathways linking sperm glycolysis with hyperactivation and those linking glycolysis with tyrosine phosphorylation, since sperm incubated with non-glycolysable substrates do not undergo hyperactivation but exhibit at least partial tyrosine phosphorylation. For example, fructose does not promote efficient hyperactivated motility, but fully supports the phosphorylation of tyrosine residues. Examination of the effects of substrates on sperm parameters in the presence of metabolic inhibitors reveals that sperm metabolizing fructose are capable of hyperactivation if oxidative phosphorylation is uncoupled from electron transport. Differences between glucose and fructose were examined further by mass-spectrometric analysis of metabolic profiles. Sperm metabolizing fructose possess higher levels of metabolites associated with antioxidant properties, suggesting a possible mechanism for the inhibition of hyperactivated motility by fructose that may facilitate proper timing of sperm capacitation in vivo.

Figure 1.1

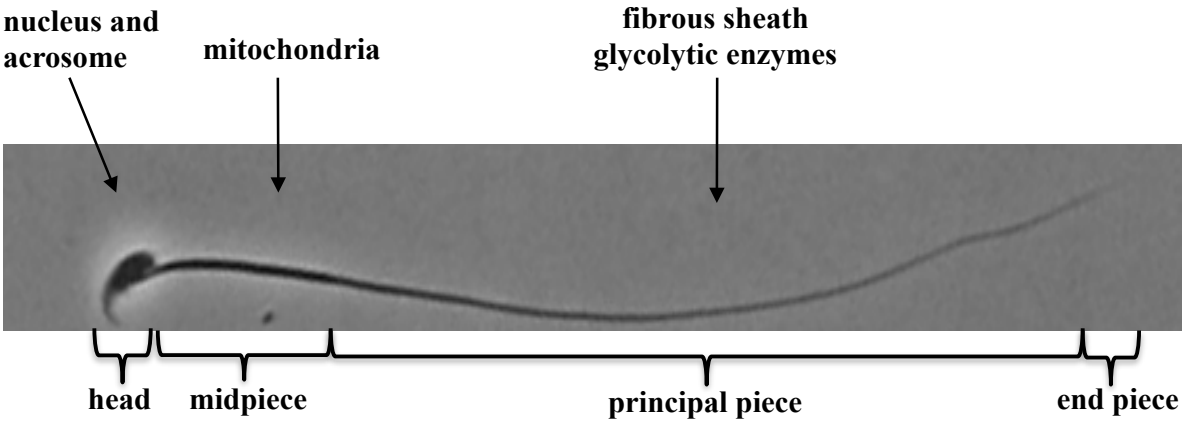

Figure 1.1 Sperm structure and metabolic compartmentalization. The nucleus and acrosome are localized to the head of sperm. The tail, organized into the midpiece, principal piece, and end piece, house the major energy-producing pathways in sperm. Mitochondria are localized to the midpiece, while glycolysis is compartmentalized in the principal piece. Several glycolytic enzymes are tightly bound to the fibrous sheath in the sperm principal piece.

Figure 1.2

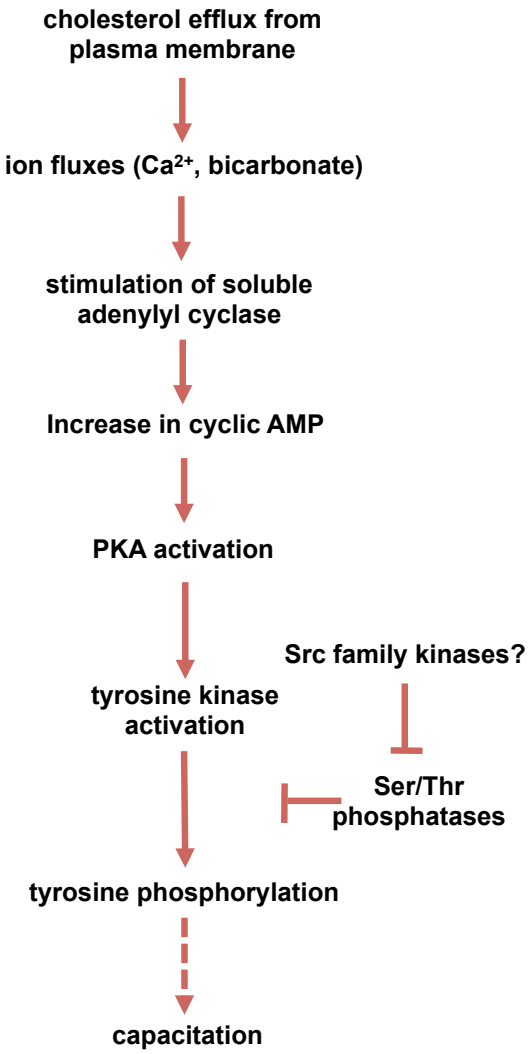

Figure 1.2 Signaling pathways controlling sperm capacitation. The exclusion of cholesterol from the membrane leads to ion fluxes. The increased presence of bicarbonate leads to activation of soluble adenylyl cyclase, stimulating the production of cyclic AMP. Cyclic AMP levels activate protein kinase A (PKA), ultimately leading to an increase in tyrosine phosphorylation and sperm capacitation. The increase in tyrosine phosphorylation is also modulated by the activity of serine/threonine (Ser/Thr) phosphatases, which may be under the control of Src family kinases.

Figure 1.3

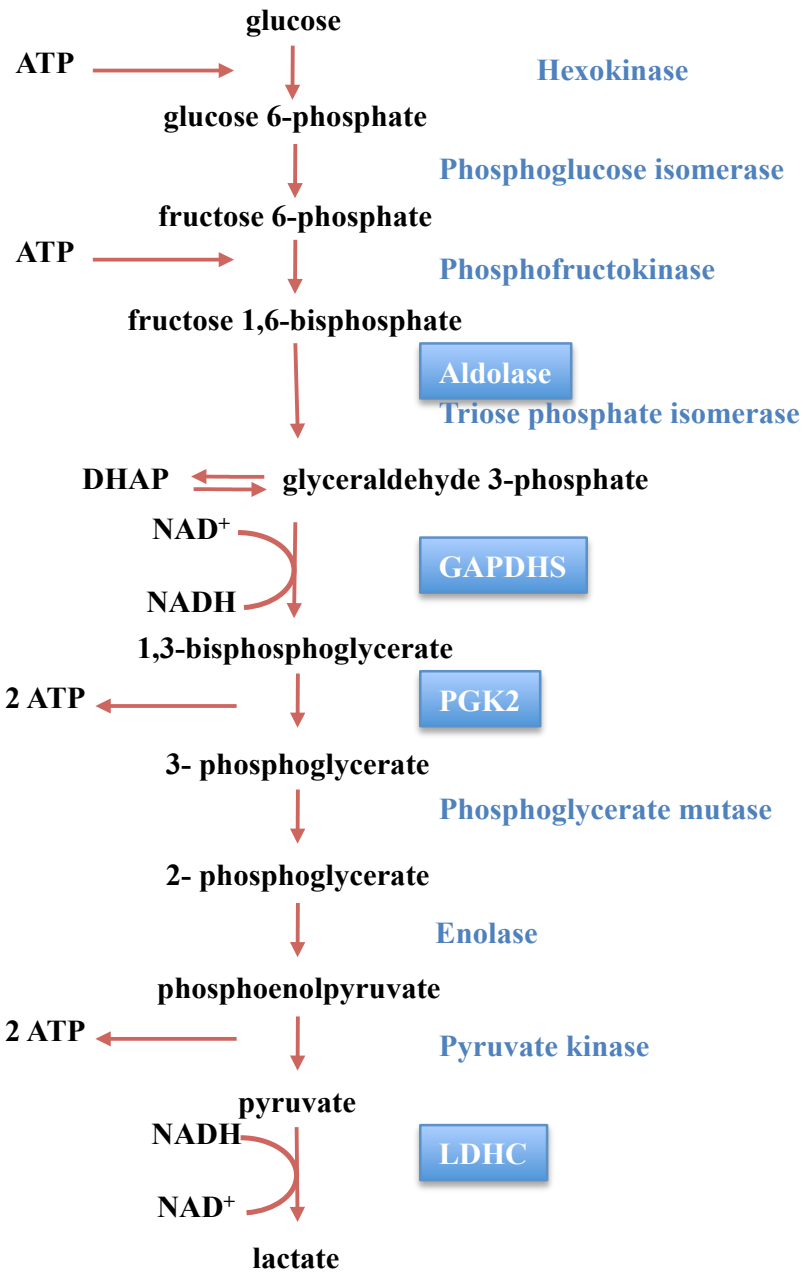

Figure 1.3 The glycolytic pathway in sperm. Glucose is metabolized via the glycolytic pathway, yielding ATP and pyruvate. Pyruvate can then enter the TCA cycle. In sperm, pyruvate can also be converted to lactate, regenerating NAD^+. Enzymes in blue are encoded by sperm-specific genes.

References

1. Yanagimachi R. Mammalian fertilization. In: Knobil E, Neill J (eds.), The Physiology of Reproduction. New York: Raven Press; 1994: 189-317.

2. Visconti PE, Westbrook VA, Chertihin O, Demarco I, Sleight S, Diekman AB. Novel signaling pathways involved in sperm acquisition of fertilizing capacity. J Reprod Immunol 2002; 53:133-150.

3. Fraser LR. Cellular biology of capacitation and the acrosome reaction. Hum Reprod 1995; 10 Suppl 1:22-30.

4. Danshina PV, Geyer CB, Dai Q, Goulding EH, Willis WD, Kitto GB, McCarrey JR, Eddy EM, O'Brien DA. Phosphoglycerate kinase 2 (PGK2) is essential for sperm function and male fertility in mice. Biol Reprod 2010; 82:136-145.

5. Miki K, Qu W, Goulding EH, Willis WD, Bunch DO, Strader LF, Perreault SD, Eddy EM, O'Brien DA. Glyceraldehyde 3-phosphate dehydrogenase-S, a sperm-specific glycolytic enzyme, is required for sperm motility and male fertility. Proc Natl Acad Sci U S A 2004; 101:16501-16506.

6. Narisawa S, Hecht NB, Goldberg E, Boatright KM, Reed JC, Millan JL. Testis-specific cytochrome c-null mice produce functional sperm but undergo early testicular atrophy. Mol Cell Biol 2002; 22:5554-5562.

7. Odet F, Duan C, Willis WD, Goulding EH, Kung A, Eddy EM, Goldberg E. Expression of the gene for mouse lactate dehydrogenase C (Ldhc) is required for male fertility. Biol Reprod 2008; 79:26-34.

8. Cummins JM, Woodall PF. On mammalian sperm dimensions. J Reprod Fertil 1985; 75:153-175.

9. Green DP. The head shapes of some mammalian spermatozoa and their possible relationship to the shape of the penetration slit through the zona pellucida. J Reprod Fertil 1988; 83:377-387.

10. Fawcett DW. The mammalian spermatozoon. Dev Biol 1975; 44:394-436.

11. Mohri H. Role of tubulin and dynein in spermatozoan motility. Mol Reprod Dev 1993; 36:221-223.

12. Turner RM. Tales from the tail: what do we really know about sperm motility? J Androl 2003; 24:790-803.

13. Eddy EM, Toshimori K, O'Brien DA. Fibrous sheath of mammalian spermatozoa. Microsc Res Tech 2003; 61:103-115.

14. Carr DW, Stofko-Hahn RE, Fraser ID, Bishop SM, Acott TS, Brennan RG, Scott JD. Interaction of the regulatory subunit (RII) of cAMP-dependent protein kinase with RII-anchoring proteins occurs through an amphipathic helix binding motif. J Biol Chem 1991; 266:14188-14192.

15. Carnegie GK, Means CK, Scott JD. A-kinase anchoring proteins: from protein complexes to physiology and disease. IUBMB Life 2009; 61:394-406.

16. Vijayaraghavan S, Goueli SA, Davey MP, Carr DW. Protein kinase A-anchoring inhibitor peptides arrest mammalian sperm motility. J Biol Chem 1997; 272:4747-4752.

17. Nolan MA, Babcock DF, Wennemuth G, Brown W, Burton KA, McKnight GS. Sperm-specific protein kinase A catalytic subunit Ca2 orchestrates cAMP signaling for male fertility. Proc Natl Acad Sci U S A 2004; 101:13483-13488.

18. Visconti PE, Moore GD, Bailey JL, Leclerc P, Connors SA, Pan D, Olds-Clarke P, Kopf GS. Capacitation of mouse spermatozoa. II. Protein tyrosine phosphorylation and capacitation are regulated by a cAMP-dependent pathway. Development 1995b; 121:1139-1150.

19. Hermo L, Pelletier RM, Cyr DG, Smith CE. Surfing the wave, cycle, life history, and genes/proteins expressed by testicular germ cells. Part 5: intercellular junctions and contacts between germs cells and Sertoli cells and their regulatory interactions, testicular cholesterol, and genes/proteins associated with more than one germ cell generation. Microsc Res Tech 2010; 73:409-494.

20. Krisfalusi M, Miki K, Magyar PL, O'Brien D A. Multiple glycolytic enzymes are tightly bound to the fibrous sheath of mouse spermatozoa. Biol Reprod 2006; 75:270-278.

21. Fujita A, Nakamura K, Kato T, Watanabe N, Ishizaki T, Kimura K, Mizoguchi A, Narumiya S. Ropporin, a sperm-specific binding protein of rhophilin, that is localized in the fibrous sheath of sperm flagella. J Cell Sci 2000; 113 (Pt 1):103-112.

22. Li YF, He W, Mandal A, Kim YH, Digilio L, Klotz K, Flickinger CJ, Herr JC. CABYR binds to AKAP3 and Ropporin in the human sperm fibrous sheath. Asian J Androl 2011.

23. Franca LR, Avelar GF, Almeida FF. Spermatogenesis and sperm transit through the epididymis in mammals with emphasis on pigs. Theriogenology 2005; 63:300-318.

24. Bedford JM, Calvin HI. Changes in -S-S- linked structures of the sperm tail during epididymal maturation, with comparative observations in sub-mammalian species. J Exp Zool 1974; 187:181-204.

25. Fraser LR. Motility patterns in mouse spermatozoa before and after capacitation. J Exp Zool 1977; 202:439-444.

26. Suarez SS, Osman RA. Initiation of hyperactivated flagellar bending in mouse sperm within the female reproductive tract. Biol Reprod 1987; 36:1191-1198.

27. Cooper TG. The onset and maintenance of hyperactivated motility of spermatozoa in the mouse. Gamete Res 1984; 9:55-74.

28. Qi H, Moran MM, Navarro B, Chong JA, Krapivinsky G, Krapivinsky L, Kirichok Y, Ramsey IS, Quill TA, Clapham DE. All four CatSper ion channel proteins are required for male fertility and sperm cell hyperactivated motility. Proc Natl Acad Sci U S A 2007; 104:1219-1223.

29. Suarez SS, Ho HC. Hyperactivated motility in sperm. Reprod Domest Anim 2003; 38:119-124.

30. Visconti PE, Ning X, Fornes MW, Alvarez JG, Stein P, Connors SA, Kopf GS. Cholesterol efflux-mediated signal transduction in mammalian sperm: cholesterol release signals an increase in protein tyrosine phosphorylation during mouse sperm capacitation. Dev Biol 1999; 214:429-443.

31. Visconti PE, Bailey JL, Moore GD, Pan D, Olds-Clarke P, Kopf GS. Capacitation of mouse spermatozoa. I. Correlation between the capacitation state and protein tyrosine phosphorylation. Development 1995a; 121:1129-1137.

32. Ren D, Navarro B, Perez G, Jackson AC, Hsu S, Shi Q, Tilly JL, Clapham DE. A sperm ion channel required for sperm motility and male fertility. Nature 2001; 413:603-609.

33. Boatman DE, Robbins RS. Bicarbonate: carbon-dioxide regulation of sperm capacitation, hyperactivated motility, and acrosome reactions. Biol Reprod 1991; 44:806-813.

34. Lee MA, Storey BT. Bicarbonate is essential for fertilization of mouse eggs: mouse sperm require it to undergo the acrosome reaction. Biol Reprod 1986; 34:349-356.

35. Neill JM, Olds-Clarke P. A computer-assisted assay for mouse sperm hyperactivation demonstrates that bicarbonate but not bovine serum albumin is required. Gamete Res 1987; 18:121-140.

36. Chen Y, Cann MJ, Litvin TN, Iourgenko V, Sinclair ML, Levin LR, Buck J. Soluble adenylyl cyclase as an evolutionarily conserved bicarbonate sensor. Science 2000; 289:625-628.

37. Urner F, Leppens-Luisier G, Sakkas D. Protein tyrosine phosphorylation in sperm during gamete interaction in the mouse: the influence of glucose. Biol Reprod 2001; 64:1350-1357.

38. Lawson C, Goupil S, Leclerc P. Increased activity of the human sperm tyrosine kinase SRC by the cAMP-dependent pathway in the presence of calcium. Biol Reprod 2008; 79:657-666.

39. Mitchell LA, Nixon B, Baker MA, Aitken RJ. Investigation of the role of SRC in capacitation-associated tyrosine phosphorylation of human spermatozoa. Mol Hum Reprod 2008; 14:235-243.

40. Varano G, Lombardi A, Cantini G, Forti G, Baldi E, Luconi M. Src activation triggers capacitation and acrosome reaction but not motility in human spermatozoa. Hum Reprod 2008; 23:2652-2662.

41. Baker MA, Hetherington L, Aitken RJ. Identification of SRC as a key PKA-stimulated tyrosine kinase involved in the capacitation-associated hyperactivation of murine spermatozoa. J Cell Sci 2006; 119:3182-3192.

42. Krapf D, Arcelay E, Wertheimer EV, Sanjay A, Pilder SH, Salicioni AM, Visconti PE. Inhibition of Ser/Thr phosphatases induces capacitation-associated signaling in the presence of Src kinase inhibitors. J Biol Chem 2010; 285:7977-7985.

43. Xie F, Garcia MA, Carlson AE, Schuh SM, Babcock DF, Jaiswal BS, Gossen JA, Esposito G, van Duin M, Conti M. Soluble adenylyl cyclase (sAC) is indispensable for sperm function and fertilization. Dev Biol 2006; 2006 Jun 7; doi:10.1016/j.ydbio.2006.05.038

44. Baker MA, Lewis B, Hetherington L, Aitken RJ. Development of the signalling pathways associated with sperm capacitation during epididymal maturation. Mol Reprod Dev 2003; 64:446-457.

45. Barbonetti A, Vassallo MR, Cinque B, Antonangelo C, Sciarretta F, Santucci R, D'Angeli A, Francavilla S, Francavilla F. Dynamics of the global tyrosine phosphorylation during capacitation and acquisition of the ability to fuse with oocytes in human spermatozoa. Biol Reprod 2008; 79:649-656.

46. Colas C, Cebrian-Perez JA, Muino-Blanco T. Caffeine induces ram sperm hyperactivation independent of cAMP-dependent protein kinase. Int J Androl 2010; 33:e187-197.

47. Marquez B, Suarez SS. Bovine sperm hyperactivation is promoted by alkaline-stimulated Ca2+ influx. Biol Reprod 2007; 76:660-665.

48. Ishijima S, Mohri H, Overstreet JW, Yudin AI. Hyperactivation of monkey spermatozoa is triggered by Ca2+ and completed by cAMP. Mol Reprod Dev 2006; 73:1129-1139.

49. Suarez SS, Dai X. Intracellular calcium reaches different levels of elevation in hyperactivated and acrosome-reacted hamster sperm. Mol Reprod Dev 1995; 42:325-333.

50. Quill TA, Sugden SA, Rossi KL, Doolittle LK, Hammer RE, Garbers DL. Hyperactivated sperm motility driven by CatSper2 is required for fertilization. Proc Natl Acad Sci U S A 2003; 100:14869-14874.

51. Jin J, Jin N, Zheng H, Ro S, Tafolla D, Sanders KM, Yan W. Catsper3 and Catsper4 are essential for sperm hyperactivated motility and male fertility in the mouse. Biol Reprod 2007; 77:37-44.

52. Marquez B, Ignotz G, Suarez SS. Contributions of extracellular and intracellular Ca2+ to regulation of sperm motility: Release of intracellular stores can hyperactivate CatSper1 and CatSper2 null sperm. Dev Biol 2007; 303:214-221.

53. Murase T, El-Kon I, Harayama H, Mukoujima K, Takasu M, Sakai K. Hyperactivated motility of frozen-thawed spermatozoa from fertile and subfertile Japanese black bulls induced by cyclic adenosine 3',5'-monophosphate analogue, cBiMPS. J Reprod Dev 2010; 56:36-40.

54. Harayama H, Miyake M. A cyclic adenosine 3',5'-monophosphate-dependent protein kinase C activation is involved in the hyperactivation of boar spermatozoa. Mol Reprod Dev 2006; 73:1169-1178.

55. Griveau JF, Renard, P., and Le Lannou, D. An in vitro promoting role for hydrogen peroxide in human sperm capacitation. International Journal of Andrology 1994; 17:300-307.

56. Ecroyd HW, Jones, R.C., Aitken, R.J. Endogenous redox activity in mouse spermatozoa and its role in regulating the tyrosine phosphorylation events associated with sperm capacitation. Biology of Reproduction 2003; 69.

57. de Lamirande E, Lamothe G. Reactive oxygen-induced reactive oxygen formation during human sperm capacitation. Free Radic Biol Med 2009; 46:502-510.

58. de Lamirande E, O'Flaherty C. Sperm activation: role of reactive oxygen species and kinases. Biochim Biophys Acta 2008; 1784:106-115.

59. Aitken RJ, Baker MA, De Iuliis GN, Nixon B. New insights into sperm physiology and pathology. Handb Exp Pharmacol 2010:99-115.

60. Dona G, Fiore, C., Tibaldi,E., Frezzato, F., Andrisani, A., Ambrosini, G. Fiorentin, D. Armanini, D., Bordin, L. and Clari, G. Endogenous reactive oxygen species content and modulation of tyrosine phosphorylation during sperm capacitation. International Journal of Andrology 2010.

61. Fraser LR, Quinn PJ. A glycolytic product is obligatory for initiation of the sperm acrosome reaction and whiplash motility required for fertilization in the mouse. J Reprod Fertil 1981; 61:25-35.

62. Hoppe PC. Glucose requirement for mouse sperm capacitation in vitro. Biol Reprod 1976; 15:39-45.

63. Urner F, Sakkas D. Glucose is not essential for the occurrence of sperm binding and zona pellucida-induced acrosome reaction in the mouse. Int J Androl 1996a; 19:91-96.

64. Travis AJ, Jorgez CJ, Merdiushev T, Jones BH, Dess DM, Diaz-Cueto L, Storey BT, Kopf GS, Moss SB. Functional relationships between capacitation-dependent cell signaling and compartmentalized metabolic pathways in murine spermatozoa. J Biol Chem 2001; 276:7630-7636.

65. Mann T, Lutwak-Mann C. Male Reproductive Function and Semen. Berlin, Heidelberg, New York: Springer-Verlag; 1981.

66. Hennig B. Change of cytochrome c structure during development of the mouse. Eur J Biochem 1975; 55:167-183.

67. Tanaka H, Kohroki J, Iguchi N, Onishi M, Nishimune Y. Cloning and characterization of a human orthologue of testis-specific succinyl CoA: 3-oxo acid CoA transferase (Scot-t) cDNA. Mol Hum Reprod 2002; 8:16-23.

68. Mori C, Nakamura N, Welch JE, Gotoh H, Goulding EH, Fujioka M, Eddy EM. Mouse spermatogenic cell-specific type 1 hexokinase (mHk1-s) transcripts are expressed by alternative splicing from the mHk1 gene and the HK1-S protein is localized mainly in the sperm tail. Mol Reprod Dev 1998; 49:374-385.

69. Mori C, Welch JE, Fulcher KD, O'Brien DA, Eddy EM. Unique hexokinase messenger ribonucleic acids lacking the porin-binding domain are developmentally expressed in mouse spermatogenic cells. Biol Reprod 1993; 49:191-203.

70. Vemuganti SA, Bell TA, Scarlett CO, Parker CE, de Villena FP, O'Brien DA. Three male germline-specific aldolase A isozymes are generated by alternative splicing and retrotransposition. Dev Biol 2007; 309:18-31.

71. Welch JE, Brown PR, O'Brien DA, Eddy EM. Genomic organization of a mouse glyceraldehyde 3-phosphate dehydrogenase gene (Gapd-s) expressed in post-meiotic spermatogenic cells. Dev Genet 1995; 16:179-189.

72. Welch JE, Schatte EC, O'Brien DA, Eddy EM. Expression of a glyceraldehyde 3-phosphate dehydrogenase gene specific to mouse spermatogenic cells. Biol Reprod 1992; 46:869-878.

73. Boer PH, Adra CN, Lau YF, McBurney MW. The testis-specific phosphoglycerate kinase gene pgk-2 is a recruited retroposon. Mol Cell Biol 1987; 7:3107-3112.

74. McCarrey JR, Thomas K. Human testis-specific PGK gene lacks introns and possesses characteristics of a processed gene. Nature 1987; 326:501-505.

75. Millan JL, Driscoll CE, LeVan KM, Goldberg E. Epitopes of human testis-specific lactate dehydrogenase deduced from a cDNA sequence. Proc Natl Acad Sci U S A 1987; 84:5311-5315.

76. Sakai I, Sharief FS, Li SS. Molecular cloning and nucleotide sequence of the cDNA for sperm-specific lactate dehydrogenase-C from mouse. Biochem J 1987; 242:619-622.

77. Goldberg E, Sberna D, Wheat TE, Urbanski GJ, Margoliash E. Cytochrome c: immunofluorescent localization of the testis-specific form. Science 1977; 196:1010-1012.

78. Tanaka H, Iguchi N, Miyagawa Y, Koga M, Kohroki J, Nishimune Y. Differential expression of succinyl CoA transferase (SCOT) genes in somatic and germline cells of the mouse testis. Int J Androl 2003; 26:52-56.

79. Nakamura Y, Tanaka H, Koga M, Miyagawa Y, Iguchi N, Egydio de Carvalho C, Yomogida K, Nozaki M, Nojima H, Matsumiya K, Okuyama A, Nishimune Y. Molecular cloning and characterization of oppo 1: a haploid germ cell-specific complementary DNA encoding sperm tail protein. Biol Reprod 2002; 67:1-7.

80. Edwards Y, West L, Van Heyningen V, Cowell J, Goldberg E. Regional localization of the sperm-specific lactate dehydrogenase, LDHC, gene on human chromosome 11. Ann Hum Genet 1989; 53:215-219.

81. Vemuganti SA, Bell TA, Scarlett CO, Parker CE, Pardo-Manuel de Villena F, O'Brien DA. Genomic and proteomic analysis of aldolase A retrogenes expressed during spermatogenesis. J Androl 2006; 27 39.

82. Kumar V, Rangaraj N, Shivaji S. Activity of pyruvate dehydrogenase A (PDHA) in hamster spermatozoa correlates positively with hyperactivation and is associated with sperm capacitation. Biol Reprod 2006; 75:767-777.

83. Mitra K, Rangaraj N, Shivaji S. Novelty of the pyruvate metabolic enzyme dihydrolipoamide dehydrogenase in spermatozoa: correlation of its localization, tyrosine phosphorylation, and activity during sperm capacitation. J Biol Chem 2005; 280:25743-25753.

84. Arcelay E, Salicioni AM, Wertheimer E, Visconti PE. Identification of proteins undergoing tyrosine phosphorylation during mouse sperm capacitation. Int J Dev Biol 2008; 52:463-472.

85. Fujinoki M, Kawamura T, Toda T, Ohtake H, Ishimoda-Takagi T, Shimizu N, Yamaoka S, Okuno M. Identification of 36 kDa phosphoprotein in fibrous sheath of hamster spermatozoa. Comp Biochem Physiol B Biochem Mol Biol 2004; 137:509-520.

86. Hinsch KD, De Pinto V, Aires VA, Schneider X, Messina A, Hinsch E. Voltage-dependent anion-selective channels VDAC2 and VDAC3 are abundant proteins in bovine outer dense fibers, a cytoskeletal component of the sperm flagellum. J Biol Chem 2004; 279:15281-15288.

87. Ford WC, Harrison A. The role of oxidative phosphorylation in the generation of ATP in human spermatozoa. J Reprod Fertil 1981; 63:271-278.

88. Hammerstedt RH, Lardy HA. The effect of substrate cycling on the ATP yield of sperm glycolysis. J Biol Chem 1983; 258:8759-8768.

89. Medrano A, Fernandez-Novell JM, Ramio L, Alvarez J, Goldberg E, Montserrat Rivera M, Guinovart JJ, Rigau T, Rodriguez-Gil JE. Utilization of citrate and lactate through a lactate dehydrogenase and ATP-regulated pathway in boar spermatozoa. Mol Reprod Dev 2006; 73:369-378.

90. Mukai C, Okuno M. Glycolysis plays a major role for adenosine triphosphate supplementation in mouse sperm flagellar movement. Biol Reprod 2004; 71:540-547.

91. Peterson RN, Freund M. ATP synthesis and oxidative metabolism in human spermatozoa. Biol Reprod 1970; 3:47-54.

92. Suter D, Chow PY, Martin IC. Maintenance of motility in human spermatozoa by energy derived through oxidative phosphorylation and addition of albumin. Biol Reprod 1979; 20:505-510.

93. Tanaka H, Takahashi T, Iguchi N, Kitamura K, Miyagawa Y, Tsujimura A, Matsumiya K, Okuyama A, Nishimune Y. Ketone bodies could support the motility but not the acrosome reaction of mouse sperm. Int J Androl 2004; 27:172-177.

94. Van Dop C, Hutson SM, Lardy HA. Pyruvate metabolism in bovine epididymal spermatozoa. J Biol Chem 1977; 252:1303-1308.

95. Williams AC, Ford WC. The role of glucose in supporting motility and capacitation in human spermatozoa. J Androl 2001; 22:680-695.

96. Carey JE, Olds-Clarke P, Storey BT. Oxidative metabolism of spermatozoa from inbred and random bred mice. J Exp Zool 1981; 216:285-292.

97. Bone W, Jones AR, Morin C, Nieschlag E, Cooper TG. Susceptibility of glycolytic enzyme activity and motility of spermatozoa from rat, mouse, and human to inhibition by proven and putative chlorinated antifertility compounds in vitro. J Androl 2001; 22:464-470.

98. Bone W, Jones NG, Kamp G, Yeung CH, Cooper TG. Effect of ornidazole on fertility of male rats: inhibition of a glycolysis-related motility pattern and zona binding required for fertilization in vitro. J Reprod Fertil 2000; 118:127-135.

99. Mahadevan MM, Miller MM, Moutos DM. Absence of glucose decreases human fertilization and sperm movement characteristics in vitro. Hum Reprod 1997; 12:119-123.

100. Cao W, Aghajanian HK, Haig-Ladewig LA, Gerton GL. Sorbitol can fuel mouse sperm motility and protein tyrosine phosphorylation via sorbitol dehydrogenase. Biol Reprod 2009; 80:124-133.

101. Okabe M, Adachi T, Kohama Y, Mimura T. Effect of glucose and phloretin-2'-beta-D-glucose (phloridzin) on in vitro fertilization of mouse ova. Experientia 1986; 42:398-399.

102. Hers HG. The conversion of fructose-1-C14 and sorbitol-1-C14 to liver and muscle glycogen in the rat. J Biol Chem 1955; 214:373-381.

103. Lippes J, Enders RG, Pragay DA, Bartholomew WR. The collection and analysis of human fallopian tubal fluid. Contraception 1972; 5:85-103.

104. Anderson RA, Jr., Oswald C, Willis BR, Zaneveld LJ. Relationship between semen characteristics and fertility in electroejaculated mice. J Reprod Fertil 1983; 68:1-7.

105. Mann T. Secretory function of the prostate, seminal vesicle and other male accessory organs of reproduction. J Reprod Fertil 1974; 37:179-188.

106. Marchlewska-Koj A. Fructose content of mouse ejaculates recovered from the uterus after mating. J Reprod Fertil 1971; 25:81-84.

107. Olds-Clarke P. Sperm from tw32/+ mice: capacitation is normal, but hyperactivation is premature and nonhyperactivated sperm are slow. Dev Biol 1989; 131:475-482.

108. Kaula N, Andrews A, Durso C, Dixon C, Graham JK. Classification of hyperactivated spermatozoa using a robust Minimum Bounding Square Ratio algorithm. Conf Proc IEEE Eng Med Biol Soc 2009; 2009:4941-4944.

109. Vulcano GJ, Moses DF, Valcarcel A, de las Heras MA. A lineal equation for the classification of progressive and hyperactive spermatozoa. Math Biosci 1998; 149:77-93.

110. Ho HC, Granish KA, Suarez SS. Hyperactivated motility of bull sperm is triggered at the axoneme by Ca2+ and not cAMP. Dev Biol 2002; 250:208-217.

111. Ishijima S, Baba SA, Mohri H, Suarez SS. Quantitative analysis of flagellar movement in hyperactivated and acrosome-reacted golden hamster spermatozoa. Mol Reprod Dev 2002; 61:376-384.

112. Wennemuth G, Carlson AE, Harper AJ, Babcock DF. Bicarbonate actions on flagellar and Ca2+ -channel responses: initial events in sperm activation. Development 2003; 130:1317-1326.

113. Cancel AM, Lobdell D, Mendola P, Perreault SD. Objective evaluation of hyperactivated motility in rat spermatozoa using computer-assisted sperm analysis. Hum Reprod 2000; 15:1322-1328.

114. Mortimer ST. CASA--practical aspects. J Androl 2000; 21:515-524.

115. Dunson DB, Weinberg CR, Perreault SD, Chapin RE. Summarizing the motion of self-propelled cells: applications to sperm motility. Biometrics 1999; 55:537-543.

116. Bray C, Son JH, Kumar P, Meizel S. Mice deficient in CHRNA7, a subunit of the nicotinic acetylcholine receptor, produce sperm with impaired motility. Biol Reprod 2005; 73:807-814.

117. Neill JM, Olds-Clarke P. Incubation of mouse sperm with lactate delays capacitation and hyperactivation and lowers fertilization levels in vitro. Gamete Res 1988; 20:459-473.

118. Si Y, Olds-Clarke P. Evidence for the involvement of calmodulin in mouse sperm capacitation. Biol Reprod 2000; 62:1231-1239.

119. Mortimer ST. Minimum sperm trajectory length for reliable determination of the fractal dimension. Reprod Fertil Dev 1998; 10:465-469.

CHAPTER 2

CLASSIFICATION OF MOUSE SPERM MOTILITY PATTERNS USING AN AUTOMATED MULTICLASS SUPPORT VECTOR MACHINES MODEL

Abstract

Vigorous sperm motility, including the transition from progressive to hyperactivated motility that occurs in the female reproductive tract, is required for normal fertilization in mammals. We developed an automated, quantitative method that objectively classifies five distinct motility patterns of mouse sperm using Support Vector Machines (SVM), a commonly used method in supervised machine learning. This multiclass SVM model is based on more than 2,000 sperm tracks that were captured by computer-assisted sperm analysis (CASA) during in vitro capacitation and visually classified as progressive, intermediate, hyperactivated, slow or weakly motile. Parameters associated with the classified tracks were incorporated into established SVM algorithms to generate a series of equations. These equations were integrated into a binary decision tree that sequentially sorts uncharacterized tracks into distinct categories. The first equation sorts CASA tracks into vigorous and non-vigorous categories. Additional equations classify vigorous tracks as progressive, intermediate or hyperactivated, and non-vigorous tracks as slow or weakly motile. Our CASAnova

software uses these SVM equations to classify individual sperm motility patterns automatically. Comparisons of motility profiles from sperm incubated with and without bicarbonate confirmed the ability of the model to distinguish hyperactivated patterns of motility that develop during in vitro capacitation. The model accurately classifies motility profiles of sperm from a mutant mouse model with severe motility defects. Application of the model to sperm from multiple inbred strains reveals strain-dependent differences in sperm motility profiles. CASAnova provides a rapid and reproducible platform for quantitative comparisons of motility in large, heterogeneous populations of mouse sperm.

Introduction

During transit through the epididymis sperm develop the capacity for progressive motility and binding to the zona pellucida, two maturational changes required for fertilization [1]. Sperm undergo further changes that are essential for fertilization in the female reproductive tract or in appropriate media in vitro. These changes, collectively known as capacitation, include changes in sperm motility [2, 3]. Sperm isolated from the cauda epididymis display progressive motility, which is characterized by high velocities and low amplitude, symmetrical flagellar bends [4]. Sperm obtained from the oviduct display motility characterized by higher amplitude, more asymmetric flagellar bends leading to more vigorous and less progressive 'whiplash' motility [5]. This change in motility, termed hyperactivation [1, 6], is required for fertilization and facilitates several processes including detachment of sperm from oviductal epithelia, navigation within the

viscoelastic oviduct environment and penetration of the zona pellucida (reviewed in [7]). In both mouse and human, several infertile phenotypes are correlated with genetic perturbations that affect either the onset of motility or the development of hyperactivated motility [8, 9].

Multiple methods have been developed to analyze physiological changes in sperm motility (reviewed in [10]). Techniques that examine flagellar movement provide detailed analyses of motion dynamics at the single sperm level, and are especially useful for analyzing changes in flagellar beat associated with hyperactivation [11-13]. Computer-assisted sperm analysis (CASA) facilitates the assessment of motility in larger populations of sperm, generating tracks for each sperm in a microscopic field based on the position of the sperm head in successive frames. Typically, at least 30 framed are captured at 60 Hz (0.5 sec), although extended tracking intervals have proven useful for evaluating hyperactivation in rat sperm [14]. Objective and quantitative measurements are provided for each track, including velocities and other kinematic parameters, along with population measures such as percentages of motile and progressive sperm [15]. When analyzed by CASA, hyperactivated sperm display vigorous, asymmetric tracks characterized by directional changes. The percentage of hyperactivated sperm has commonly been assessed by setting thresholds based on specific combinations of CASA parameters, such as curvilinear velocity and straightness [9, 16-20]. Thresholds were developed for human sperm by first analyzing flagellar movement to identify hyperactivated sperm, followed by the derivation of kinematic parameters applicable to CASA [14, 21]. Hyperactivation thresholds based on CASA parameters from tracks captured at 60 Hz have also been proposed for other species, including mouse, rat [14],

macaque [22], and stallion [23]. In the mouse, this gating approach has been reported to underestimate the percentage of hyperactivated sperm at relevant time points [20] or falsely detect hyperactivation at early time points before capacitation takes place [19, 24]. Our preliminary studies agreed with these conclusions. We tested multiple threshold gates and found underestimates of hyperactivated mouse sperm with percentile gates [20] and overestimates with other proposed thresholds [9, 16, 19], including ~5-12% of sperm classified as hyperactivated immediately after isolation.

Other gating-independent methods have been developed to simultaneously identify progressive and hyperactivated CASA tracks, including Minimum Bounding Square Ratio algorithms for stallion sperm and lineal equations for ram [25, 26]. To our knowledge, similar approaches have not yet been validated for mouse sperm. Therefore, an automated, objective, and reproducible method that distinguishes distinct patterns of sperm motility would significantly enhance our understanding of perturbations that effect mouse sperm function. To that end, we utilized Support Vector Machines (SVM), a common method of supervised machine learning [27], to develop a multiclass SVM model and CASAnova software to classify hyperactivated sperm and four other distinct patterns of mouse sperm motility based on standard CASA parameters.

Materials and Methods

Reagents and Media

All reagents were purchased from Sigma-Aldrich Co. (St. Louis, MO) except sodium chloride and glucose (Fisher Scientific), sodium pyruvate (Invitrogen, Carlsbad,

CA), sodium bicarbonate (EM Science, Gibbstown, NJ), potassium chloride, magnesium sulfate heptahydrate, and potassium phosphate (Mallinckrodt Chemical, Phillipsburg, NJ), and penicillin/streptomycin 100x stock solution containing 10,000 U/ml penicillin G and 10 mg/ml streptomycin (Gemini Bioproducts, West Sacramento, CA).

HTF, the medium used for all sperm motility assays, is based on the composition of human oviductal fluid and has been used extensively for both mouse and human in vitro fertilization (IVF) [28, 29]. HTF complete medium consists of 101.6 mM NaCl, 4.7 mM KCl, 0.37 mM KH_2PO_4, 0.2 mM $MgSO_4 \cdot 7\ H_2O$, 2 mM $CaCl_2$, 25 mM $NaHCO_3$, 2.78 mM glucose, 0.33 mM pyruvate, 21.4 mM lactate, 5mg/ml BSA, 100 U/ml penicillin G and 0.1mg/ml streptomycin. HTF medium without energy substrates did not include glucose, lactate, or pyruvate. Bicarbonate-free HTF replaced 25 mM sodium bicarbonate with 21 mM HEPES. For all media, the osmolality was adjusted to ~315 mOsm/kg with 5M NaCl using a Model 3300 micro-osmometer (Advanced Instruments, Norwood, MA).

Animals and Sperm Collection

Adult CD1 male mice were purchased from Charles River Laboratories (Raleigh, NC) and allowed to acclimatize before use. C57BL/6J, 129S1/SvImJ, and PWK /PhJ male mice were kindly provided by Fernando Pardo-Manuel de Villena (University of North Carolina). *Gapdhs*$^{-/-}$ and wildtype mice were obtained from an established breeding colony [30]. At least three mice of each strain or genotype were used for each experiment. All procedures involving mice were approved in advance by the Institutional Animal Care and Use Committee of the University of North Carolina at Chapel Hill.

Sperm were collected from the cauda epididymides of sexually mature (>8 weeks) mice. Each cauda was carefully trimmed to remove adipose and other tissue, rinsed in PBS (140 mM NaCl, 3mM KCl, 4 mM $NaH_2PO_4 \cdot 7H_2O$, 1.4 mM KH_2PO_4, pH 7.4), and placed in 1 ml HTF media lacking both bicarbonate and energy substrates. Four to six cuts were made in each cauda using iris scissors, and sperm were released into the media by incubation for 10 min at 37° C under 5% CO_2 and air. After the incubation, the tissue was removed and the suspension was mixed gently by swirling. This suspension was then diluted 1:20 to 1:60 in HTF complete medium to a concentration of ~2-4 x 10^5 sperm/ml, equivalent to 50-120 sperm per microscope field for CASA when using the following equipment and settings. For the analysis of motility under non-capacitating conditions, sperm were diluted at the same ratio into bicarbonate-free HTF.

Analysis of Sperm Motility

After dilution in HTF complete medium or bicarbonate-free HTF, sperm were incubated for 2 h at 37° C under 5% CO_2 in air, and motility was assessed at 30 min intervals. Initial time points were completed within two minutes of dilution into HTF. Quantitative parameters of sperm motility were recorded by CASA using the CEROS sperm analysis system (software version 12.3, Hamilton Thorne Biosciences, Beverly, MA). The CEROS system includes an Olympus CX41 microscope equipped with a MiniTherm stage warmer and a Sony model XC-ST50 CCD camera. Sperm tracks (1.5 sec) were captured at 37°C with a 4x negative phase contrast objective and a frame acquisition rate of 60 Hz. The default Mouse 2 analysis settings provided by Hamilton

Thorne were used, except that 90 frames were recorded and slow cells were counted as motile. These settings include: 60 frames per second, 90 frames acquired, minimum contrast = 30, minimum size = 4 pixels, default cell size = 13 pixels, default cell intensity = 75, cells progressive if VAP >50 μm/sec and STR > 50%, slow cells counted as motile, low VAP cut off = 10 μm/sec, low VSL cutoff = 0 μm/sec, minimum intensity gate = 0.10, maximum intensity gate = 1.52, minimum size gate = 0.13 pixels, maximum size gate = 2.43 pixels, minimum elongation gate = 5 pixels, and maximum elongation gate = 100 pixels.

Sperm suspensions were gently mixed before measuring motility. For each motility measurement, a 25 μl aliquot of sperm suspension was loaded by capillary action using a large bore pipet tip into one chamber of a pre-warmed Leja slide (100 μm-deep, Leja, The Netherlands). To minimize drift in the media, excess liquid was removed from the outside of the slide by blotting with a laboratory tissue as recommended by the manufacturer, and loading was examined to ensure the absence of air pockets in the chamber. At least 10 fields were recorded for each sample analyzed, covering the entire viewable area of the chamber without overlapping successive fields. Tracks and kinematic parameters were recorded for individual sperm. Tracks included in subsequent analyses were required to have a minimum of 45 points which represents half the number of total frames, as in previous studies using extended tracking intervals [9, 14]. Individual database text (DBT) files with track details were generated for every sperm population analyzed at every time point, providing Field #, Track #, average path velocity (VAP), straight-line velocity (VSL), curvilinear velocity (VCL), amplitude of lateral head

displacement (ALH), beat cross frequency (BCF), straightness (STR), and linearity (LIN) values for every track.

SVM Model Training

A training set was created from sperm analyzed after 90 min of incubation in HTF complete medium at 37^{o} in an atmosphere of 5% CO_2 and air. This time point was selected because high levels of vigorous motility were maintained consistently at 90 min and five motility patterns (progressive, intermediate, hyperactivated, slow, and weakly motile) were well represented. Individual sperm tracks were assessed visually and assigned to one of these five motility patterns (see results for details of the criteria for each group). The kinematic parameters for these tracks were identified in the CASA-generated DBT files and copied into an Excel worksheet, along with their visual classification to create the training data set. All classified tracks and parameters were loaded into Matlab (software version 2009b, The Mathworks, Natick, MA). The "svmtrain" LibSVM function [31] was used to generate the SVM equations that we incorporated into the CASAnova software program for automated sperm motility analyses. First, classified tracks were labeled as "vigorous" (progressive, intermediate, hyperactivated) or "non-vigorous" (slow and weakly motile). The function then generated an equation that best separates the two groups of data in multidimensional space (SVM1, see Results). This process was repeated within the vigorous and non-vigorous groups to generate four equations used to classify motility patterns. We have

submitted a patent application for the use of support vector machines to classify sperm motility patterns based on CASA parameters [32].

Statistical Analysis

Statistical analyses were performed using GraphPad Prism 5 (GraphPad Software, La Jolla, CA). All data are shown as mean ± SEM. Statistical significance was determined using either two-tailed unpaired t-tests or by one-way ANOVA after arcsine transformation of percentages. Differences were considered significant if $P < 0.05$. The percent agreement of the model was evaluated by calculating Cohen's Kappa Coefficient [33].

Results

Characterization of Sperm Motility Patterns

Current CASA instruments capture multiple images and generate tracks for each sperm by marking the position of the head in successive frames (Fig. 1). Visual examination of tracks recorded immediately after isolation of sperm from the cauda epididymis (Fig. 1A) and after in vitro capacitation for 90 min (Fig. 1B) indicates that motility changes during this interval from predominantly progressive to more varied profiles that are less linear. The first step in developing a quantitative model that distinguishes these different types of motility was to generate a training set of sperm tracks for analysis. We collected CASA tracks of sperm incubated for 90 minutes in HTF

complete medium and assessed both sperm motion and track pattern with the playback function in the software. Tracks of sperm from 12 CD1 mice were classified as progressive, intermediate, hyperactivated, slow, or weakly motile. Figure 1 shows examples of all motility patterns and Table 1 provides the mean values of all kinematic parameters associated with each group. Sperm with vigorous motility (progressive, intermediate or hyperactivated) in our training set had mean VCL values >279 μm/sec, while the non-vigorous groups (slow and weakly motile) had mean VCL values <176 μm/sec. Additional examples of each motility pattern are shown at higher magnification in Supplemental Figure S1. Tracks classified as progressive were typically very straight with little deviation of the head from the average path and angles between consecutive points of less than 90 degrees along the majority of the track (track a in Fig. 1A and B, Supplemental Fig. S1A). Intermediate sperm tracks showed more vigorous motion, with larger deviations from the net direction of movement and angles of approximately 90 degrees along most of the track length (track b in Fig. 1B, Supplemental Figure S1B). Sperm were classified as hyperactivated if they displayed highly vigorous motility accompanied by turns of greater than 90 degrees between consecutive points along the majority of the track. This category includes both the classic star-spin pattern of motility (track c in Fig. 1B, Supplemental Fig. S1C) and sperm tracks that exhibit large deviations from the average path but maintain a more defined direction of movement (track d in Fig. 1B, Supplemental Fig. S1C) [34, 35]. Slow sperm tracks covered much less distance than progressive sperm and generally did not show a high level of displacement of the head from the path of movement (track e in Fig. 1B, Supplemental Fig. S1D). Tracks that were motile but were not vigorous and did not have significant forward motion were

characterized as weakly motile (track f in Fig. 1B, Supplemental Fig. S1E). To maintain very strict criteria for defining the five motility patterns, we excluded tracks that were derived from sperm with abnormalities such as flagellar bending at the annulus or adherence to other sperm (~400 tracks), were the result of sperm collisions (~300 tracks), or could not be identified confidently (~400 tracks). A total of 2,043 tracks were included in the final training set used to develop the CASAnova equations.

Development of the Multiclass SVM Model and CASAnova Software

The Hamilton Thorne CASA systems generate data files that list parameter values for each sperm track analyzed in an experiment. Independent kinematic parameters, including VAP (μm/sec), VSL (μm/sec), VCL (μm/sec), ALH (μm) and BCF (Hz) were used to develop our multiclass SVM model. Since STR (VSL/VAP) and LIN (VSL/VCL) are ratios of other parameters, they were not used in building our prediction model. CASA parameters for visually classified tracks in our training set were grouped into separate Excel files for each motility pattern. This set of tracks from sperm incubated for 90 min under capacitating conditions included 539 progressive tracks, 236 intermediate tracks, 515 hyperactivated tracks, 556 slow tracks, and 197 weakly motile tracks. After generating the model using tracks from 90 min time points, progressive tracks recorded at time 0 were incorporated to determine their effect on the SVM equations. Since these time 0 tracks did not significantly alter the multiclass SVM model equations (data not shown), they were not included in the final model.

Three-dimensional scatter plots of CASA parameters associated with the five motility groups revealed clustering of tracks according to their visual classification (Fig. 2A). Hyperactivated sperm tracks (blue data points) clustered separately from progressive sperm tracks (red data points). Intermediate tracks (green data points) clustered between these groups, indicating that this motility pattern may constitute a phase that occurs between progressive and hyperactivated states. Tracks classified as weakly motile (cyan data points) generally had the lowest velocities and were grouped below the slow tracks (black points).

The clustering of sperm tracks based on their visual classification (Fig. 2A) suggested that sperm motility patterns could be mathematically separated into groups using support vector machines. We developed a set of equations that mathematically define the boundaries which distinguish these clusters (Table 2). Each equation includes all independent CASA parameters, and the number multiplied by each parameter reflects its relative importance in that equation. In equation SVM1, for example, VAP is the most important determinant and BCF is the least important. The decision tree shown in Figure 2B summarizes how these equations are sequentially applied to sort sperm tracks into the five motility groups. We first used established algorithms available in LibSVM to divide the tracks into two principal groups: vigorous (progressive, intermediate, hyperactivated) and non-vigorous (slow and weakly motile). The program generated a binary equation that separates these two groups in the training set (Table 2, SVM1). If CASA parameters from an unclassified track are applied to this equation and the result is greater than 0, the track is classified as vigorous. Otherwise, the track is classified as non-vigorous. After

defining two groups with the initial equation, the process was repeated to further subdivide these populations into discrete motility groups.

Within the vigorous group, we developed two additional SVM equations, SVM2 and SVM3 (Table 2). SVM2 classifies tracks as hyperactivated if the value of SVM2 is greater than 0, and removes them from further examination. Vigorous sperm tracks that have a SVM2 <0 are further analyzed by SVM3. Tracks are classified as intermediate if their SVM3 >0, or progressive if SVM3 <0.

Tracks with SVM1 values less than 0 are classified as non-vigorous. This non-vigorous group can be further classified as slow or weakly motile based on SVM4 (Table 2). The SVM4 equation classifies a sperm track as slow if its value is greater than 0, while SVM4 values less than 0 are categorized as weakly motile.

A software program, which we named CASAnova, incorporates these four SVM equations for the automated classification of the motility patterns of individual sperm. This program utilizes CASA-generated DBT files with all CASA parameters for each motile track. CASAnova applies the SVM equations to individual CASA tracks, generates a summary showing the number of sperm that were classified into each motility group, and calculates the percentage of tracks in each group as a function of the motile population. This program also generates a detailed list showing each track analyzed, along with its CASA parameters and multiclass SVM classification. The CASAnova software and instructions for use can be downloaded for non-profit purposes at http://www.csbio.unc.edu/CASAnova/.

Accuracy of Track Identification with CASAnova

To assess the ability of CASAnova to accurately classify sperm motility tracks, we visually classified the motility patterns of 1,068 sperm tracks from four additional CD1 mice after incubation for 90 min in HTF complete medium. We then determined how many of these tracks were correctly assessed by CASAnova, and calculated the percent agreement (Table 3). All tracks were included in these assessments. In agreement with our visual classification, we noted that tracks of sperm with hairpin bends at the annulus were identified almost exclusively as slow or progressive. Tracks from agglutinated sperm were typically excluded from the analysis because of size exclusions in the software or short tracks with less than 45 points. Tracks derived from sperm collisions and errors in tracking were also greatly reduced by requiring a minimum of 45 points. Agreement in all groups, except intermediate, exceeded 83% and the overall agreement was 88.2%. Just over half of the visually identified intermediate tracks in this set (52.1%) agreed with the model classification, while CASAnova classified the remaining tracks in this group as progressive or hyperactivated in approximately equal proportions. We also employed Cohen's Kappa, a measurement of interrater reliability [33], to assess the overall level of agreement between visual and CASAnova classifications. This index indicates that the strength of agreement between these classifications is very good, with a Kappa coefficient of 0.848, which is within the 95% confidence interval.

Motility Profiles of Sperm Incubated in Capacitating and Non-capacitating Medium

Bicarbonate is required for sperm capacitation as well as the acquisition of hyperactivated motility [17, 36-38]. To assess the ability of the model to distinguish motility pattern distributions of capacitated and non-capacitated sperm, we generated motility profiles of sperm from six CD1 mice incubated in HTF complete medium ± 25 mM bicarbonate over a 2 hr time course (Fig. 3). While the percentage of motile sperm in both media remained above 50% throughout the time course (Supplemental Fig. S2A), there were marked differences in the sperm motility profiles. In complete medium containing bicarbonate (Fig. 3A), the number of progressive tracks steadily decreased over time. This decrease in progressive motility was accompanied by increases in all other motility groups. Among vigorously motile tracks, both intermediate and hyperactivated tracks increased by 60 min and reached maximum values by 90 min (red box, Fig. 3A). In this experiment, progressive tracks declined to 22.2% of all motile tracks by 90 min, while intermediate tracks increased to 9% and hyperactivated tracks increased to 18.9%. The proportion of sperm with non-vigorous motility (slow or weakly motile) also increased during in vitro capacitation, reaching 49.9% by 90 min. Further increases in non-vigorous motility were frequently observed by the 2 h time point. We confirmed that CASAnova is effective when sperm are analyzed in chambers with depths of either 100 μm (Leja) or 80 μm (2X-cel slides, Hamilton Thorne) (Supplemental Fig. S3).

Sperm incubated in medium that does not stimulate capacitation (Fig. 3B) showed a significantly different motility distribution than sperm incubated for the same period in HTF complete medium (Fig. 3A). When bicarbonate was omitted from the medium, the mean proportion of progressive sperm tracks remained above 50% over the entire time

course, in agreement with visual observations. The proportion of non-vigorous tracks increased throughout the incubation, although the percentage of weakly motile sperm remained lower than observed in HTF complete medium. As expected, intermediate and hyperactivated tracks were rarely observed throughout the incubation, reaching mean values of 0.4% and 1.2%, respectively, by 90 min (red box, Fig. 3B).

Analysis of Sperm with Motility Defects

To determine how CASAnova classifies sperm with severe defects in motility, we assessed the motility distribution of mice lacking the sperm-specific glycolytic enzyme glyceraldehyde 3-phosphate dehydrogenase (GAPDHS) (Fig. 4). These males are infertile and produce sperm that are motile (Supplemental Fig. 2B), but exhibit little forward progression [30]. CASAnova classified 99% of GAPDHS-null sperm as weakly motile or slow (Figure 4, open bars). Sperm from wild-type mice with the same genetic background (mixed 129S6/SvEvTac and C57BL/6NCrl) displayed predominantly progressive motility (Fig. 4, black bars). Approximately 17% of wild-type sperm were classified as slow immediately after isolation, perhaps reflecting contributions of the C57BL/6 genetic background (see next section).

Motility Profiles of Sperm from Inbred Mouse Strains

We developed CASAnova using sperm tracks from CD1 outbred mice. To determine its suitability for assessing sperm motility in other mouse strains, we assessed

sperm from C57BL/6J (BL6), 129S1/SvImJ (129) and PWK/PhJ (PWK) inbred mouse strains over a 90 min incubation in HTF complete medium (assayed in parallel, n = 4 mice per strain). Motility profiles were generated for each strain and compared to CD1 profiles (Fig. 5A). Sperm from two inbred strains (129 and PWK) exhibited motility profiles that were comparable to CD1 sperm immediately after isolation, except that a higher percentage of 129 sperm were classified as slow (0 min). At this initial time point, BL6 sperm tracks contained significantly fewer progressive tracks (mean = 23%, $P < 0.001$) and significantly more slow tracks (mean = 66.4%, $P < 0.001$) compared to CD1 sperm (79.2% progressive, 4.2% slow). This proportion of slow tracks persisted in BL6 sperm throughout the assay.

Throughout the time course, sperm from the three inbred strains showed the expected decrease in the percentage of progressive motility and concomitant increase in other motility classes (Fig. 5A). After 90 min of incubation, the mean percentage of slow tracks was significantly higher for both BL6 (59.5%) and 129 (60.6%) sperm than for CD1 (40.9%) sperm. At this time point, the mean percentages of hyperactivated sperm in both BL6 (16%) and 129 (15%) mice were significantly lower than the levels observed in CD1 mice (32%), while PWK hyperactivation was comparable to CD1. To determine whether reduced hyperactivation was due to the inability of the model to identify hyperactivated sperm in BL6 and 129 mice, we visually assessed the percentage of hyperactivated sperm for each strain. There were no statistically significant differences between hyperactivation levels determined visually or by using CASAnova (Supplemental Fig. S4). BL6 sperm did display more asymmetric tracks than 129 sperm

at 90 min, but many of these tracks had low velocities and were not classified as hyperactivated by the model or visual assessment.

CASAnova classifies all motile sperm in each population. When the number of sperm analyzed or the percent motility varies substantially between animals, additional considerations may be needed for a more complete assessment of motility. We typically recovered fewer sperm from these inbred strains (mean = 5.7 - 16.7 x 10^6) than from CD1 mice (mean = 31 x 10^6), but analyzed >150 tracks/mouse at each time point to provide robust assessments of sperm motility in each strain. We also found that the percentage of motile sperm at later time points was significantly lower in PWK mice (mean = 26.5% at 90 minutes) compared to the other strains (37% - 50%, Supplemental Fig. 2C). Therefore, we also calculated the percentage of hyperactivated sperm as a function of the total number of sperm analyzed by CASA at the 90 min time point (Fig. 5B). When immotile sperm are included in the calculation, the percentage of hyperactivated sperm in PWK mice falls to levels that are comparable to those observed for the other two inbred strains.

Discussion

During capacitation sperm motility patterns shift from largely progressive tracks at early time points to more varied patterns of movement, including hyperactivation. CASA-based approaches for identifying sperm motility patterns in the mouse have focused predominantly on distinguishing progressive and hyperactivated sperm populations [9, 16-20, 30, 39, 40], although there is no consensus on the parameters that

best define hyperactivation. We used CASA parameters from 2,043 sperm tracks (1.5 sec, 90 frames) to develop an automated model that identifies and quantitates five distinct patterns of sperm movement in large populations of mouse sperm. CASAnova is built upon a series of SVM equations (Table 2) that take into account both the relationships between CASA parameters and the relative importance of each parameter in assigning tracks to specific motility groups. This approach classifies all recorded tracks simultaneously, providing a more comprehensive analysis of the changes in motility that occur during capacitation compared to identifying only the percentage of hyperactivated sperm by visual assessment or the use of thresholds for selected CASA parameters. CASAnova was developed with mouse sperm tracks captured at 60 Hz using a Hamilton Thorne CEROS instrument. Although CASA systems typically calculate similar kinematic parameters, further validation studies will be necessary to test the applicability of this model for other CASA platforms.

Immediately after isolation from the cauda epididymis, mouse sperm display vigorous motility with ~80% of the motile population classified as progressive by CASAnova. The percentage of motile sperm is typically maintained during a 120 min in vitro capacitation period. In addition, the percentage of sperm displaying progressive motility does not change substantially during this interval when standard CASA cutoffs are used. The Mouse 2 default settings recommended by Hamilton Thorne categorize sperm as progressive if VAP >50 μm/sec and STR >50, a broad definition that includes virtually all linear tracks. The Hamilton Thorne software also identifies sperm as rapid if VAP exceeds the progressive threshold of 50μm/sec. In contrast, the progressive tracks in our training set were linear and had mean values for VAP of 146.9 ± 31.5 μm/sec.

CASAnova classifies sperm as progressive only if they have motility that is both linear and vigorous, while sperm that have linear tracks with substantially lower velocities (mean VAP = 85.2 ± 19.0 in our training set) are classified as slow. Inclusion of the non-vigorous classifications in this model provides better discrimination of sperm velocities and clearly shows that the motility of many sperm becomes less vigorous as capacitation proceeds, with ≥40% of the sperm classified as slow or weakly motile by 60 min (Fig. 3).

CASAnova also identifies intermediate and hyperactivated tracks, the vigorous patterns of sperm motility that develop during capacitation. In our training set both intermediate and hyperactivated sperm had higher mean values for VCL and ALH than progressive sperm (Table 1), reflecting the increased vigor expected during hyperactivation [14]. Hyperactivated motility patterns, including both star-spin tracks and tracks that show some directional movement, were classified with 94% accuracy. At initial time points, hyperactivation is essentially absent by visual inspection of sperm tracks (Fig. 1) and multiclass analysis reflects this observation (Fig. 3). Consequently, CASAnova eliminates the need for the subtraction of noise detected at time zero from the levels of hyperactivation detected at later time points [24]. As expected, this model detects an increase in the proportion of hyperactivated sperm over the course of a 2 h period of in vitro capacitation. The percentage of hyperactivated sperm reaches ~15%-35% by 90 min, consistent with levels reported in mouse and other species using validated approaches [14, 25, 34, 41, 42].

The percentage of intermediate tracks increases to ~9% of the motile population over the same time course (Fig. 3). Analyses of multidimensional scatter plots show that

the intermediate tracks cluster between the progressive and hyperactivated groups (Fig. 2), suggesting that the intermediate category may represent sperm shifting from progressive to hyperactivated motility. Similar transitional patterns of sperm motility have been described in other species [14, 35, 43]. The loss of both intermediate and hyperactivated tracks when bicarbonate is omitted from the medium (Fig. 3) provides support for considering intermediate sperm as a subset of the population developing asymmetric flagellar beats, and highlights the ability of CASAnova to accurately identify physiological alterations in motility that occur during capacitation.

The design of CASAnova to quickly distinguish and quantitate five patterns of motility, along with its applicability to sperm from multiple mouse strains, suggests that this model will be useful for more detailed analyses of sperm motility under a variety of experimental conditions. Inclusion of the slow category in CASAnova revealed that sperm from C57BL/6J mice are substantially less vigorous at initial time points than sperm from two other inbred strains (129S1/SvImJ and PWK/PhJ). This difference is interesting since both C57BL/6J and 129S1/SvImJ strains are used extensively in the production of knockout and transgenic mouse lines. In addition, all three of these inbred strains are founder strains of the Collaborative Cross, a project that is producing a large number of recombinant inbred lines with extensive genetic diversity [44]. Given the phenotypic variation that we observed in these inbred lines, it will be interesting to complete a similar analysis of sperm motility with fully inbred Collaborative Cross lines. We anticipate that use of CASAnova will contribute to more quantitative analyses of genetic factors that influence the complex traits of sperm motility and male fertility.

Gene targeting strategies have produced more than forty mutant mouse models with defects in sperm motility [8]. These include a broad range of structural, metabolic and signaling defects that reduce the proportion of motile sperm and/or impair required aspects of sperm movement such as forward progression [30, 45] or hyperactivation [46]. The inclusion of multiple categories in CASAnova will facilitate rapid assessment of motility deficits, as demonstrated for GAPDHS-null sperm. Although further validation will be required for sperm with severe structural defects or unusual motility patterns, CASAnova could be useful for establishing a standardized assessment of sperm motility that automatically discriminates between motility patterns based on the mathematical relationship of CASA parameters. Standardization would facilitate more meaningful comparisons among mutant mouse lines that may significantly enhance our understanding of the regulation of motility transitions required for fertilization.

Toxicological studies are being conducted to investigate the effects of various compounds on reproductive function in mice [40, 47, 48]. In cases where male reproductive toxicity is observed, use of CASAnova could improve discrimination of effects on physiologically relevant patterns of motility that are not easily discerned by comparison of individual CASA parameters. Similarly, the model could serve as an important screening tool for evaluating compounds as potential contraceptives that impair sperm motility, particularly when mechanisms that regulate hyperactivation are targeted.

Motility classification by CASAnova is rapid, reproducible and quantitative. This model provides an objective assessment of the entire motile population of sperm analyzed by CASA that is consistent between experiments, thereby facilitating standardization of motility pattern analyses. The CASAnova program is easy to use and quickly calculates

both the number and percentage of motile sperm in each of the five categories. It also generates a list showing the CASA parameters and multiclass SVM classification for each track. Classification of sperm motility patterns using CASAnova shows good agreement with visual classifications by observers with extensive training (Table 3), eliminating the need for visual verification of results or complex training to achieve accurate, detailed analyses. By combining CASA and standard machine learning tools to identify physiologically relevant patterns of sperm movement, CASAnova has the potential for being a valuable tool for assessing genetic, biomolecular, and pharmaceutical effects on sperm motility.

Figure 2.1

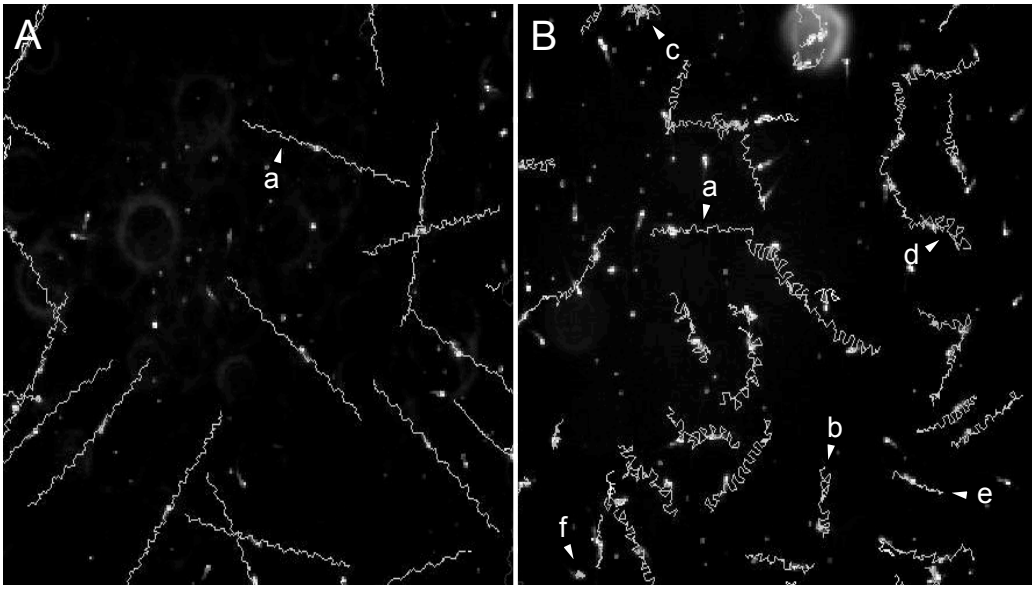

Figure 2.1. **Changes in sperm motility patterns during in vitro capacitation**. Representative CASA fields showing sperm tracks immediately after isolation (0 min, **A**) and after 90 min (**B**) incubation in HTF complete medium. Lower case letters in each panel denote representative tracks corresponding to five distinct motility groups used to generate the multiclass SVM model—progressive (a), intermediate (b), hyperactivated (c and d), slow (e), and weakly motile (f).

Figure 2.2

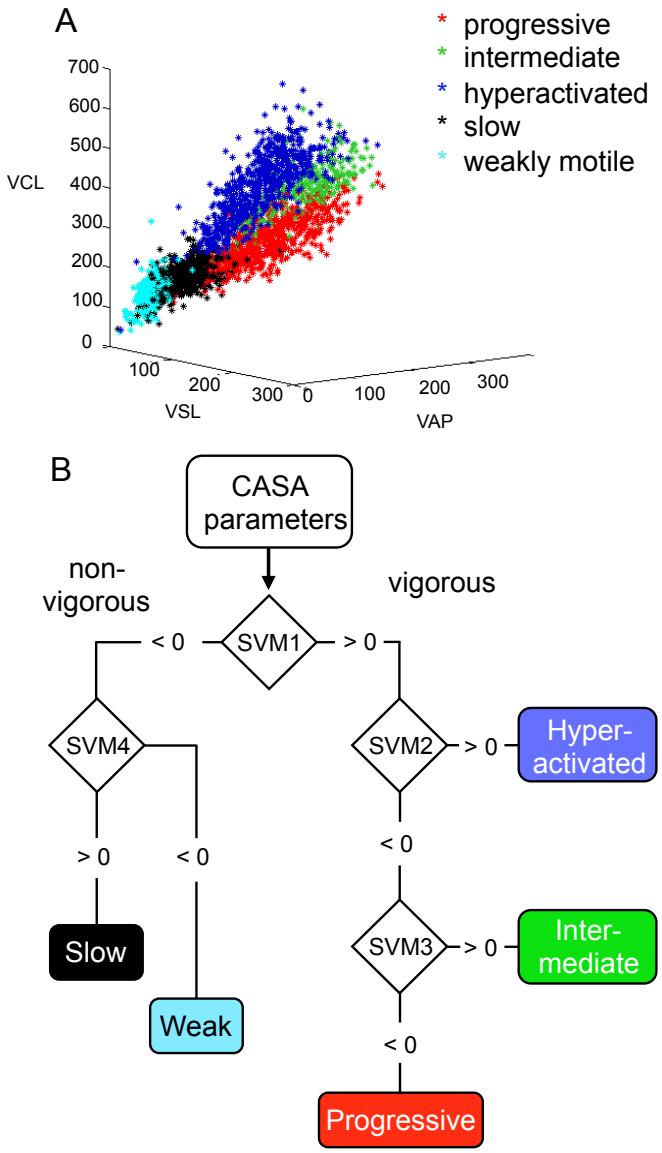

Figure 2.2. Generation of a multiclass SVM model to identify sperm motility patterns. A) In a multidimensional scatter plot of CASA velocity parameters (VCL, VSL, VAP) associated with sperm tracks in the training set, the tracks are clustered based on their visual classification. **B**) This decision tree diagrams how the multiclass SVM equations (Table 2) are used to classify sperm motility patterns.

Figure 2.3

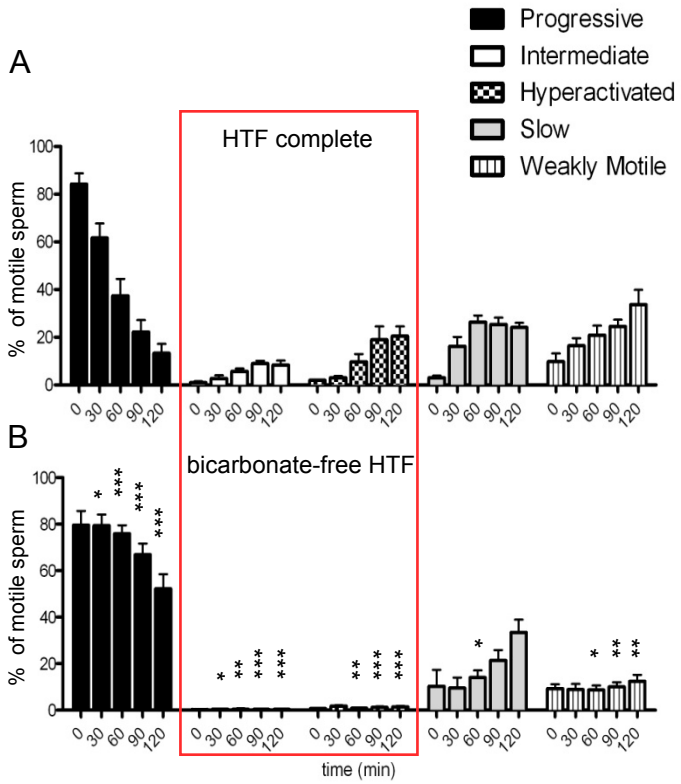

Figure 2.3. Time-dependent changes in the distribution of sperm motility patterns during in vitro capacitation. Motility of sperm from 6 CD1 mice was assessed at 30 min intervals during incubation in HTF complete medium with (**A**) or without (**B**) 25 mM sodium bicarbonate, and CASA parameters were subjected to analysis by CASAnova. The red box highlights significant differences in the appearance of intermediate and hyperactivated tracks under capacitating conditions. Bars represent the mean percentage ± SEM of motile tracks identified in each group at each time point. Differences between motility groups in A and B at corresponding time points were analyzed using one-way ANOVA. * $P < 0.05$; ** $P < 0.01$; *** $P < 0.001$.

Figure 2.4

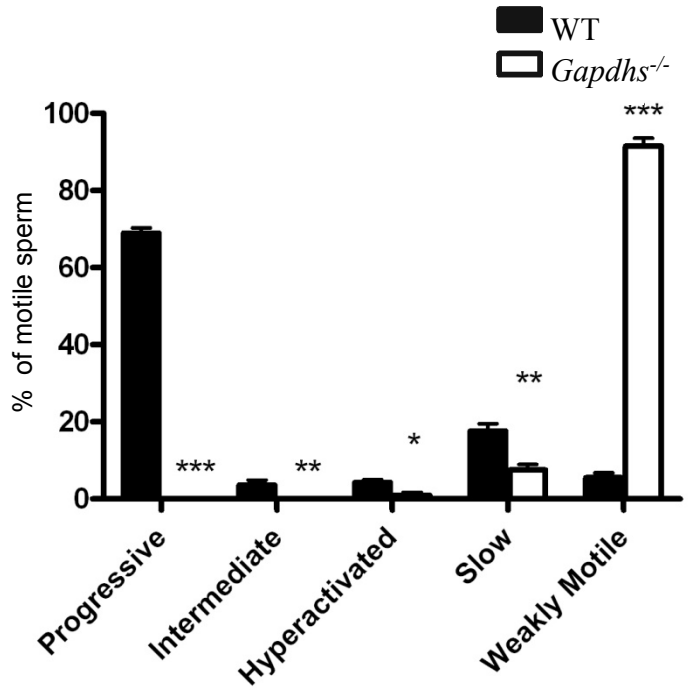

Figure 2.4. Distribution of sperm motility patterns in wildtype (WT) and *Gapdhs*$^{-/-}$ mice. CASAnova analysis of CASA parameters was used to compare motility patterns of sperm from wild-type (black bars, n = 3) and *Gapdhs*$^{-/-}$ mice (white bars, n = 3). Bars represent the mean percentage ± SEM of motile tracks identified in each group immediately after isolation in HTF complete medium (time 0). Significance was determined using a two-tailed unpaired t-test. * $P < 0.05$; ** $P < 0.01$; *** $P < 0.001$.

Figure 2.5

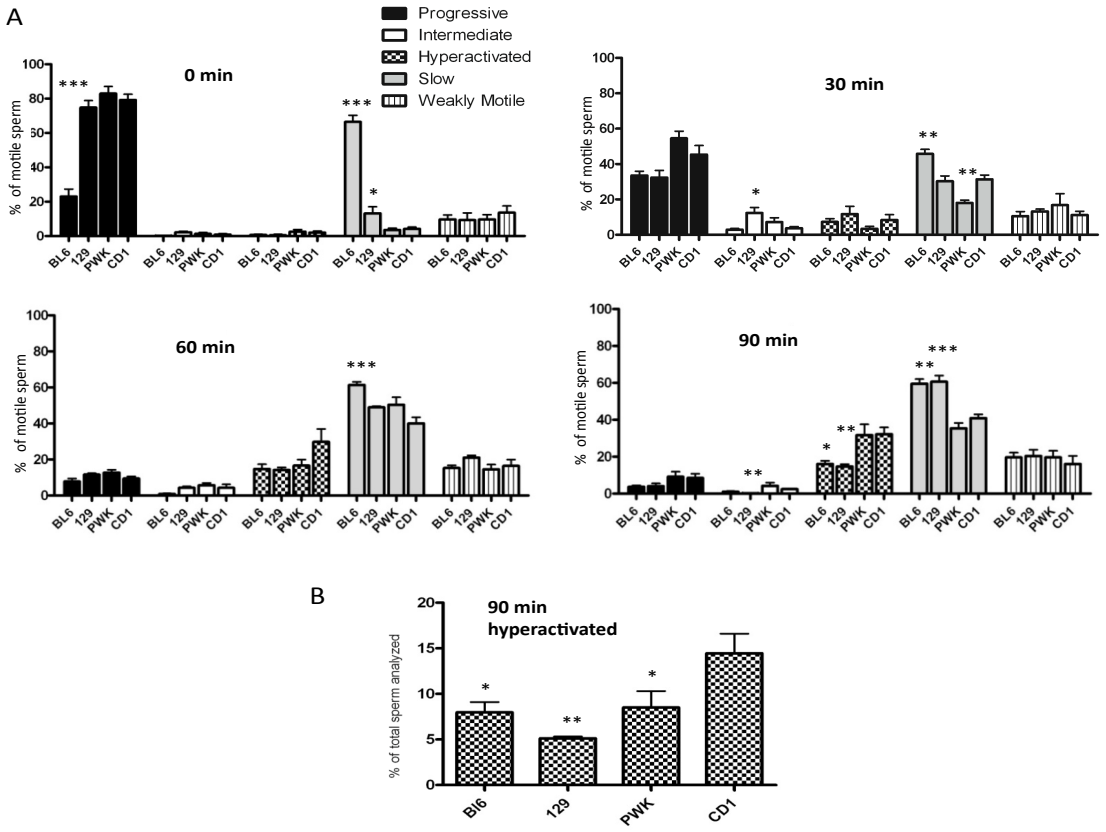

Figure 2.5. Differences in motility profiles between inbred and outbred mouse strains. (**A**) Sperm from C57BL/6J (BL6), 129S1/SvlmJ (129), PWK/PhJ (PWK), and CD1 mice (n = 4 mice per strain) were incubated in HTF complete medium and assayed by CASA over a 90 min time course, followed by analysis by CASAnova. Bars represent the mean percentage ± SEM of motile tracks identified in each group at each time point. (**B**) The percentage of hyperactivated sperm at 90 min (mean ± SEM) was determined as a function of the total number of sperm analyzed by CASA (motile + immotile). Differences between motility groups at corresponding time points were analyzed using one-way ANOVA followed by Dunnett's posttest to determine significance relative to the outbred CD1 strain. * $P < 0.05$; ** $P < 0.01$; *** $P < 0.001$.

Table 2.1. CASA parameter means for groups identified in the multiclass training set.*

Group	VAP	VSL	VCL	ALH	BCF
Progressive	146.9 ± 31.5	119.5 ± 29.5	279.6 ± 59.1	16.7 ± 4.5	25.4 ± 5.2
Intermediate	183.3 ± 31.1	140.4 ± 28.5	406.3 ± 61.5	23.7 ± 4.1	21.1 ± 4.1
Hyperactivated	171.1 ± 37.9	73.3 ± 36.1	373.6 ± 78.4	22.7 ± 5.4	29.1 ± 11.8
Slow	85.2 ± 19.0	40.2 ± 20.5	175.6 ± 32.4	12.3 ± 4.3	33.8 ± 10.3
Weakly Motile	56.2 ± 16.5	13.6 ± 6.8	127.2 ± 36.4	9.9 ± 4.0	45.3 ± 12.6

* Values are means ± standard deviation. VAP = average path velocity in μm/sec, VSL = straight line velocity in μm/sec, VCL = curvilinear velocity in μm/sec, ALH = amplitude of lateral head displacement in μm, BCF = beat cross frequency in Hz.

Table 2.2. CASAnova Multiclass Support Vector Machine (SVM) equations.

SVM1	(0.0388 x VAP) + (0.0335 x VSL) + (0.0225 x VCL) - (0.0248 x ALH) + (0.0051 x BCF) - 10.9540
SVM2	(0.0123 x VAP) - (0.1034 x VSL) + (0.0307 x VCL) + (0.0427 x ALH) + (0.0175 x BCF) - 3.6222
SVM3	(0.0146 x VAP) - (0.0701 x VSL) + (0.0371 x VCL) + (0.0167 x ALH) - (0.0132 x BCF) - 6.4943
SVM4	(0.0418 x VAP) + (0.1115 x VSL) + (0.0163 x VCL) - (0.0243 x ALH) - (0.0471 x BCF) - 4.7717

VAP = average path velocity in μm/sec, VSL = straight line velocity in μm/sec, VCL = curvilinear velocity in μm/sec, ALH = amplitude of lateral head displacement in μm, BCF = beat cross frequency in Hz.

Table 2.3. Agreement between visual and model-assigned tracks.

Track group	agree/total	% agreement
Progressive	192/231	83.2
Intermediate	38/73	52.1
Hyperactivated	251/265	94.7
Slow	232/248	93.5
Weakly Motile	229/251	91.2
Total	**942/1068**	**88.2**

Supplemental Figure 2.1

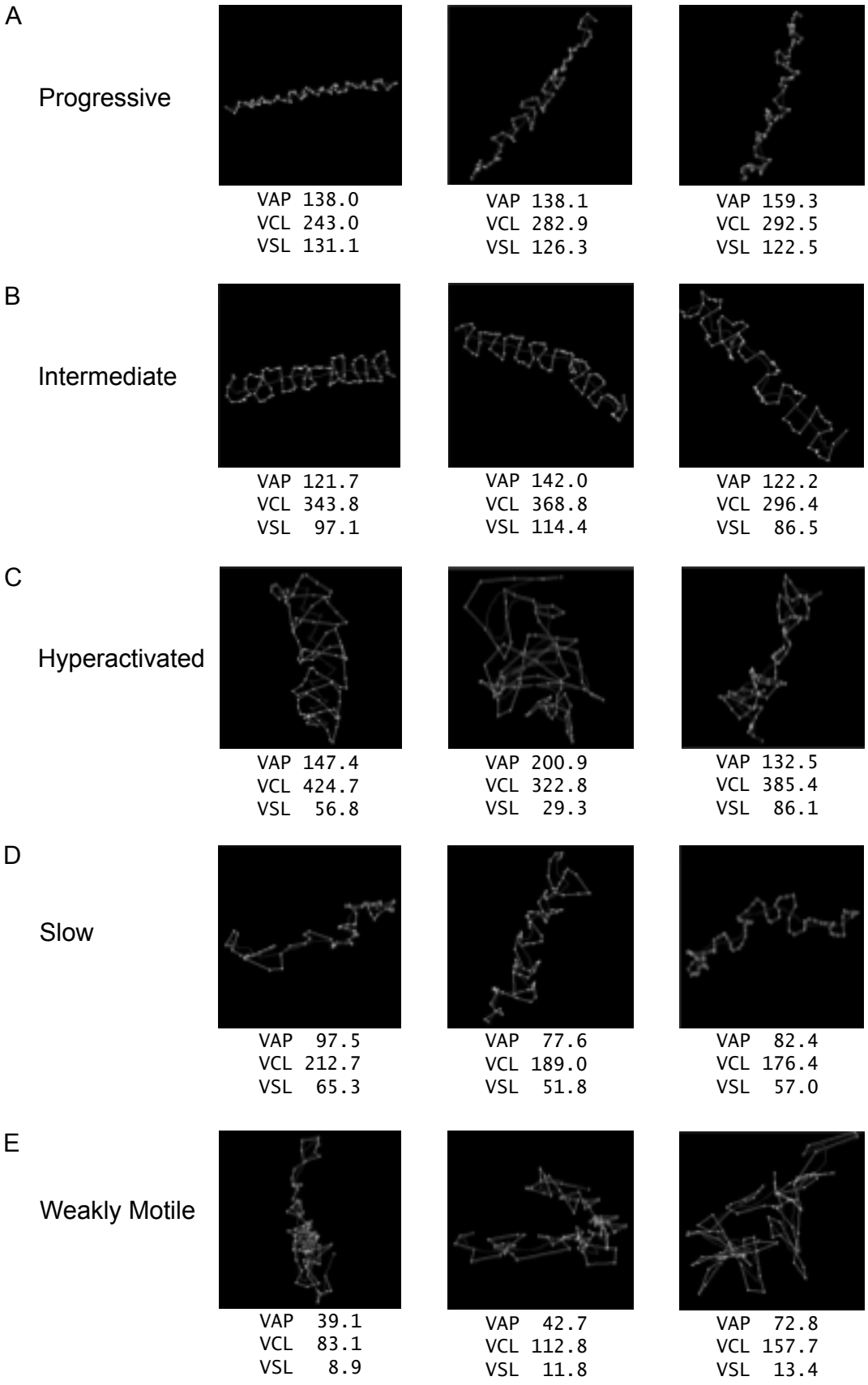

Supplemental Figure 2.1. Examples of sperm motility patterns identified during in vitro capacitation. Representative CASA tracks of sperm identified as progressive (**A**), intermediate (**B**), hyperactivated (**C**), slow (**D**), and weakly motile (**E**) after 90 min incubation in HTF complete medium. VAP, VCL, and VSL values for each track are shown. All tracks were identified by the both the multiclass SVM model and visual inspection as belonging to their respective groups. Track images are magnified to better illustrate the patterns of movement, but are not to the same scale relative to each other.

Supplemental Figure 2.2

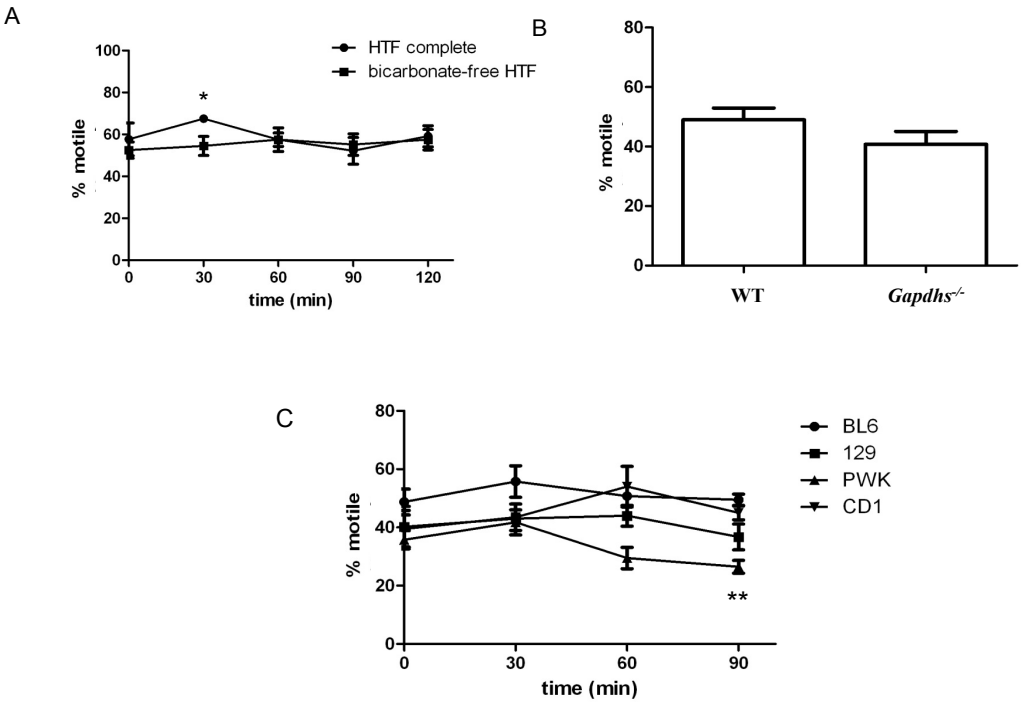

Supplemental Figure 2.2. Percent motility of sperm populations analyzed in this study. The percentage of motile sperm was assessed by CASA for: **A**) samples used in Fig. 3 incubated under capacitating (●) or non-capacitating conditions (■), B) samples from WT or *Gapdhs*$^{-/-}$ mice compared in Fig. 4, and **C**) samples from C57BL/6J (BL6, ●), 129S1/SvlmJ (129, ■), PWK/PhJ (PWK, ▲), and CD1 (▼) mice compared in Fig. 5. Data are shown as mean values ± SEM. Differences between percent motility at corresponding time points were analyzed using two-tailed unpaired t-test for **A** and **B**. For **C**, one-way ANOVA followed by Dunnett's posttest was used to determine significance relative to the outbred CD1 strain. * $P < 0.05$; ** $P < 0.01$

Supplemental Figure 2.3

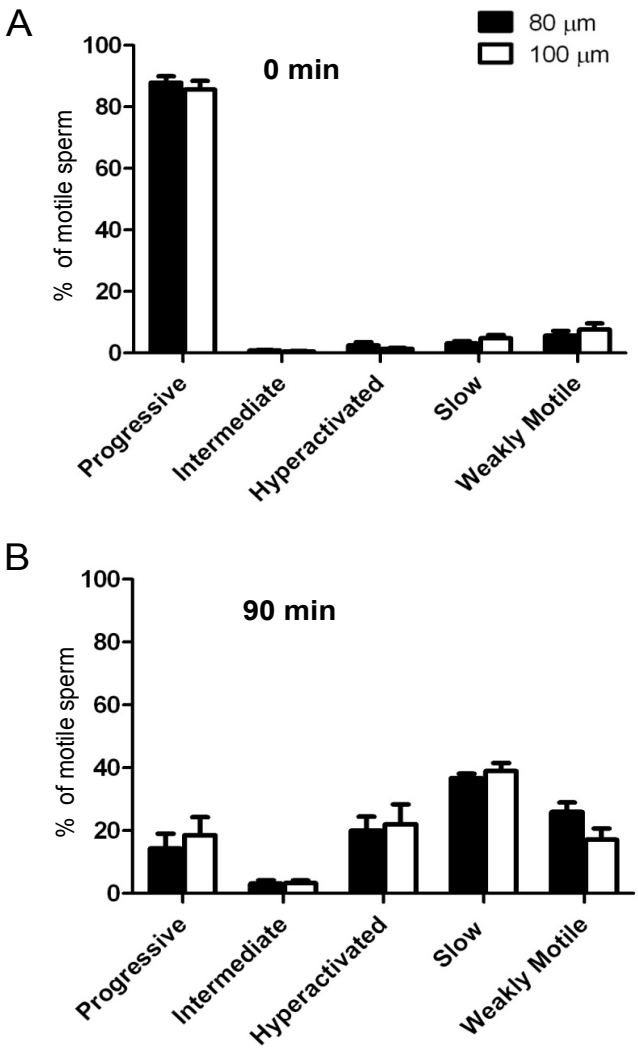

Supplemental Figure 2.3. Motility profiles of sperm analyzed in 80 μm vs. 100 μm CASA chambers. Sperm from CD1 mice (n = 6) were incubated for 0 min (**A**) or 90 min (**B**) in HTF complete medium. At each time point, aliquots of sperm were placed in either 80 μm (black bars) or 100 μm (open bars) chambers and motility was assessed by CASA. Motility profiles were generated using the multiclass SVM model. Bars represent mean percentages ± SEM of motile tracks. No significant differences were detected between the two chambers with the two-tailed unpaired t-test.

Supplemental Figure 2.4

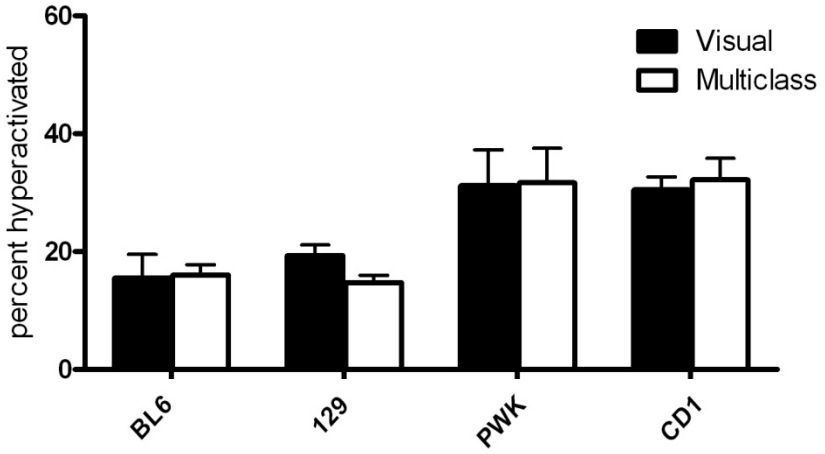

Supplemental Figure 2.4. Comparison of visual and multiclass SVM assessments of hyperactivation levels in inbred strains (n = 4 mice/strain). The percentage of the motile population exhibiting hyperactivated motility after 90 min in HTF complete medium was determined visually (black bars) and with the multiclass SVM model (open bars). No significant differences were detected between the two methods with the two-tailed unpaired t-test.

References

1. Yanagimachi R. Mammalian fertilization. In: Knobil E, Neill J (eds.), The Physiology of Reproduction. New York: Raven Press; 1994: 189-317.

2. Fraser LR. The "switching on" of mammalian spermatozoa: molecular events involved in promotion and regulation of capacitation. Mol Reprod Dev 2010; 77:197-208.

3. Visconti PE, Westbrook VA, Chertihin O, Demarco I, Sleight S, Diekman AB. Novel signaling pathways involved in sperm acquisition of fertilizing capacity. J Reprod Immunol 2002; 53:133-150.

4. Fraser L. Motility patterns in mouse spermatozoa before and after capacitation. Journal of Experimental Zoology 1977; 202:439-444.

5. Suarez SS, Osman RA. Initiation of hyperactivated flagellar bending in mouse sperm within the female reproductive tract. Biol Reprod 1987; 36:1191-1198.

6. Yanagimachi R. The movement of golden hamster spermatozoa before and after capacitation. J Reprod Fertil 1970; 23:193-196.

7. Suarez SS. Control of hyperactivation in sperm. Hum Reprod Update 2008; 14:647-657.

8. Matzuk MM, Lamb DJ. The biology of infertility: research advances and clinical challenges. Nat Med 2008; 14:1197-1213.

9. Si Y, Olds-Clarke P. Evidence for the involvement of calmodulin in mouse sperm capacitation. Biol Reprod 2000; 62:1231-1239.

10. Mortimer ST. A critical review of the physiological importance and analysis of sperm movement in mammals. Hum Reprod Update 1997; 3:403-439.

11. Ho HC, Granish KA, Suarez SS. Hyperactivated motility of bull sperm is triggered at the axoneme by Ca2+ and not cAMP. Dev Biol 2002; 250:208-217.

12. Ishijima S, Baba SA, Mohri H, Suarez SS. Quantitative analysis of flagellar movement in hyperactivated and acrosome-reacted golden hamster spermatozoa. Mol Reprod Dev 2002; 61:376-384.

13. Wennemuth G, Carlson AE, Harper AJ, Babcock DF. Bicarbonate actions on flagellar and Ca2+ -channel responses: initial events in sperm activation. Development 2003; 130:1317-1326.

14. Cancel AM, Lobdell D, Mendola P, Perreault SD. Objective evaluation of hyperactivated motility in rat spermatozoa using computer-assisted sperm analysis. Hum Reprod 2000; 15:1322-1328.

15. Mortimer ST. CASA--practical aspects. J Androl 2000; 21:515-524.

16. Bray C, Son JH, Kumar P, Meizel S. Mice deficient in CHRNA7, a subunit of the nicotinic acetylcholine receptor, produce sperm with impaired motility. Biol Reprod 2005; 73:807-814.

17. Neill JM, Olds-Clarke P. A computer-assisted assay for mouse sperm hyperactivation demonstrates that bicarbonate but not bovine serum albumin is required. Gamete Res 1987; 18:121-140.

18. Neill JM, Olds-Clarke P. Incubation of mouse sperm with lactate delays capacitation and hyperactivation and lowers fertilization levels in vitro. Gamete Res 1988; 20:459-473.

19. Odet F, Duan C, Willis WD, Goulding EH, Kung A, Eddy EM, Goldberg E. Expression of the gene for mouse lactate dehydrogenase C (Ldhc) is required for male fertility. Biol Reprod 2008; 79:26-34.

20. Quill TA, Sugden SA, Rossi KL, Doolittle LK, Hammer RE, Garbers DL. Hyperactivated sperm motility driven by CatSper2 is required for fertilization. Proc Natl Acad Sci U S A 2003; 100:14869-14874.

21. Mortimer ST, Swan MA. Kinematics of capacitating human spermatozoa analysed at 60 Hz. Hum Reprod 1995; 10:873-879.

22. Baumber J, Meyers SA. Hyperactivated motility in rhesus macaque (Macaca mulatta) spermatozoa. J Androl 2006; 27:459-468.

23. McPartlin LA, Suarez SS, Czaya CA, Hinrichs K, Bedford-Guaus SJ. Hyperactivation of stallion sperm is required for successful in vitro fertilization of equine oocytes. Biol Reprod 2009; 81:199-206.

24. Cao W, Aghajanian HK, Haig-Ladewig LA, Gerton GL. Sorbitol can fuel mouse sperm motility and protein tyrosine phosphorylation via sorbitol dehydrogenase. Biol Reprod 2009; 80:124-133.

25. Kaula N, Andrews A, Durso C, Dixon C, Graham JK. Classification of hyperactivated spermatozoa using a robust Minimum Bounding Square Ratio algorithm. Conf Proc IEEE Eng Med Biol Soc 2009; 2009:4941-4944.

26. Vulcano GJ, Moses DF, Valcarcel A, de las Heras MA. A lineal equation for the classification of progressive and hyperactive spermatozoa. Math Biosci 1998; 149:77-93.

27. Wang L. Support vector machines: theory and applications. Berlin: Springer; 2005.

28. Quinn P, Kerin JF, Warnes GM. Improved pregnancy rate in human in vitro fertilization with the use of a medium based on the composition of human tubal fluid. Fertil Steril 1985; 44:493-498.

29. Byers SL, Payson SJ, Taft RA. Performance of ten inbred mouse strains following assisted reproductive technologies (ARTs). Theriogenology 2006; 65:1716-1726.

30. Miki K, Qu W, Goulding EH, Willis WD, Bunch DO, Strader LF, Perreault SD, Eddy EM, O'Brien DA. Glyceraldehyde 3-phosphate dehydrogenase-S, a sperm-specific glycolytic enzyme, is required for sperm motility and male fertility. Proc Natl Acad Sci U S A 2004; 101:16501-16506.

31. Chih-Chung Chang and Chih-Jen Lin Lalfsvm, 2001. Software available at http://www.csie.ntu.edu.tw/~cjlin/libsvm

32. Goodson SG, O'Brien, DA, Zhang, Z, Tsuruta, JK, Wang, W, (inventors) The United States of American as represented by the University of North Carolina at Chapel Hill, assignee. Sperm Motility Analyzer and Related Methods. U.S. Patent Application 61/409,688; 2010.

33. Cohen J. A coefficient of agreement for nominal scales. Educational and Psychological Measurement 1960; 20:37-46.

34. Robertson L, Wolf DP, Tash JS. Temporal changes in motility parameters related to acrosomal status: identification and characterization of populations of hyperactivated human sperm. Biol Reprod 1988; 39:797-805.

35. Mortimer ST, Mortimer D. Kinematics of human spermatozoa incubated under capacitating conditions. J Androl 1990; 11:195-203.

36. Lee MA, Storey BT. Bicarbonate is essential for fertilization of mouse eggs: mouse sperm require it to undergo the acrosome reaction. Biol Reprod 1986; 34:349-356.

37. Boatman DE, Robbins RS. Bicarbonate: carbon-dioxide regulation of sperm capacitation, hyperactivated motility, and acrosome reactions. Biol Reprod 1991; 44:806-813.

38. Visconti PE, Bailey JL, Moore GD, Pan D, Olds-Clarke P, Kopf GS. Capacitation of mouse spermatozoa. I. Correlation between the capacitation state and protein tyrosine phosphorylation. Development 1995a; 121:1129-1137.

39. Shao M, Ghosh A, Cooke VG, Naik UP, Martin-DeLeon PA. JAM-A is present in mammalian spermatozoa where it is essential for normal motility. Dev Biol 2008; 313:246-255.

40. Wang RS, Ohtani K, Suda M, Kitagawa K, Nakayama K, Kawamoto T, Nakajima T. Reproductive toxicity of ethylene glycol monoethyl ether in Aldh2 knockout mice. Ind Health 2007; 45:574-578.

41. Burkman LJ. Characterization of hyperactivated motility by human spermatozoa during capacitation: comparison of fertile and oligozoospermic sperm populations. Arch Androl 1984; 13:153-165.

42. Young RJ, Bodt BA, Heitkamp DH. Action of metallic ions on the precocious development by rabbit sperm of motion patterns that are characteristic of hyperactivated motility. Mol Reprod Dev 1995; 41:239-248.

43. Suarez SS, Katz DF, Owen DH, Andrew JB, Powell RL. Evidence for the function of hyperactivated motility in sperm. Biol Reprod 1991; 44:375-381.

44. Chesler EJ, Miller DR, Branstetter LR, Galloway LD, Jackson BL, Philip VM, Voy BH, Culiat CT, Threadgill DW, Williams RW, Churchill GA, Johnson DK, et al. The Collaborative Cross at Oak Ridge National Laboratory: developing a powerful resource for systems genetics. Mamm Genome 2008; 19:382-389.

45. Danshina PV, Geyer CB, Dai Q, Goulding EH, Willis WD, Kitto GB, McCarrey JR, Eddy EM, O'Brien DA. Phosphoglycerate kinase 2 (PGK2) is essential for sperm function and male fertility in mice. Biol Reprod 2010; 82:136-145.

46. Carlson AE, Quill TA, Westenbroek RE, Schuh SM, Hille B, Babcock DF. Identical phenotypes of CatSper1 and CatSper2 null sperm. J Biol Chem 2005; 280:32238-32244.

47. Elangovan N, Chiou TJ, Tzeng WF, Chu ST. Cyclophosphamide treatment causes impairment of sperm and its fertilizing ability in mice. Toxicology 2006; 222:60-70.

48. Bone W, Jones AR, Morin C, Nieschlag E, Cooper TG. Susceptibility of glycolytic enzyme activity and motility of spermatozoa from rat, mouse, and human to inhibition by proven and putative chlorinated antifertility compounds in vitro. J Androl 2001; 22:464-470.

CHAPTER 3

METABOLIC SUBSTRATES EXHIBIT DIFFERENTIAL EFFECTS ON FUNCTIONAL PARAMETERS OF MOUSE SPERM CAPACITATION

Abstract

Glycolysis is critical for sperm function since mice deficient in sperm-specific glycolytic enzymes are infertile due to marked defects in both ATP production and motility, while mice lacking functional mitochondria retain fertility. Despite the evidence of the importance of glycolysis in sperm capacitation, there are reports that sperm motility in several species can be supported by substrates that are not metabolized through this pathway. However, those studies did not determine if motility characteristics or other aspects of sperm function were supported. To better understand the roles of glycolysis and other metabolic pathways in supporting sperm function, we conducted quantitative studies to determine the metabolic requirements of mouse sperm throughout a 2 h in vitro capacitation period by measuring ATP, motility, and motility patterns. We also assessed sperm capacitation by tyrosine phosphorylation. Our results indicate that sperm are capable of metabolizing both glycolytic and non-glycolytic substrates but that glycolysis is required to support the full spectrum of events associated with sperm fertilizing ability. Analyses of selected substrates in the presence of metabolic inhibitors reveals that sperm incubated in medium containing fructose are capable of hyperactivation when their

mitochondria are uncoupled. We demonstrated that glucose support of hyperactivation is a function of its active utilization. Finally, metabolic profiles of sperm metabolizing glucose or fructose and detected differences in metabolites with antioxidant functions, perhaps accounting for the ability of CCCP to restore hyperactivation in the presence of fructose.

Introduction

During epididymal maturation, sperm acquire the ability to achieve progressive motility and to bind the zona pellucida [1]. However, sperm are not considered functionally mature until they have resided for a time in the female reproductive tract or in defined media mimicking this environment. During this time, sperm undergo a set of biochemical changes rendering them competent for fertilization [2]. These events, collectively termed capacitation, include the ability to undergo the acrosome reaction and to achieve hyperactivated motility. In order for capacitation to occur, sperm must initiate the appropriate signaling pathways, including PKA-dependent tyrosine phosphorylation of specific proteins and the inhibition of specific protein phosphatases [3, 4].

Both mitochondrial respiration and glycolysis are active in sperm. While oxidative phosphorylation yields more ATP per molecule of glucose, studies indicate that sperm from different species show variable dependency on mitochondrial function to drive functional processes [5-8]. For example, bull sperm have highly active mitochondria, whereas mitochondria from mouse sperm are less efficient [9]. A great deal of conflicting literature exists on the importance of oxidative phosphorylation versus

glycolysis in supporting ATP and other sperm functions in human sperm. While some reports demonstrate that mitochondrial substrates can support ATP and motility, others suggest that glycolysable substrates are needed [7, 10-12].

Sperm glycolysis has several unique features that differentiate it from glycolysis in somatic cells. The glycolytic machinery is compartmentalized to the principal piece of the sperm flagellum, whereas the mitochondria are localized to the midpiece in sperm [13]. Glyceraldehyde phosphate dehydrogenase (GAPDHS), phosphoglycerate kinase 2 (PGK2), and lactate dehydrogenase C (LDHC) are all germ cell-specific enzymes [14-17]. In addition, sperm express three germline-specific isoforms of aldolase [18, 19]. Other sperm glycolytic enzymes display unique structural and functional properties [20, 21].

Sperm mitochondria also have novel properties. The mitochondria are surrounded by protein structures known as capsules [22]. Both the testis-specific cytochrome c and succinyl-CoA transferase are encoded by genes expressed only during spermatogenesis [23, 24]. In addition, some proteins typically confined to the mitochondria have been detected in extramitochondrial locations in sperm. The pyruvate dehydrogenase (PDH) complex has been localized in the principal piece in hamster sperm, where it has been shown to undergo capacitation-associated tyrosine phosphorylation [25, 26]. Voltage-dependent anion channels (VDAC) VDAC2 and VDAC3 have also been found extramitochondrially in association with outer dense fibers in the sperm flagellum [27]. These findings suggest that sperm may possess unique metabolic pathways and interactions not found in somatic cells.

Mouse sperm is an ideal model system for the study of human sperm function, since mitochondrial function in both species is less efficient and glycolytic rates are high. A great deal of evidence supports the importance of glycolysis in sperm function in mice. Knockout mouse models disrupting distinct sperm glycolytic isozymes exhibit severe reproductive defects due to abnormal sperm motility, whereas a knockout mouse lacking testis-specific cytochrome is fertile [28-31]. Moreover, studies have demonstrated that glycolysable substrates are required to support events such as capacitation-associated tyrosine phosphorylation, hyperactivation, and penetration of the zona pellucida [32-35]. While many reports provide evidence for the role of glycolysable substrates in supporting sperm function, nonglycolysable substrates have also been shown to support sperm ATP and motility [8, 11, 36, 37]. However, these experiments were performed under a variety of conditions and did not investigate multiple parameters of sperm function, such as hyperactivation and capacitation.

In order to understand the energy pathways involved in sperm ATP production and motility and to investigate potential novel sperm metabolic pathways and regulatory mechanisms, we conducted a comprehensive analysis of the impact of glycolysable and nonglycolysable substrates on sperm functional parameters over an in vitro capacitation period. We monitored sperm energy production, capacitation-associated tyrosine phosphorylation, and motility. To understand the changes in the types of motility, including hyperactivation, in the presence of single substrates, we conducted multiclass motility analysis using CASAnova, a tool developed to describe changes in sperm motility more precisely [38]. A subset of these substrates were selected for investigations of their metabolism in the presence of an inhibitor of glycolysis and an uncoupler of

oxidative phosphorylation. We explored intrinsic differences in the effects of fructose and glucose on sperm hyperactivation, and have obtained metabolic profiles of sperm incubated in the presence of these substrates.

Materials and Methods

Reagents

Reagents for media preparation and sperm functional analyses were purchased from Sigma-Aldrich (St. Louis, MO) with the exception of sodium chloride, glucose, Tris, EDTA, sodium dodecyl sulfate, glycerol, TCEP reducing agent and Tween 20 (Thermo Fisher Scientific, Waltham, MA), sodium pyruvate (Invitrogen, Carlsbad, CA), sodium bicarbonate (EM Science, Gibbstown, NJ), potassium chloride, magnesium sulfate heptrahydrate, and potassium phosphate (Mallinckrodt Chemical, Phillipsburg, NJ), and penicillin/streptomycin solution (Gemini Bioproducts, West Sacramento, CA).

For mass spectrometry analyses, methanol (Optima LC-MS), acetonitrile (Optima LC-MS), water (Optima LC/MS), hexane, chloroformate and methanol (HPLC grade) were purchased from Thermo Fisher Scientific. Methoxyamine HCl, bis(trimethylsilyl)trifluoroacetamide (BSTFA, with 1% trimethylchlorosilane, TMCS) and alkanes C10-C40 were purchased from Sigma-Aldrich.

Animals

Adult CD1 male mice were purchased from Charles River Laboratories (Raleigh, NC) and allowed to acclimatize before use. All procedures involving mice were approved in advance by the Institutional Animal Care and Use Committee of the University of North Carolina at Chapel Hill.

Sperm In Vitro Capacitation

All sperm incubations were performed in HTF medium, shown to support both mouse and human in vitro fertilization [39, 40]. HTF complete medium consists of 101.6 mM NaCl, 4.7 mM KCL, 0.37 mM KH_2PO_4, 0.2 mM $MgSO_4 \cdot 7H_2O$, 2 mM $CaCl_2$, 25 mM $NaHCO_3$, 5 mg/ml BSA, 100U penicillin G, 0.1 mg streptomycin, 2.78 mM glucose, 0.33 mM pyruvate, and 21.4 mM lactate, pH 7.4. Bicarbonate-free HTF replaced 25 mM sodium bicarbonate with 21 mM HEPES. For experiments without energy substrates, glucose, lactate, and pyruvate were omitted. To assess the efficacy of both glycolysable and non-glycolysable substrates to support capacitation, HTF media were prepared with individual substrates at appropriate concentrations. For all media, the osmolality was adjusted to ~315 mOsm/kg with 5M NaCl using a Model 3300 micro-osmometer (Advanced Instruments, Norwood, MA.)

Sperm were collected from the cauda epididymides of sexually mature (>8 weeks) mice. Each cauda was carefully trimmed to remove adipose and other tissue, rinsed in PBS (140 mM NaCl, 3mM KCl, 4 mM $NaH_2PO_4 \cdot 7H_2O$, 1.4 mM KH_2PO_4, pH 7.4), and placed in 1 ml HTF medium lacking bicarbonate and energy substrates. Four to six cuts were made in each cauda using iris scissors, and sperm were released into the medium by

incubation for 10 min at 37° C under 5% CO_2 and air. The tissue was removed and the suspension was mixed gently by swirling. A 10 μl aliquot was reserved for calculating sperm concentration for ATP and western blot analysis.

Control samples were diluted at least 1:10 in HTF complete medium and incubated for 2 h at 37°C under 5% CO_2 and air, conditions that support sperm capacitation. Other samples were diluted similarly in HTF media containing 25mM bicarbonate and individual test substrates. Multiple substrates were tested on sperm from each mouse. At appropriate time points, aliquots of sperm suspensions were taken for analyses of sperm motility, ATP levels, and tyrosine phosphorylation.

Sperm Viability

Sperm viability was measured after incubating for 2 h in HTF medium with appropriate substrates. Aliquots were taken and propidium iodide was added to a final concentration of 12 μM. Viability was determined by counting at least 100 cells for each condition and determining the proportion of membrane-intact sperm that exclude this DNA intercalating agent.

Sperm Motility

Cauda epididymal sperm were diluted 1:20 to 1:60 with HTF media containing appropriate substrates to a concentration (typically 2-4 x 10^5 sperm/ml) that yields ~50 sperm per microscope field for motility assessment by computer assisted sperm analysis

(CASA). Motility was assessed at 30 min intervals throughout the 2 h in vitro capacitation period. Initial time points for each condition were completed within two minutes of dilution. Quantitative parameters of sperm motility were recorded by CASA using the CEROS sperm analysis system (software version 12.3, Hamilton Thorne Biosciences, Beverly, MA). The CEROS system includes an Olympus CX41 microscope equipped with a MiniTherm stage warmer and a Sony model XC-ST50 CCD camera. Sperm tracks (1.5 sec) were captured at 37^{o}C with a 4x negative phase contrast objective and a frame acquisition rate of 60 Hz. The default Mouse 2 analysis settings provided by Hamilton-Thorne were used, except that 90 frames were recorded and slow cells were counted as motile. Motile sperm tracks were also required to have a minimum of 45 points. For each motility measurement, a 25 μl aliquot of sperm suspension was loaded by capillary action using a large bore pipet tip into one chamber of a 100 μm-deep Leja slide (Leja, The Netherlands). Excess liquid was blotted with a laboratory tissue, and loading was examined to ensure the absence of air in the chamber. At least 10 fields were recorded for each sample analyzed, with tracks and kinetic parameters saved for individual sperm in each field. Individual database text (DBT) files were generated from the CASA images and used to generate motility profiles using CASAnova software (http://www.csbio.unc.edu/CASAnova/) [38].

Sperm ATP Levels

Sperm were diluted at least 1:10 from epididymal suspensions and incubated for 2 h in HTF with appropriate substrates. At relevant time points, sperm samples were

swirled gently and triplicate 50 μl aliquots were removed and diluted into individual tubes containing 450 μl hot Tris-EDTA buffer (0.1M Tris-HCl, 4 mM EDTA, pH 7.75). The resulting suspensions were boiled for 5 min and then frozen in liquid nitrogen. Upon thawing, each sample was centrifuged at 15,000 x g for 5 min at room temperature. A 20 μl aliquot of the supernatant was mixed with 80 μl water, and then 50 μl were utilized for quantifying ATP. ATP content was determined using the ATP Bioluminescence Assay Kit CLS II (Roche Applied Science, Indianapolis, IN) according to the manufacturer's protocol.

Capacitation-associated Tyrosine Phosphorylation

To assess the status of sperm tyrosine phosphorylation during capacitation, sperm were diluted at least 1:10 from epididymal suspensions into HTF media containing various substrates. One ml aliquots were removed from each test medium at time 0 and 2 h and centrifuged at 1,000 x g for 3 min. The supernatant was removed and the sperm pellet was resuspended in 1ml PBS and then centrifuged briefly at 10,000 x g. After removing the supernatant, the pellet was resuspended in 2X sample buffer (4.6% SDS, 125 mM Tris pH 6.8, 18% glycerol, 1% bromophenol blue, 50 mM TCEP) and boiled for 5 min. Equivalents of 10^6 sperm per sample were resolved by SDS-PAGE on 10% polyacrylamide gels, and tyrosine phosphorylation was detected using the anti-phosphotyrosine 4G10 monoclonal antibody (Millipore, Billerica, MA) as described [41] with minor modifications. Briefly, blots were blocked overnight at 4^oC in PBS + 0.1% Tween 20 (PBST) and 5% fish gelatin and then incubated for 1h at room temperature

with 4G10 diluted 1:5,000 in PBST with 5% fish gelatin. Blots were washed 3 times with PBST for 5 min each and then incubated for 30 min at room temperature with horseradish peroxidase-conjugated goat-anti-mouse secondary antibody (KPL, Gaithersburg, Maryland) diluted 1:30,000 in PBST with 5% fish gelatin. Blots were washed in 2 changes of PBST for 1h each before detection of chemiluminescence using Supersignal West Pico (Pierce, Rockford, IL).

Analysis of Sperm Function in the Presence of Metabolic Inhibitors

To determine the effect of inhibition of metabolic pathways on sperm function, epididymal sperm were isolated as describe above and incubated with HTF media containing single substrates supplemented with either 10 mM α-chlorohydrin (ACH, supplied as 3-chloro-1,2-propanediol), 10 μM carbonyl cyanide 3-chlorophenylhydrazone (CCCP), or DMSO as a vehicle control. Aliquots were taken at time 0 and 90 min for analysis of ATP levels, determination of percent motility by CASA, and analysis of motility profiles generated with CASAnova.

Substrate Pre-incubation Experiments

Cauda epididymal sperm were isolated in bicarbonate-free, substrate-free HTF as described above. Sperm were diluted 1:10 in 6 ml HTF medium containing either 2.78 mM glucose or 5 mM fructose and incubated for 30 min at 37^{o}C under 5% CO_2 in air. Each suspension was then diluted to 30 ml with substrate-free HTF, divided in half and

centrifuged at 500 x g for 10 min at room temperature. Each sperm pellet was washed again with 5 ml substrate-free HTF and centrifuged at 1,000 x g for 5 min. The supernatant was removed and sperm were gently resuspended in the remaining liquid (approximately 150 μl). The sperm suspension was then evenly divided into 1ml of HTF media containing 2.78 mM glucose, 5 mM fructose, or no substrates. Sperm were incubated at 37^{o}C under 5% CO_2 in air for 30 min before taking aliquots for CASA analysis. Additional time points were taken at 60 and 90 min after resuspension with substrates. The percent of sperm undergoing hyperactivation was determined from motility profiles generated by CASAnova.

Preparation of Sperm for Metabolomic Analyses following Incubation with Glucose or Fructose

Sperm samples for metabolomic analyses were pooled from 6 CD1 mice after isolation in substrate-free HTF (1 ml/cauda) as described above. The sperm suspension was mixed by gently swirling, diluted to 100 ml with PBS and centrifuged at 1,000 x g for 10 minutes. The pellets were resuspended in residual PBS, divided equally into 25 ml HTF + 2.78 mM glucose or 25 ml HTF + 5 mM fructose and incubated for 90 min at 37^{o}C under 5% CO_2 in air. At the end of the incubation period, each sperm suspension was diluted to 50 ml with ice cold PBS to quench metabolic reactions and centrifuged at 1,000 x g for 10 min at 4^{o}C. After removing the supernatant, the pellet was transferred to a 1.5 ml microfuge tube and diluted to 1 ml with ice-cold PBS. The pellets were resuspended by gentle mixing and 10 μl was reserved for sperm counting. Suspensions

were spun briefly at high 14,000 x g to pellet, the supernatants were removed, and pellets were snap frozen in liquid nitrogen and stored at -80^{o}C until processing.

Sperm pellets from different experiments were combined to yield a minimum of 45 x 10^{6} sperm per sample. A total of 8 pools for each substrate were analyzed, comparing sperm from the same mice after incubation with glucose or fructose. Sperm metabolites were extracted from each pellet using 500 µl ice-cold methanol-chloroform (ratio 2:1). The mixture was added to sperm pellets on ice, and pellets were resuspended and briefly sonicated. Samples were incubated for 30 min on ice and briefly sonicated again prior to the addition of 500 µl of a 1:1 chloroform-water mixture. After mixing by vortexing, samples were centrifuged at 15,000 x g for 20 min. Aqueous and organic phases were separated into glass crimp top vials (Agilent, Santa Clara, CA) and stored at -80^{o}C. Samples were shipped on dry ice to the North Carolina Research Campus (Kannapolis, NC) for analysis.

Metabolomic Analysis by High Performance Liquid Chromatography Time-of-flight Mass Spectrometry (HPLC-TOFMS)

Aqueous and organic layers from sperm samples were vacuum dried in the same vial at room temperature. The dried samples were reconstituted in 150 µl of methanol: water (80:20, v/v) and filtered through 0.20 µm membrane (Millipore, Bedford, MA) for HPLC-TOFMS analysis.

An Agilent HPLC 1200 system equipped with a binary solvent delivery manager and a sample manager (Agilent Corporation, Santa Clara, CA, USA) was used, with

chromatographic separations performed on a 4.6 × 150 mm 5µm Agilent ZORBAX Eclipse XDB-C18 chromatography column. The LC elution conditions were optimized as follows: isocratic at 1% B (0–0.5 min), linear gradient from 1% to 20% B (0.5-9.0 min), 20-75% B (9.0-15.0 min), 75-100% B (15.0-18.0 min), isocratic at 100% B (18–19.5 min); linear gradient from 100% to 1% B (19.5-20.0 min) and isocratic at 1% B (20.0–25.0 min). Here, A = water with 0.1% formic acid and B = acetonitrile with 0.1% formic acid. The column was maintained at 30°C. A 10 µl aliquot sample was injected onto the column. Mass spectrometry was performed using an Agilent model 6220 MSD TOF mass spectrometer equipped with a dual sprayer electrospray ionization (ESI) source (Agilent Corporation, Santa Clara, CA, USA). The system was tuned for optimum sensitivity and resolution using an Agilent ESI-L low concentration tuning mix in both positive (ES+) and negative (ES-) electrospray ionization modes. Agilent API-TOF reference mass solution kit was used to obtain accurate mass time-of-flight data in both positive and negative mode operation. The TOF mass spectrometer was operated with the following optimized conditions: (1) ES+ mode, capillary voltage 3500 V, nebulizer 45 psig, drying gas temperature 325 °C, drying gas flow 11 L/min, and (2) ES- mode, similar conditions as ES+ mode except the capillary voltage was adjusted to 3000 V. The TOF mass spectrometer was calibrated routinely in ES+ and ES- modes using the Agilent ESI-L low concentration tuning mix. During metabolite profiling experiments, both plot and centroid data were acquired for each sample from 50 to 1,000 Da over a 25 min analysis time.

The resulting data files were centroided, deisotoped, and converted to mzData xml files using the MassHunter Qualitative Analysis Program (vB.03.01, Agilent).

Following conversion, xml files were analyzed using the open source XCMS package (v1.24.1) (http://metlin.scripps.edu), which runs in the statistical package R (v.2.12.1, http://www.r-project.org), to pick, align, and quantify features (chromatographic events corresponding to specific *m/z* values and retention times). The software was used with default settings as described (http://metlin.scripps.edu) except for xset (bw = 5) and rector (plottype = "m", family = "s"). The created .tsv file was opened using Excel software and saved as an excel file. The resulting data sheet was used for the further analysis.

Metabolomic Analysis by Gas Chromatography Time-of-flight Mass Spectrometry (GC-TOFMS)

After LC-MS analysis, all liquid from each sample was transferred into a glass vial and vacuum dried at room temperature. The residue was derivatized using a two-step procedure. First, 80 µl methoxyamine (15 mg/ml in pyridine) was added to the vial and kept at 30°C for 90 minutes. After the addition of 10µl retention index compounds (the mixture of C10-C40, 50µg/ml) and 80 µL BSTFA (1%TMCS) to the reaction vials, the samples were subjected to a 70°C derivatization reaction for 120 minutes.

Each 1 µl aliquot of derivatized solution was injected in splitless mode into an Agilent 7890N gas chromatograph coupled with a Pegasus HT time-of-flight mass spectrometer (Leco Corporation, St Joseph, USA). Separation was achieved on a DB-5 ms capillary column (30 m × 250 µm I.D., 0.25-µm film thickness; Agilent J&W Scientific, Folsom, CA, USA), with helium as the carrier gas at a constant flow rate of 1.0 ml/min. The temperature of injection, transfer interface, and ion source were set to

260°C, 260°C, and 210°C, respectively. The GC temperature programming was set to 2 min isothermal heating at 80°C, followed by 10°C/min oven temperature ramps to 220 °C, 5 °C/min to 240°C, and 25°C/min to 290 °C, and a final 8 min maintenance at 290°C. Electron impact ionization (70 eV) at full scan mode (m/z 40-600) was used, with an acquisition rate of 20 spectra/second in the TOFMS setting. The acquired data were analyzed by ChromaTOF software (v4.22, Leco Co., CA, USA). Internal standards and any known artificial peaks, such as peaks caused by noise, column bleed and BSTFA derivatization procedure, were removed from the data set. Compound identification was performed by comparing the mass fragments with NIST 05 Standard mass spectral databases in NIST MS search 2.0 (NIST, Gaithersburg, MD) software with a similarity of more than 70% and verified by available reference compounds.

Statistical Analysis

Statistical analyses were performed using GraphPad Prism 5 (Graphpad Software, La Jolla, CA). All data are shown as mean ± SEM. Statistical significance was determined using either two-tailed unpaired t-tests or by one-way ANOVA after arcsine transformation of percentages. Differences were considered significant if $P < 0.05$.

Results

Effects of Eliminating Endogenous Substrates on Sperm ATP Levels and Motility

Several studies have shown that HTF complete medium (containing 2.78 mM glucose, 21.4 mM lactate, and 0.33 mM pyruvate as energy substrates) supports tyrosine phosphorylation, hyperactivation and other changes required for successful in vitro fertilization in multiple species [39, 40]. In our metabolic studies, sperm from individual mice were divided into multiple aliquots so that functional parameters in each test medium were compared directly with those in HTF complete medium. Sperm were assessed every 30 min over a 2 h time course for total ATP content, percent motility, and the distribution of multiple patterns of motility.

To minimize the influence of endogenous substrates on our analyses, initial experiments determined conditions that reduce epididymal substrates to levels that do not sustain sperm ATP. When sperm were collected in 1 ml/cauda substrate-free HTF and further diluted at least 1:10 in the same medium, the mean ATP content fell to 12% of the initial level (2.89 ± 0.33 nmoles per 10^7 sperm) within 30 min (Fig. 1A). ATP declined further throughout the incubation period, reaching mean values <5% of initial levels by 60 min. In contrast, mean ATP content was 4.20 ± 0.14 nmoles/10^7 sperm immediately after dilution into HTF complete medium and was maintained at >65% of this level throughout the 2 h incubation. Subsequent experiments evaluating single substrates used this same dilution strategy to minimize the contribution of epididymal energy substrates.

In parallel with ATP measurements, CASA was used to determine the effects of omitting substrates on sperm motility. In HTF complete medium 50 - 60% of sperm remained motile throughout the 2 h capacitation interval (Fig. 1B). Initial percentages of motile sperm in the absence of substrates were comparable to those in HTF complete medium. However, the mean percentage of motile sperm in substrate-free HTF declined

significantly after 60 min and reached levels <5% by 90 min. In the absence of added substrates, sperm ATP levels fell more rapidly than percent motility, suggesting possible reductions in vigorous motility under these conditions.

We used CASAnova, a recently developed method for quantitative analyses of mouse sperm motility [38]to assess this possibility (Fig. 1C-E). CASA tracks and DBT files for sperm analyzed in Fig. 1B were used to compare motility profiles in substrate-free HTF with those observed in HTF complete medium. CASAnova assesses parameters of individual sperm tracks and assigns each sperm to vigorous (progressive, intermediate, and hyperactivated) or non-vigorous (slow, and weakly motile) categories of motility. Analysis of percent hyperactivation during incubation in HTF complete medium showed a steady increase in hyperactivated sperm, reaching mean values of 24.0 ± 4.3% after 90 min (Fig. 1C). No appreciable hyperactivation was observed at any time point when sperm were incubated in substrate-free HTF. Furthermore, comparison of all CASAnova categories reveals the rapid loss of all vigorous motility when substrates are omitted. As in previous studies [38], sperm in HTF complete medium exhibited a transition from predominantly progressive at time 0 to other vigorous (intermediate and hyperactivated) and non-vigorous (slow and weakly motile) patterns of motility during capacitation (Fig. 1D). Sperm incubated in substrate-free HTF had a reduced percentage of progressive sperm and more slow sperm at the initial time point (Fig. 1E). Moreover, greater than 99% of the motile population in substrate-free HTF was classified as non-vigorous after 30 min and in the weakly motile category by the end of the 2 h time course. These results confirm the importance of examining changes in the types of sperm motility, rather than

the overall percentage of motile sperm, when assessing the efficacy of metabolic substrates in supporting functional changes required for fertilization.

Effects of Single Substrates on Sperm Motility Parameters

Four glycolysable substrates (glucose, mannose, fructose, and sorbitol) and four non-glycolysable substrates (lactate, pyruvate, D-β-hydroxybutyrate (DHB), and citrate) were tested to determine their effects on motility transitions during capacitation. Sperm from at least four mice were tested with each substrate, with direct comparisons of each medium to HTF complete medium. Glucose (2.78 mM), lactate (21.4 mM), and pyruvate (0.33 mM) were initially tested at the concentrations in HTF complete medium [40]. Other substrates were tested at concentrations shown previously to support sperm motility and other aspects of capacitation, including 5 mM mannose, 5 mM fructose, 5 mM sorbitol, 5 mM DHB (5 mM) and 10 mM citrate [7, 36, 37, 42-45]. We also tested glucose, lactate, pyruvate and citrate at 5 mM concentrations, but found that changing the concentration did not have significant effects on the sperm motility parameters described below (data not shown).

Motility profiles were first compared for the four substrates metabolized through the glycolytic pathway (Fig. 2). When sperm were incubated in HTF with glucose, mannose, fructose or sorbitol for 2 h, there were no statistically significant differences in percent motility assessed by CASA compared to HTF complete medium (Fig. 2A). However, we did observe decreases in motility of ~30% in half the samples incubated with fructose. CASAnova was used to classify the motility profiles of sperm analyzed in

Fig. 2A. HTF with 2.78 mM glucose or 5 mM mannose supported hyperactivation at mean levels that were comparable or higher than those supported by HTF complete medium (Fig. 2B). Sperm incubated with 5 mM fructose as the sole energy substrate displayed significantly lower levels of hyperactivation throughout the incubation. Although 5 mM sorbitol supported a short burst of hyperactivation 30 min after addition of substrate, the mean percentage of hyperactivated motility decreased steadily thereafter, generating a time course of hyperactivation markedly different from the HTF complete control.

Complete CASAnova motility profiles were compared at 90 min, the time point where levels of hyperactivated motility typically begin to plateau (Fig. 2C). The mean percentages of vigorous (progressive, intermediate and hyperactivated) and non-vigorous (slow and weakly motile) motility patterns in HTF with glucose or mannose were comparable to those seen in HTF complete medium. Sperm incubated in HTF with fructose displayed higher levels of progressive motility at 90 min, suggesting that sperm retain the progressive pattern of motility for longer periods when hyperactivation is inhibited. Unlike other glycolysable substrates tested, sorbitol did not sustain vigorous motility patterns throughout the incubation period. Greater than 93% of motile sperm were classified as non-vigorous after 90 min incubation in HTF with sorbitol.

We also assessed the ability of non-glycolysable substrates (lactate, pyruvate, DHB, and citrate) to support sperm motility. In HTF with pyruvate or lactate, approximately half the mice tested showed a 25% decrease in the percentage of motile sperm over time. However, we found no statistical significant reductions in percent motility compared to HTF complete medium when sperm were incubated in HTF with

0.33 mM pyruvate, 21.4 mM lactate or 5 mM DHB, except at the 60 min time point with pyruvate (Fig. 3A). In contrast, percent motility declined significantly after incubation in HTF with 10 mM citrate for 60 min and reached mean levels of ~20% by the end of the incubation period. The viability of sperm in HTF with citrate at this time point was comparable to HTF complete medium (means ≥ 54% in both media), indicating that the reduction in percent motility did not result from a loss of cell viability.

None of the non-glycolysable substrates supported hyperactivation at the levels observed in HTF complete (Fig. 3B). When the motility profiles of sperm analyzed in Fig. 3A were classified by CASAnova, hyperactivation reached maximum mean levels of 6.1% after 60 min with pyruvate, 5.3% after 120 min with lactate, and 4.5% after 90 min with DHB. Within 2 min of dilution into HTF medium containing citrate, a small but significant portion of sperm displayed hyperactivated motility (mean = 8.0% vs. 2.36% in HTF compete medium). However, hyperactivation was not observed at all subsequent time points in this medium. We also compared complete CASAnova motility profiles after incubation for 90 min with different non-glycolysable substrates (Fig. 3C). Although hyperactivated motility was significantly lower in HTF with pyruvate, lactate or DHB, these substrates maintained progressive motility at comparable or higher mean levels than HTF complete medium. Of the low percentage of sperm (mean = 30.4%) that remained motile after 90 min of incubation in HTF with citrate, >99% were classified in the non-vigorous categories of slow or weakly motile.

Our basic CASA analyses demonstrated that all single substrates examined, except citrate, supported comparable percentages of sperm motility. CASAnova analysis of sperm motility profiles revealed additional differences in the ability of these substrates

to support capacitation-associated changes in sperm motility. Vigorous motility was not supported by sorbitol or citrate, and hyperactivation was fully supported by only glucose and mannose.

Effects of Single Substrates on Capacitation-associated Tyrosine Phosphorylation

Sperm capacitation is correlated with the tyrosine phosphorylation of a distinct subset of proteins [46], previously reported to occur at highest levels in the presence of glucose [45, 47]. We incubated sperm for 2 h in HTF with single substrates and examined tyrosine phosphorylation patterns by Western blotting using the phosphotyrosine-specific antibody 4G10. Three glycolysable substrates (glucose, mannose and fructose) supported the full, robust tyrosine phosphorylation pattern seen in HTF complete medium (Fig. 4A). However, sorbitol did not support capacitation-dependent tyrosine phosphorylation, even though sorbitol dehydrogenase present in mouse sperm flagella [45] should convert this monosaccharide to fructose.

We observed more variability in the tyrosine phosphorylation patterns of sperm incubated in media containing nonglycolysable substrates (Fig. 4B). DHB supported the full pattern of tyrosine phosphorylation at a similar intensity to HTF complete medium in 4 of 6 replicate experiments. Both lactate and pyruvate supported tyrosine phosphorylation patterns that were comparable to HTF complete medium, except for the absence of a phosphorylated doublet with apparent molecular weights of 84,000 and 88,000 (arrows). We occasionally observed phosphorylation of these bands when sperm were incubated with lactate or pyruvate, although the signal was much weaker than that

seen with the positive control. Citrate did not support capacitation-dependent tyrosine phosphorylation.

Effects of Inhibitors of Glycolysis and Mitochondrial Function on Sperm ATP Levels and Motility

Our studies indicate that both glycolysable and non-glycolysable substrates can maintain sperm motility throughout 2 h in vitro incubation periods, and that both types of substrates support at least partial capacitation-dependent tyrosine phosphorylation. However, individual substrates within these two categories have variable capacities to sustain motility or support the molecular and physiological changes associated with sperm capacitation. To assess these substrate differences in more detail, we assayed sperm ATP and motility parameters in the presence of the glycolytic inhibitor α-chlorohydrin (ACH, Fig. 5) or carbonyl cyanide 3-chlorophenylhydrazone (CCCP), an uncoupler of oxidative phosphorylation (Fig. 6). These experiments compared two glycolysable substrates (glucose and fructose) that varied in their ability to support hyperactivation and two nonglycolysable substrates (pyruvate and DHB) that varied in their ability to support capacitation-dependent tyrosine phosphorylation.

We first monitored ATP levels throughout 2 h in vitro capacitation intervals and found no statistically significant differences between sperm incubated in HTF with any single substrate and sperm incubated in HTF complete medium (data not shown). We then tested the ability of these substrates to support ATP and motility in the presence of 10 mM ACH or DMSO as a vehicle control. As anticipated, ATP levels of sperm

incubated with glycolysable substrates (2.78 mM glucose or 5 mM fructose) were dramatically reduced after 90 min incubation in the presence of ACH (Fig. 5A). The percentage of motile sperm also declined under these conditions, although the reduction was not significant with fructose as the sole substrate (Fig. 5B). However, examination of CASAnova motility profiles demonstrates that >90% of motile sperm incubated with glucose (Fig. 5C) or fructose (Fig. 5D) were classified as weakly motile when glycolysis was inhibited by the addition of ACH.

When sperm were incubated with non-glycolysable substrates (0.33 mM pyruvate or 5 mM DHB), the addition of ACH caused no significant changes in ATP levels (Fig. 5A) or percent motility (Fig. 5B). Motility profiles of sperm incubated in DHB + ACH were also unaltered compared to the vehicle control (Fig. 5F). However, there was a significant increase in the percentage of weakly motile sperm after incubation for 90 min in pyruvate + ACH, suggesting that inhibition of sperm glycolysis has an impact on pyruvate metabolism.

Analysis of CASAnova motility profiles also revealed unexpected differences when sperm were incubated for 90 min with single substrates in the presence of CCCP. As expected, this uncoupling agent reduced both ATP levels (Fig. 6A) and percent motility (Fig. 6B) to near zero levels when added to sperm incubated with pyruvate or DHB, substrates typically metabolized in the mitochondria. Sperm that retained motility under these conditions were classified as weakly motile (Fig. 6 E, F). ATP levels and percent motility were unaffected when CCCP was added to sperm incubated with glycolysable substrates (glucose or fructose, Figs. 6A, B). When motility profiles were compared, sperm incubated in glucose + CCCP displayed only small, but significant,

reductions in the mean percentages of progressive and intermediate motility patterns (Fig. 6C). The addition of CCCP to sperm incubated with fructose caused more substantial shifts in motility profiles. The mean percentage of hyperactivated sperm increased to 30% in fructose + CCCP (Fig. 6D), comparable to the levels achieved with glucose, mannose or HTF complete medium. This change was accompanied by decreased progressive and increased non-vigorous motility profiles, similar to the motility transitions observed during capacitation in HTF compete medium (Fig. 1D). The stimulation of hyperactivation by an uncoupling agent suggests that the differential abilities of fructose, mannose, and glucose to support hyperactivation may lie in differences in the metabolism of fructose related to mitochondrial function.

Substrate Preincubation Experiments

Previous studies reported that glucose is required for the initiation of sperm capacitation, but may not be necessary for the completion of functional transitions leading to fertilization [48]. We incubated sperm sequentially in HTF with glucose or fructose to determine if glucose priming was sufficient to induce hyperactivation. Sperm were pre-incubated for 30 min in HTF containing either 2.78 mM glucose (Fig. 7A) or 5 mM fructose (Fig. 7B), followed by washing and resuspension in medium containing no substrates, glucose or fructose. Hyperactivation levels were determined at 30, 60, and 90 min after resuspension in each medium. In the absence of energy substrates, sperm pre-incubated in glucose maintained some hyperactivation at all time points analyzed (Fig. 7A), while sperm pre-incubated in fructose did not (Fig. 7B). After pre-incubation in

glucose, sperm resuspended in glucose achieved levels of hyperactivation comparable to levels observed in HTF complete medium (Fig. 7A). Sperm resuspended in fructose after glucose pre-incubation did not exhibit increased hyperactivation above the levels observed following resuspension in substrate-free medium. Hyperactivation levels also remained low in sperm pre-incubated and resuspended in fructose (Fig 7B). However, pre-incubation of sperm in fructose did not prevent them from achieving high levels of hyperactivation when resuspended in glucose (Fig. 7B). These results suggest that continuous glucose metabolism is required for stimulating hyperactivation to the levels typically achieved in HTF complete medium.

Analysis of Metabolic Differences Between Sperm Incubated in Glucose or Fructose

To further explore differences between the ability of fructose and glucose to support hyperactivation, we analyzed the metabolic profiles of sperm incubated in each of these substrates (Table 1). For these assays, eight sperm samples pooled from multiple mice were divided in half for parallel 90 min incubations in HTF with either 2.78 mM glucose or 5mM fructose. We analyzed both the aqueous and organic phases of extracts and metabolites were detected using both GC/MS and LC/MS. Significantly altered peaks were identified ($P < 0.05$), and metabolites were confirmed using biochemical standards. Our analyses showed that flux through the glycolytic pathway was not significantly different between the two substrates, since lactate production was comparable (G:F ratio = 1.08, $P = 0.37$). Metabolic profiles also revealed an increase in the abundance of four confirmed metabolites in fructose-incubated samples: azelaic acid, mannose, taurine, and

carnosine. The most striking difference between glucose and fructose-metabolizing sperm was azelaic acid, which was 40 times higher when sperm were incubated in HTF + fructose. Azelaic acid is an end product of linoleic acid peroxidation and has been shown to possess a number of properties, including tyrosinase inhibition [49], inhibition of mitochondrial enzymes [50], ROS scavenging [51], inhibition of anaerobic glycolysis [52], and inhibition of thioredoxins in melanoma cells [53]. While the anti-mitochondrial and anti-glycolytic properties of azelaic acid are potential reasons for the difference between glucose and fructose effects on sperm, metabolic profiling did not detect significant differences in TCA intermediates.

Taurine was also more abundant in sperm incubated in medium containing fructose. Taurine is an end product of cysteine metabolism and is a key organic osmolyte [54]. Taurine is present at high levels in both human semen and sperm [55], and was shown to inhibit sodium-potassium ATPase activity in hamster sperm [56]. In addition, taurine protected rabbit sperm from lipid peroxidation and maintained sperm motility [57]. The presence of taurine in fructose-incubated sperm may indicate increased osmotic stress in these cells due to altered ion channel function. However, it is also possible that taurine is evidence of increased antioxidant activity in these sperm, since the antioxidant hypotaurine interacts with free radicals in a complex reaction that results in the production of taurine [55].

Carnosine, a natural dipeptide composed of β-alanine and histidine [58], was elevated in sperm incubated with fructose. It has been tested in Tris-based diluents for the storage of ram sperm [59], and is a powerful antioxidant capable of inhibiting lipid peroxidation [60-62]. Carnosine was 70% more abundant in sperm metabolizing fructose,

while its precursor, histidine, was elevated two-fold in sperm metabolizing glucose. These differences suggest that there may processes which induce general lipid peroxidation in sperm metabolizing fructose, and that as a result sperm have upregulated antioxidant systems to combat cellular damage.

In addition to histidine, only one other metabolite, dimethylsuccinate, was increased in sperm utilizing glucose. While dimethylsuccinate has been used to supply an exogenous source of succinate, its endogenous function is unknown [63, 64].

Discussion

A great deal of controversy exists over the relative contribution of mitochondria versus glycolytic metabolism in supporting motility and other functional parameters in both mouse and human sperm. While some studies suggest that mitochondrial substrates are sufficient to support sperm ATP and motility, other evidence suggests the need for a glycolysable substrate [7, 8, 10-12, 36, 37]. We conducted these studies to assess the ability of individual glycolysable or nonglycolysable substrates to support sperm energy production, motility and functional changes that occur throughout capacitation. We examined individual sperm processes instead of the endpoint of fertilization, as the egg has its own metabolic requirements [32, 65]. Our results suggest that both glycolysable and nonglycolysable substrates maintain ATP levels and percent motility throughout a 2 h capacitation period. However, these substrates exhibit differential abilities to support hyperactivation and tyrosine phosphorylation.

With the exception of 10 mM citrate, all tested substrates were capable of supporting both ATP levels and percent motility as well as HTF complete medium,

indicating that both the mitochondrial and the glycolytic pathway are functional in mouse sperm. Citrate was shown to support sperm motility and viability in boar, although neither the quantity nor quality of motility was described [37]. The motility of mouse sperm was higher in the presence of citrate than in substrate-free medium, suggesting at least partial metabolism of this substrate. Phosphofructokinase (PFK) has been shown to be an important point of control in sperm glycolysis in mouse [47], and the presence of citrate, in conjunction with ATP, can inhibit PFK function in boar [66] Therefore, the possibility exists that mouse sperm motility is not efficiently maintained in the presence of citrate due to substrate inhibition of glycolysis.

The differences between glycolysable and non-glycolysable substrates became evident as we investigated other sperm parameters. Among glycolysable substrates, only mannose and glucose were capable of supporting hyperactivation comparable to HTF complete medium (Fig. 2B). Previous reports of substrate-dependent hyperactivation found that mannose, sorbitol, and fructose did not support hyperactivation as well as glucose [43]. However, the high ionic strength of media used in this study may have interfered with the ability of substrates other than glucose to support hyperactivated motility [67]. In our assays sorbitol did not maintain hyperactivation after 30 min, and the loss of hyperactivated motility was also correlated with the loss of vigorous sperm patterns (Fig. 2C). Sorbitol can be converted to fructose by sorbitol dehydrogenase (SORD), a reaction that requires NAD^+ [45]. As glycolysis requires NAD^+ at the GAPDHS step, the conversion of sorbitol to fructose may deplete available NAD^+ stores in sperm, lowering glycolytic rates and leading to a greater proportion of nonvigorous sperm motility in the presence of sorbitol.

Evaluation of sperm motility patterns in the presence of non-glycolysable substrates indicated that sperm were not capable of efficiently undergoing hyperactivated motility (Fig. 3B). These results were expected, as there is ample evidence in the literature that glycolysis is required for hyperactivation [7, 34, 35, 43, 68]. Our findings further support these conclusions on the importance of the glycolytic pathway.

All glycolysable substrates tested, with the exception of sorbitol, support the full pattern of capacitation-dependent increases in tyrosine phosphorylation. In addition, we found that some non-glycolysable substrates can support at least partial tyrosine phosphorylation. These results suggest that other pathways may work in concert with glycolysis to promote capacitation. Sperm incubated with lactate or pyruvate showed a lack of phosphorylation of a doublet immediately below the constitutively phosphorylated hexokinase band.

Assessment of the effects of glycolytic and mitochondrial inhibitors on sperm function in the presence of single substrates suggests that multiple pathways regulate sperm functional changes that occur during capacitation. The addition of ACH to pyruvate did not affect ATP levels or percent motility but caused a drastic loss of vigorous forms of motility compared to controls. This raises the possibility that inhibition of sperm glycolysis, perhaps by altering NAD^+/NADH ratios, may influence the metabolism of substrates typically utilized by the mitochondria.

The restoration of hyperactivated motility in the presence of fructose and CCCP may be due to an increase in the production of reactive oxygen species (ROS) that occurs when cells are incubated with mitochondrial inhibitors such as CCCP [69]. While high

ROS levels have been correlated with infertility in human sperm [70], low levels of ROS production facilitated capacitation in both human and mouse sperm [71-73]. Treatment of human sperm with hydrogen peroxide also stimulated hyperactivation [72]. In rat hepatocytes, fructose prevented cell death after reoxygenation by increasing intracellular pools of the antioxidant glutathione (possibly via the increased generation of NADPH). Mouse sperm have been shown to possess a high glutathione peroxidase content [74, 75]. Therefore, incubation of sperm in fructose may result in disruption of the redox state of sperm, preventing them from undergoing hyperactivation unless ROS production is stimulated sufficiently.

Previous studies have showed that sperm could fertilize oocytes in the absence of substrates if they had been previously incubated in glucose, leading to the hypothesis that glucose 'priming' was sufficient for sperm to become fertilization competent [34, 48]. In our experiments, sperm pre-incubated in glucose for 30 min did not exhibit increase hyperactivation when transferred to fructose-containing medium. Fraser and Quinn [34] preincubated sperm in glucose-containing medium for 2h before mixing with oocytes, a period that is typically sufficient for the development of maximal levels of hyperactivation. Okabe et al. [48] preincubated sperm in glucose medium for 40 min and observed zona penetration within 10 min of mixing with oocytes. However, these experiments did not quantitate the percentage of sperm undergoing hyperactivation. In control conditions where sperm were preincubated in HTF+glucose and then resuspended in substrate-free HTF, we observed that sperm were capable of maintaining some hyperactivated motility after being resuspended in media without substrates (Fig. 7a). This residual hyperactivity may be due to glucose metabolites still functioning in the

sperm. Similar residual hyperactivation could contribute to zona penetration observed by Okabe and colleagues. In order for sperm to exhibit high levels of hyperactivation in our system glucose was required to be present in the medium, suggesting that active glucose metabolism is required both for the initiation and maintenance of hyperactivated motility during in vitro capacitation.

The analysis of metabolic profiles of sperm incubated with glucose or fructose identified several significant differences (Table 1). Since we used unlabeled sugars, we were unable to determine which metabolites were direct products of substrate utilization. However, this approach produces a universal profile of both primary and secondary metabolic pathways. The results indicated that in the presence of fructose, sperm possess higher levels of metabolites that are associated with the inhibition of lipid peroxidation and antioxidant activity. We hypothesize that the metabolism of fructose, which is abundant in mammalian seminal fluid [76-78], increases the production of antioxidants, providing increase protection from oxidative damage and preventing premature hyperactivation. Upon entering the oviduct, sperm increase the utilization of glucose. Our metabolic profiles suggest that this change of substrates should decrease antioxidants, and the resulting increase in ROS production would stimulate hyperactivated motility. Future studies will test this hypothesis by measuring ROS levels in the sperm incubated in fructose or glucose ± CCCP and by determining the effect of adding cell-permeable antioxidants on hyperactivation.

Figure 3.1

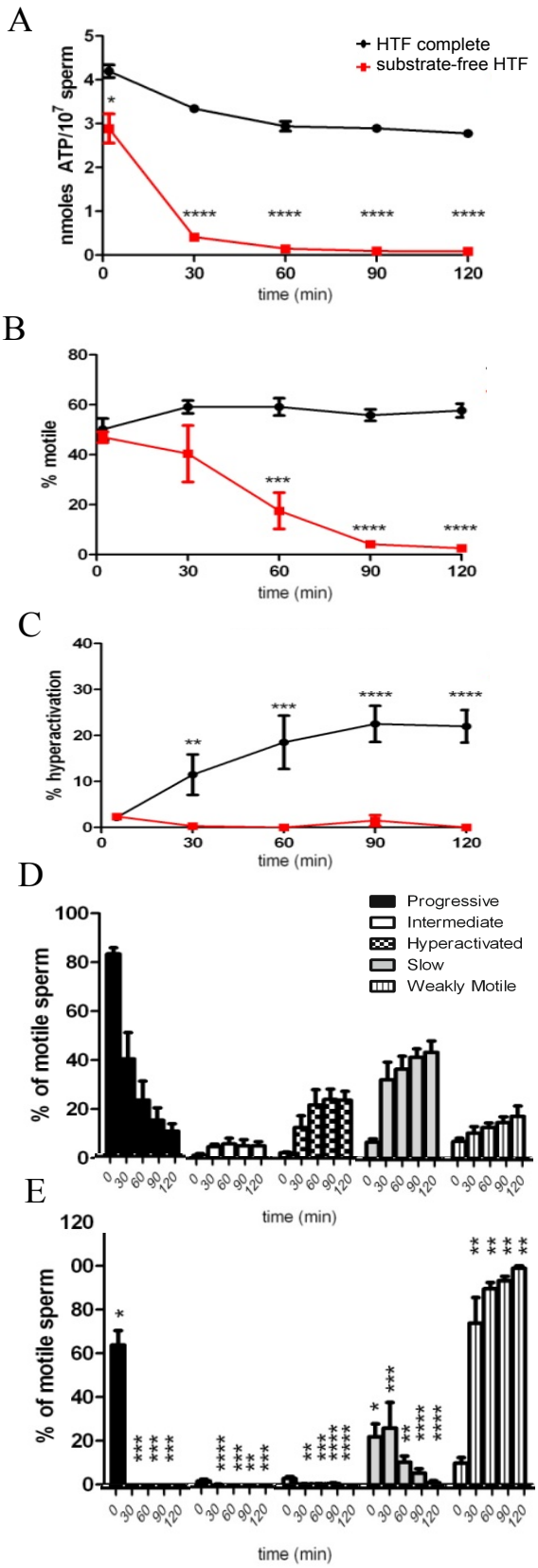
A
HTF complete
substrate-free HTF
nmoles ATP/10^7 sperm
time (min)
B
% motile
time (min)
C
% hyperactivation
time (min)
D
Progressive
Intermediate
Hyperactivated
Slow
Weakly Motile
% of motile sperm
time (min)
E
% of motile sperm
time (min)

Figure 3.1. ATP and motility parameters of sperm incubated in the presence or absence of energy substrates. Sperm were incubated in the presence of substrates (HTF complete, A-D) or in the absence of substrates (substrate-free HTF, A-C, E) and analyzed at 30 minute time points over a 2h in vitro capacitation period. **A**) Sperm ATP levels in the presence and absence of substrates. **B**) Total sperm motility assessed by CASA. **C**) The percentage of motile sperm displaying hyperactivated motility over the time course. **D**) Motility profiles of sperm incubated in HTF complete media. **E**) Motility profiles of sperm incubated without energy substrates. Data are represented as the mean ± SEM of sperm from 7 mice. Differences between conditions at corresponding time points were analyzed using two-tailed, unpaired t-test. * $P < 0.05$, ** $P < 0.01$, *** $P < 0.001$, **** $P < 0.0001$.

Figure 3.2

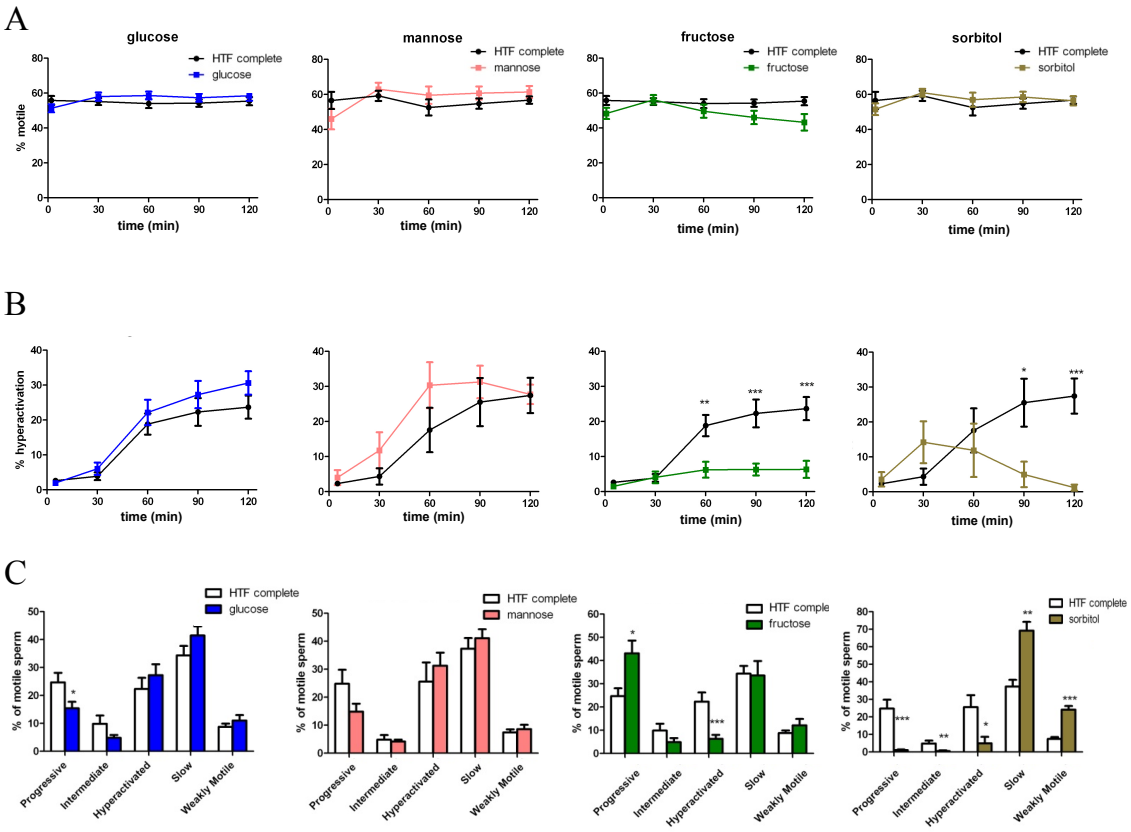

Figure 3.2. Total motility, hyperactivation, and motility profiles of sperm incubated with glycolysable substrates. Sperm were incubated in HTF complete medium or HTF media with either 2.78 mM glucose (blue), 5 mM mannose (pink), 5 mM fructose (green), or 5 mM sorbitol (olive) as the sole energy substrate. At the indicated time points, sperm were analyzed for total motility (**A**) or percent hyperactivation (**B**). **C**) Motility profiles of sperm incubated in HTF complete medium (open bars) or HTF with a glycolysable substrate (colored bars) for 90 minutes. Data are represented as the mean ± SEM of sperm from ≥ 5 mice. Differences between conditions at corresponding time points were analyzed using two-tailed, unpaired t-test. * $P < 0.05$, ** $P < 0.01$, *** $P < 0.001$, **** $P < 0.0001$.

Figure 3.3

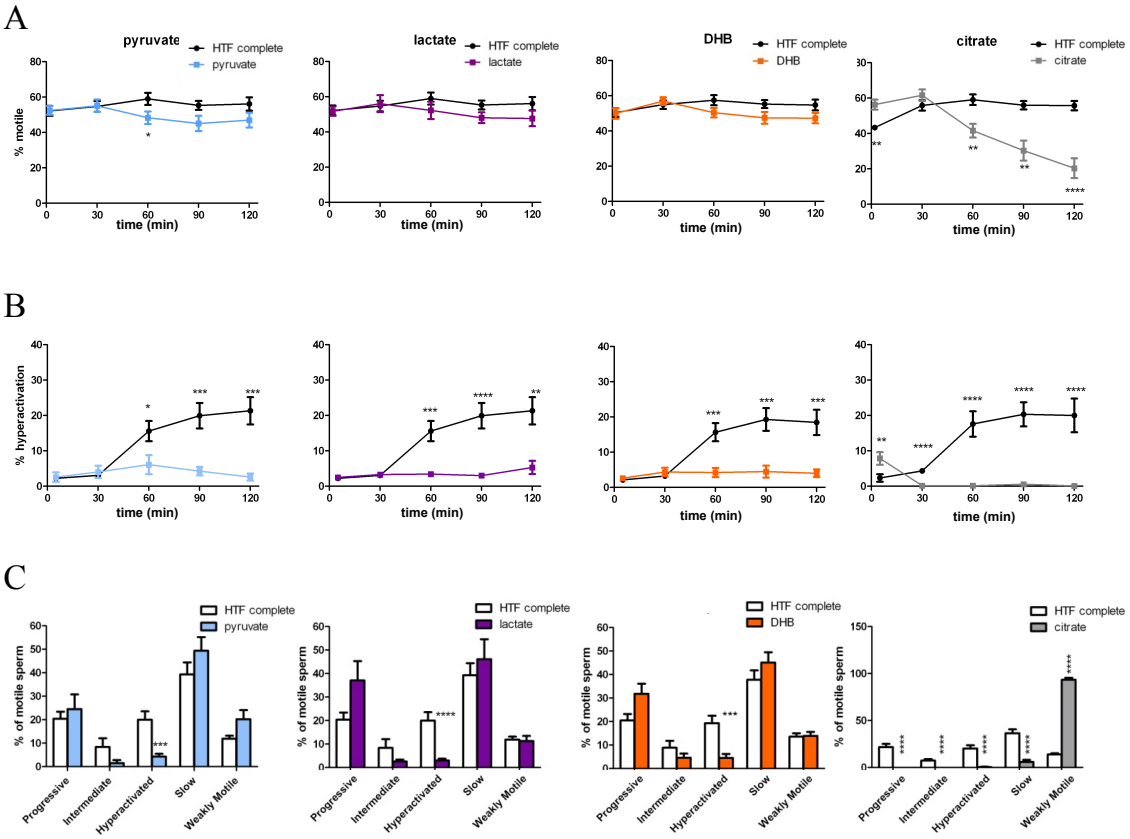

Figure 3.3. Total motility, hyperactivation, and motility profiles of sperm incubated with nonglycolysable substrates. Sperm were incubated in HTF complete medium or HTF media with either 0.33 mM pyruvate(light blue), 21.4 mM lactate (purple), 5 mM DHB (orange), or 10 mM citrate (gray) as the sole energy substrate. At the indicated time points, sperm were analyzed for total motility (**A**) or percent hyperactivation (**B**). **C**) Motility profiles of sperm incubated in HTF complete medium (open bars) or HTF with a glycolysable substrate (colored bars) for 90 minutes. Data are represented as the mean ± SEM of sperm from ≥ 8 mice. Differences between conditions at corresponding time points were analyzed using two-tailed, unpaired t-test. * $P < 0.05$, ** $P < 0.01$, *** $P < 0.001$, **** $P < 0.0001$.

Figure 3.4

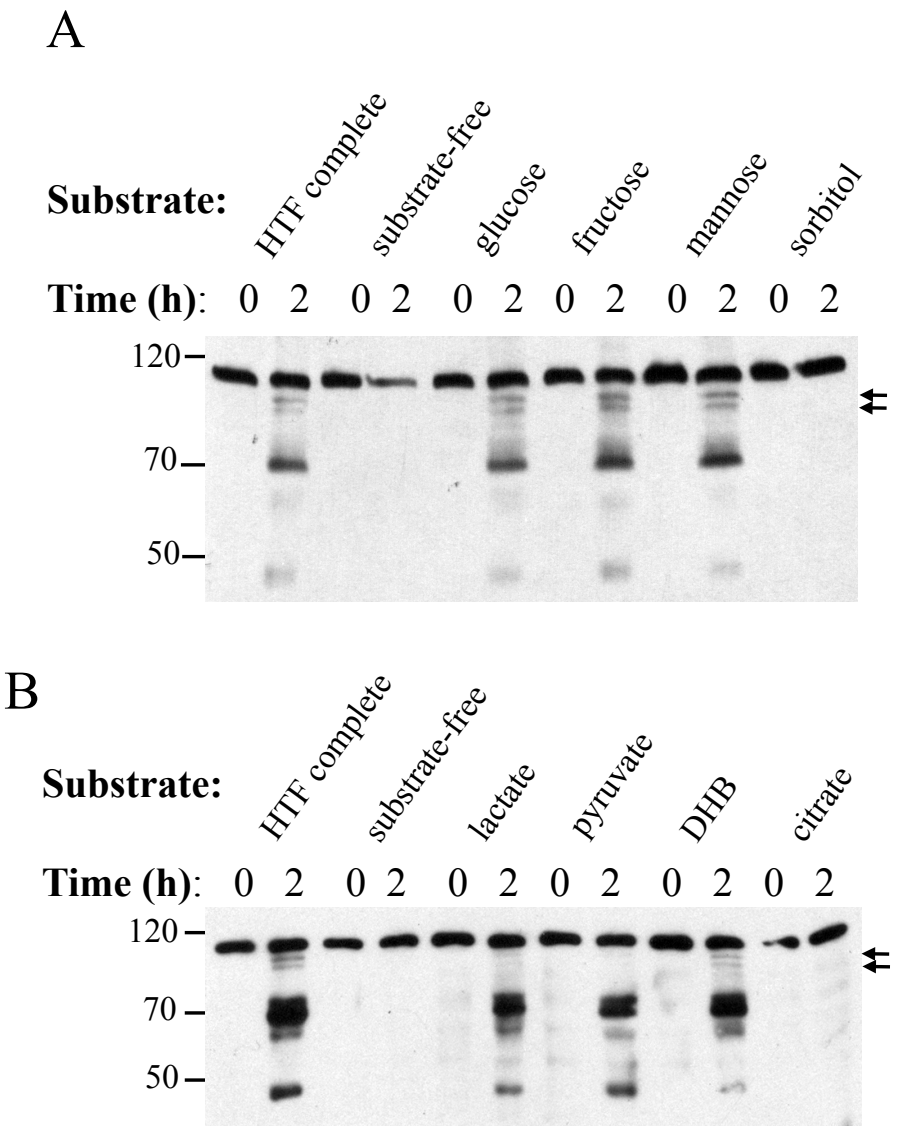

Figure 3.4. Capacitation-associated tyrosine phosphorylation of sperm incubated in glycolysable or nonglycolysable substrates. Sperm were incubated for 0 or 90 min in the HTF complete medium, substrate-free medium, or media supplemented with glycolysable substrates (**A**), or nonglycolysable substrates (**B**). Sperm were lysed and subjected to SDS-PAGE, followed by western blotting with 4G10. Experiments were repeated a minimum of 5 times for each substrate.

Figure 3.5

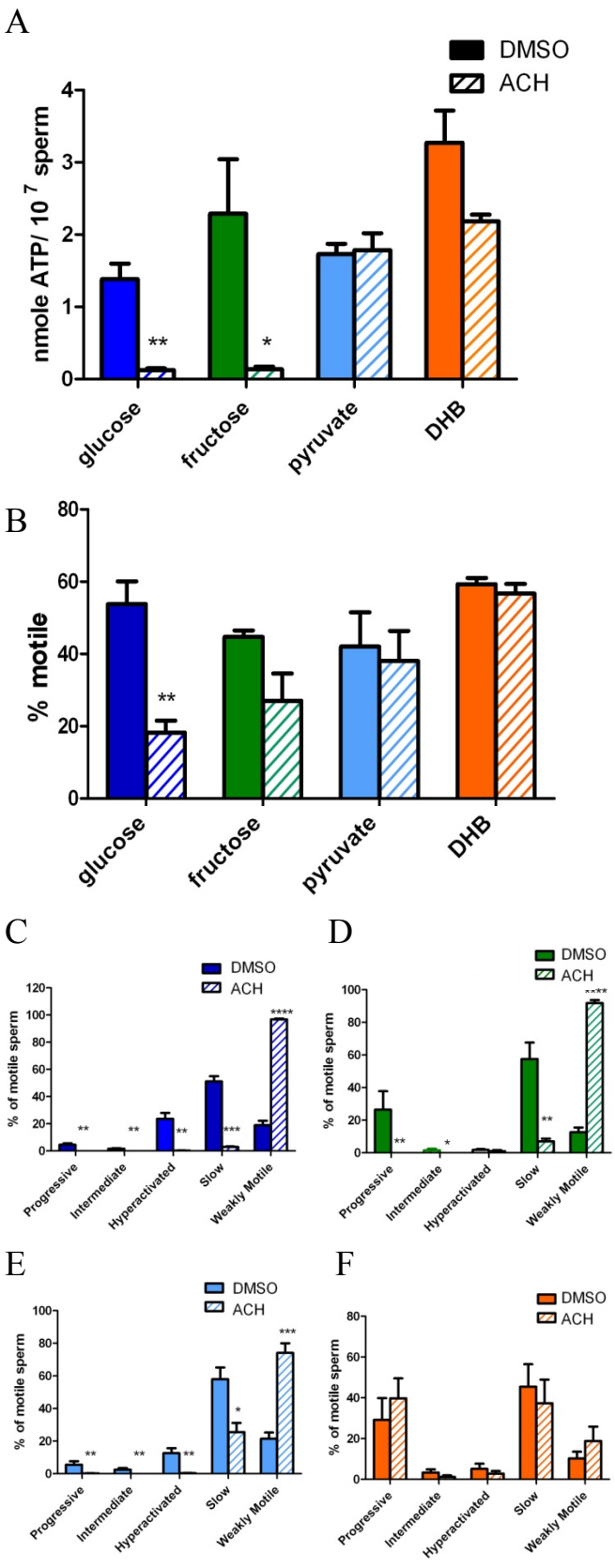
A
DMSO
ACH
nmole ATP/ 10 7 sperm
glucose
fructose
pyruvate
DHB
B
% motile
C
D
E
F
% of motile sperm
Progressive
Intermediate
Hyperactivated
Slow
Weakly Motile

Figure 3.5. ATP levels, percent motility, and motility profiles incubated in the presence of an inhibitor of glycolysis. Sperm were incubated in HTF media containing 2.78 mM glucose, 5 mM fructose, 0.33 mM pyruvate, or 5 mM DHB in the presence of either 10 mM ACH or the vehicle control. After 90 minutes of incubation, sperm were analyzed for ATP content (**A**), percent motility (**B**) and motility profiles (**C**, glucose, **D**, fructose, **E**, pyruvate, and **F**, DHB. Data are represented as the mean ± SEM of sperm from ≥ 3 mice. Differences between conditions at corresponding time points were analyzed using two-tailed, unpaired t-test. * $P < 0.05$, ** $P < 0.01$, *** $P < 0.001$, **** $P < 0.0001$.

Figure 3.6

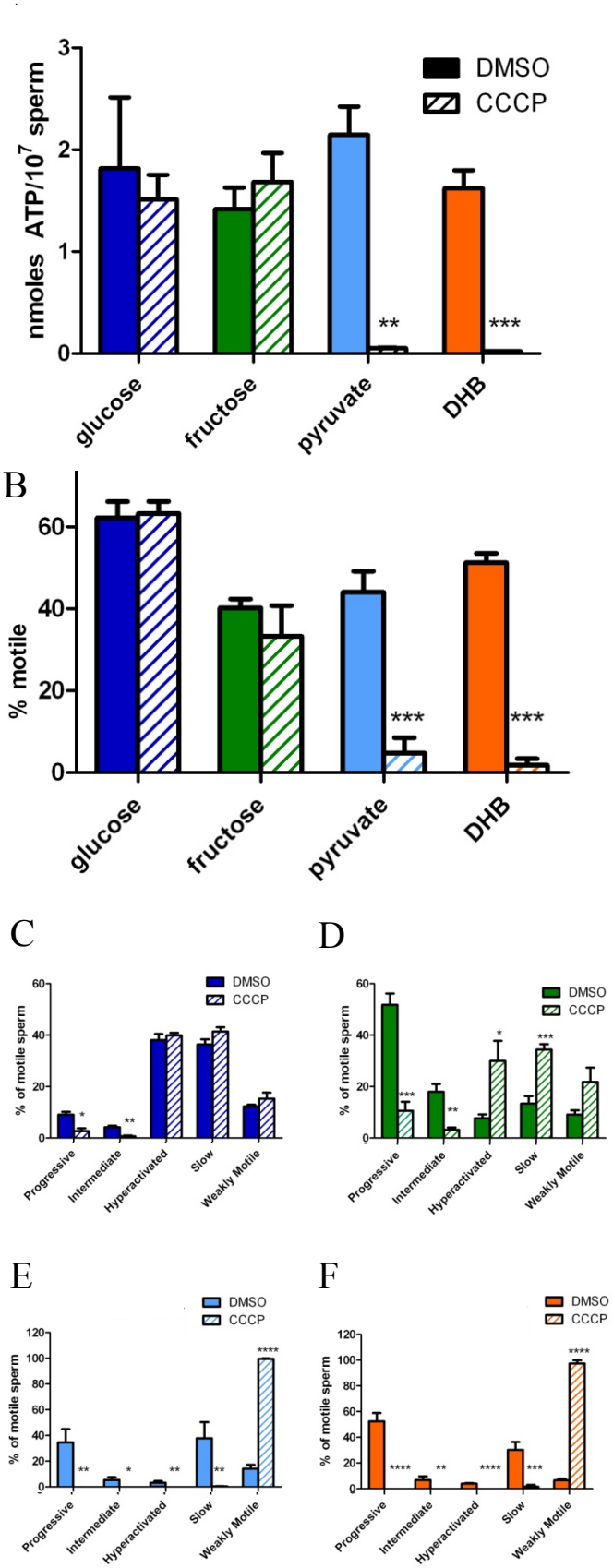
nmoles ATP/10^7 sperm
DMSO
CCCP
glucose
fructose
pyruvate
DHB
B
% motile
C
D
E
F
% of motile sperm
Progressive
Intermediate
Hyperactivated
Slow
Weakly Motile

Figure 3.6. ATP levels, percent motility, and motility profiles incubated in the presence of an uncoupler of oxidative phosphorylation. Sperm were incubated in HTF media containing 2.78 mM glucose, 5 mM fructose, 0.33 mM pyruvate, or 5 mM DHB in the presence of either 10 μM ACH or the vehicle control. After 90 minutes of incubation, sperm were analyzed for ATP content (**A**), percent motility (**B**) and motility profiles (**C**, glucose, **D**, fructose, **E**, pyruvate, and **F**, DHB. Data are represented as the mean ± SEM of sperm from ≥ 3 mice. Differences between conditions at corresponding time points were analyzed using two-tailed, unpaired t-test. * $P < 0.05$, ** $P < 0.01$, *** $P < 0.001$, **** $P < 0.0001$.

Figure 3.7

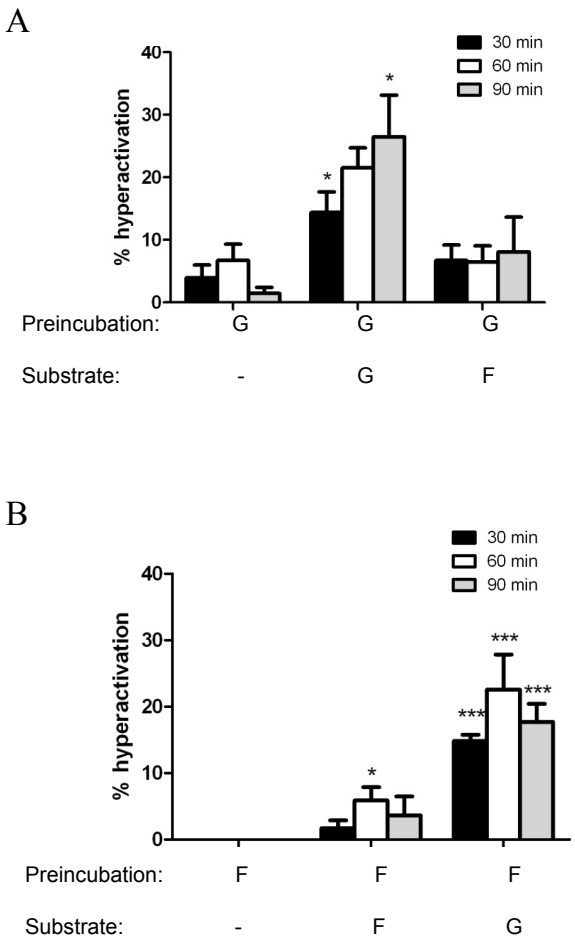

Figure 3.7. Hyperactivation after preincubation in glucose or fructose-containing HTF. Sperm were preincubated in media containing HTF + 2.78 mM glucose (**A**) or 5 mM fructose (**B**) for 30 min, washed, and then resuspended in either substrate-free HTF, HTF+ 2.78 mM glucose, or 5 mM fructose. The percentage of the motile population displaying hyperactivate motility was determined 30 min (black bars), 60 min (open bars), or 90 min (gray bars) after resuspension. . Data are represented as the mean ± SEM of sperm from 4 mice. Differences between conditions at corresponding time points were analyzed using one-way ANOVA. * $P < 0.05$, ** $P < 0.01$, *** $P < 0.001$, **** $P < 0.0001$.

TABLE 3.1. Confirmed metabolites differentially present in glucose or fructose- incubated sperm

	Metabolite	Increased Abundance	Glucose/Fructose Ratio	P
	Azelaic acid	Fructose	0.021	0.021
	Mannose	Fructose	0.262	0.003
	Taurine	Fructose	0.576	0.024
	Carnosine	Fructose	0.592	0.005
	Dimethyl succinic acid	Glucose	1.312	0.046
	Histidine	Glucose	2.007	0.041
Glycolytic metabolites	Lactate	N/A	1.087	0.374
	Pyruvate	N/A	1.502	0.088
TCA metabolites	Citrate	N/A	0.303	0.300
	Fumarate	N/A	0.595	0.070
	Succinate	N/A	1.306	0.205
	Malate	N/A	1.595	0.092

References

1. Yanagimachi R. Mammalian fertilization. In: Knobil E, Neill J (eds.), The Physiology of Reproduction. New York: Raven Press; 1994: 189-317.

2. Visconti PE, Westbrook VA, Chertihin O, Demarco I, Sleight S, Diekman AB. Novel signaling pathways involved in sperm acquisition of fertilizing capacity. J Reprod Immunol 2002; 53:133-150.

3. Fraser LR. The "Switching on" of Mammalian Spermatozoa: Molecular Events Involed in Promotion and Regulation of Capacitation. Molecular Reproduction and Development 2009; 77:197-208.

4. Krapf D, Arcelay E, Wertheimer EV, Sanjay A, Pilder SH, Salicioni AM, Visconti PE. Inhibition of Ser/Thr phosphatases induces capacitation-associated signaling in the presence of Src kinase inhibitors. J Biol Chem 2010; 285:7977-7985.

5. Van Dop C, Hutson SM, Lardy HA. Pyruvate metabolism in bovine epididymal spermatozoa. J Biol Chem 1977; 252:1303-1308.

6. Hammerstedt RH, Lardy HA. The effect of substrate cycling on the ATP yield of sperm glycolysis. J Biol Chem 1983; 258:8759-8768.

7. Williams AC, Ford WC. The role of glucose in supporting motility and capacitation in human spermatozoa. J Androl 2001; 22:680-695.

8. Mukai C, Okuno M. Glycolysis plays a major role for adenosine triphosphate supplementation in mouse sperm flagellar movement. Biol Reprod 2004; 71:540-547.

9. Carey JE, Olds-Clarke P, Storey BT. Oxidative metabolism of spermatozoa from inbred and random bred mice. J Exp Zool 1981; 216:285-292.

10. Suter D, Chow PY, Martin IC. Maintenance of motility in human spermatozoa by energy derived through oxidative phosphorylation and addition of albumin. Biol Reprod 1979; 20:505-510.

11. Ford WC, Harrison A. The role of oxidative phosphorylation in the generation of ATP in human spermatozoa. J Reprod Fertil 1981; 63:271-278.

12. Peterson RN, Freund M. ATP synthesis and oxidative metabolism in human spermatozoa. Biol Reprod 1970; 3:47-54.

13. Eddy EM, Toshimori K, O'Brien DA. Fibrous sheath of mammalian spermatozoa. Microsc Res Tech 2003; 61:103-115.

14. Welch JE, Brown PR, O'Brien DA, Eddy EM. Genomic organization of a mouse glyceraldehyde 3-phosphate dehydrogenase gene (Gapd-s) expressed in post-meiotic spermatogenic cells. Dev Genet 1995; 16:179-189.

15. Boer PH, Adra CN, Lau YF, McBurney MW. The testis-specific phosphoglycerate kinase gene pgk-2 is a recruited retroposon. Mol Cell Biol 1987; 7:3107-3112.

16. McCarrey JR, Thomas K. Human testis-specific PGK gene lacks introns and possesses characteristics of a processed gene. Nature 1987; 326:501-505.

17. Millan JL, Driscoll CE, LeVan KM, Goldberg E. Epitopes of human testis-specific lactate dehydrogenase deduced from a cDNA sequence. Proc Natl Acad Sci U S A 1987; 84:5311-5315.

18. Vemuganti SA, Bell TA, Scarlett CO, Parker CE, de Villena FP, O'Brien DA. Three male germline-specific aldolase A isozymes are generated by alternative splicing and retrotransposition. Dev Biol 2007; 309:18-31.

19. Vemuganti SA, Bell TA, Scarlett CO, Parker CE, Pardo-Manuel de Villena F, O'Brien DA. Genomic and proteomic analysis of aldolase A retrogenes expressed during spermatogenesis. J Androl 2006; 27 39.

20. Eddy EM, Welch, J.E., Mori, C., Fulcher, K.D., O'Brien, D.A. Role and regulation of spermatogenic cell-specific gene expression: enzymes of glycolysis. In: Bartke A (ed.) Function of somatic cells in the testis. New Rork: Springer; 1994: 362-372.

21. Vemuganti SA, de Villena FP, O'Brien DA. Frequent and recent retrotransposition of orthologous genes plays a role in the evolution of sperm glycolytic enzymes. BMC Genomics 2010; 11:285.

22. Nayernia K, Adham IM, Burkhardt-Gottges E, Neesen J, Rieche M, Wolf S, Sancken U, Kleene K, Engel W. Asthenozoospermia in mice with targeted deletion of the sperm mitochondrion-associated cysteine-rich protein (Smcp) gene. Mol Cell Biol 2002; 22:3046-3052.

23. Hennig B. Change of cytochrome c structure during development of the mouse. Eur J Biochem 1975; 55:167-183.

24. Tanaka H, Kohroki J, Iguchi N, Onishi M, Nishimune Y. Cloning and characterization of a human orthologue of testis-specific succinyl CoA: 3-oxo acid CoA transferase (Scot-t) cDNA. Mol Hum Reprod 2002; 8:16-23.

25. Mitra K, Rangaraj N, Shivaji S. Novelty of the pyruvate metabolic enzyme dihydrolipoamide dehydrogenase in spermatozoa: correlation of its localization,

tyrosine phosphorylation, and activity during sperm capacitation. J Biol Chem 2005; 280:25743-25753.

26. Kumar V, Rangaraj N, Shivaji S. Activity of pyruvate dehydrogenase A (PDHA) in hamster spermatozoa correlates positively with hyperactivation and is associated with sperm capacitation. Biol Reprod 2006; 75:767-777.

27. Hinsch KD, De Pinto V, Aires VA, Schneider X, Messina A, Hinsch E. Voltage-dependent anion-selective channels VDAC2 and VDAC3 are abundant proteins in bovine outer dense fibers, a cytoskeletal component of the sperm flagellum. J Biol Chem 2004; 279:15281-15288.

28. Miki K, Qu W, Goulding EH, Willis WD, Bunch DO, Strader LF, Perreault SD, Eddy EM, O'Brien DA. Glyceraldehyde 3-phosphate dehydrogenase-S, a sperm-specific glycolytic enzyme, is required for sperm motility and male fertility. Proc Natl Acad Sci U S A 2004; 101:16501-16506.

29. Odet F, Duan C, Willis WD, Goulding EH, Kung A, Eddy EM, Goldberg E. Expression of the gene for mouse lactate dehydrogenase C (Ldhc) is required for male fertility. Biol Reprod 2008; 79:26-34.

30. Danshina PV, Geyer CB, Dai Q, Goulding EH, Willis WD, Kitto GB, McCarrey JR, Eddy EM, O'Brien DA. Phosphoglycerate kinase 2 (PGK2) is essential for sperm function and male fertility in mice. Biol Reprod 2010; 82:136-145.

31. Narisawa S, Hecht NB, Goldberg E, Boatright KM, Reed JC, Millan JL. Testis-specific cytochrome c-null mice produce functional sperm but undergo early testicular atrophy. Mol Cell Biol 2002; 22:5554-5562.

32. Hoppe PC. Glucose requirement for mouse sperm capacitation in vitro. Biol Reprod 1976; 15:39-45.

33. Urner F, Leppens-Luisier G, Sakkas D. Protein tyrosine phosphorylation in sperm during gamete interaction in the mouse: the influence of glucose. Biol Reprod 2001; 64:1350-1357.

34. Fraser LR, Quinn PJ. A glycolytic product is obligatory for initiation of the sperm acrosome reaction and whiplash motility required for fertilization in the mouse. J Reprod Fertil 1981; 61:25-35.

35. Urner F, Sakkas D. Glucose is not essential for the occurrence of sperm binding and zona pellucida-induced acrosome reaction in the mouse. Int J Androl 1996a; 19:91-96.

36. Tanaka H, Takahashi T, Iguchi N, Kitamura K, Miyagawa Y, Tsujimura A, Matsumiya K, Okuyama A, Nishimune Y. Ketone bodies could support the

motility but not the acrosome reaction of mouse sperm. Int J Androl 2004; 27:172-177.

37. Medrano A, Fernandez-Novell JM, Ramio L, Alvarez J, Goldberg E, Montserrat Rivera M, Guinovart JJ, Rigau T, Rodriguez-Gil JE. Utilization of citrate and lactate through a lactate dehydrogenase and ATP-regulated pathway in boar spermatozoa. Mol Reprod Dev 2006; 73:369-378.

38. Goodson SG, Zhang Z, Tsuruta JK, Wang W, O'Brien DA. Classification of Mouse Sperm Motility Patterns Using an Automated Multiclass Support Vector Machines Model. Biol Reprod 2011.

39. Byers SL, Payson SJ, Taft RA. Performance of ten inbred mouse strains following assisted reproductive technologies (ARTs). Theriogenology 2006; 65:1716-1726.

40. Quinn P, Kerin JF, Warnes GM. Improved pregnancy rate in human in vitro fertilization with the use of a medium based on the composition of human tubal fluid. Fertil Steril 1985; 44:493-498.

41. Kalab P, Visconti P, Leclerc P, Kopf GS. p95, the major phosphotyrosine-containing protein in mouse spermatozoa, is a hexokinase with unique properties. J Biol Chem 1994; 269:3810-3817.

42. Rigau T, Rivera M, Palomo MJ, Fernandez-Novell JM, Mogas T, Ballester J, Pena A, Otaegui PJ, Guinovart JJ, Rodriguez-Gil JE. Differential effects of glucose and fructose on hexose metabolism in dog spermatozoa. Reproduction 2002; 123:579-591.

43. Cooper TG. The onset and maintenance of hyperactivated motility of spermatozoa in the mouse. Gamete Res 1984; 9:55-74.

44. Niwa K, Iritani A. Effect of various hexoses on sperm capacitation and penetration of rat eggs in vitro. J Reprod Fertil 1978; 53:267-271.

45. Cao W, Aghajanian HK, Haig-Ladewig LA, Gerton GL. Sorbitol can fuel mouse sperm motility and protein tyrosine phosphorylation via sorbitol dehydrogenase. Biol Reprod 2009; 80:124-133.

46. Visconti PE, Bailey JL, Moore GD, Pan D, Olds-Clarke P, Kopf GS. Capacitation of mouse spermatozoa. I. Correlation between the capacitation state and protein tyrosine phosphorylation. Development 1995a; 121:1129-1137.

47. Travis AJ, Jorgez CJ, Merdiushev T, Jones BH, Dess DM, Diaz-Cueto L, Storey BT, Kopf GS, Moss SB. Functional relationships between capacitation-dependent cell signaling and compartmentalized metabolic pathways in murine spermatozoa. J Biol Chem 2001; 276:7630-7636.

48. Okabe M, Adachi T, Kohama Y, Mimura T. Effect of glucose and phloretin-2'-beta-D-glucose (phloridzin) on in vitro fertilization of mouse ova. Experientia 1986; 42:398-399.

49. Nazzaro-Porro M, Passi, S. Identification of tyrosinase inhibitors in cultures of Pityrosporum. Journal of Investigative Dermatology 1978; 71:205-208.

50. Passi S, Picardo M, Nazzaro-Porro M, Breathnach A, Confaloni AM, Serlupi-Crescenzi G. Antimitochondrial effect of saturated medium chain length (C8-C13) dicarboxylic acids. Biochem Pharmacol 1984; 33:103-108.

51. Passi S, Picardo M, Zompetta C, De Luca C, Breathnach AS, Nazzaro-Porro M. The oxyradical-scavenging activity of azelaic acid in biological systems. Free Radic Res Commun 1991; 15:17-28.

52. Bargoni NaT, O. On the effect of aliphatic saturated dicarboxylic acids on anaerobic glycolysis in chicken embryo. Italian Journal of Biochemistry 1983; 32:385-390.

53. Schallreuter KU, Wood JM. Azelaic acid as a competitive inhibitor of thioredoxin reductase in human melanoma cells. Cancer Lett 1987; 36:297-305.

54. Huxtable RJ. Physiological actions of taurine. Physiological reviews 1992; 72:101-163.

55. Holmes RP, Goodman HO, Shihabi ZK, Jarow JP. The taurine and hypotaurine content of human semen. J Androl 1992; 13:289-292.

56. Mrsny RJ, Meizel, S. Inhibition of hamster sperm Na+, K+-ATPase activity by taurine and hypotaurine. Life Sciences 1985; 36:271-275.

57. Alvarez JG, Storey BT. Taurine, hypotaurine, epinephrine and albumin inhibit lipid peroxidation in rabbit spermatozoa and protect against loss of motility. Biol Reprod 1983; 29:548-555.

58. Quinn PJ, Boldyrev, A.A., and Formazuyk, V.E. Carnosine: Its properties, functions, and potential therapeutic applications. Molecular Aspects of Medicine 1992; 13:379-444.

59. Sanchez-Partida LG, Setchell BP, Maxwell WM. Epididymal compounds and antioxidants in diluents for the frozen storage of ram spermatozoa. Reprod Fertil Dev 1997; 9:689-696.

60. Babizhayev MA, Costa EB. Lipid peroxide and reactive oxygen species generating systems of the crystalline lens. Biochim Biophys Acta 1994; 1225:326-337.

61. Babizhayev MA, Seguin MC, Gueyne J, Evstigneeva RP, Ageyeva EA, Zheltukhina GA. L-carnosine (beta-alanyl-L-histidine) and carcinine (beta-alanylhistamine) act as natural antioxidants with hydroxyl-radical-scavenging and lipid-peroxidase activities. Biochem J 1994; 304 (Pt 2):509-516.

62. Kang JH, Kim, K.S., Choi, S.Y., Kwon, H.Y., Won, M.H., Kang, T.C. Carnosine and related dipepetides protect human ceruloplasmin against peroxyl radical-mediated modification. Molecules and Cells 2002; 13:498-502.

63. MacDonald MJ. Differences between mouse and rat pancreatic islets: succinate responsiveness, malic enzyme, and anaplerosis. Am J Physiol Endocrinol Metab 2002; 283:E302-310.

64. Yang L, Kasumov T, Kombu RS, Zhu SH, Cendrowski AV, David F, Anderson VE, Kelleher JK, Brunengraber H. Metabolomic and mass isotopomer analysis of liver gluconeogenesis and citric acid cycle: II. Heterogeneity of metabolite labeling pattern. J Biol Chem 2008; 283:21988-21996.

65. Summers MC, Biggers JD. Chemically defined media and the culture of mammalian preimplantation embryos: historical perspective and current issues. Hum Reprod Update 2003; 9:557-582.

66. Kamp G, Schmidt H, Stypa H, Feiden S, Mahling C, Wegener G. Regulatory properties of 6-phosphofructokinase and control of glycolysis in boar spermatozoa. Reproduction 2007; 133:29-40.

67. Fraser LR, Herod JE. Expression of capacitation-dependent changes in chlortetracycline fluorescence patterns in mouse spermatozoa requires a suitable glycolysable substrate. J Reprod Fertil 1990; 88:611-621.

68. Rogers BJ, Perreault SD. Importance of glycolysable substrates for in vitro capacitation of human spermatozoa. Biol Reprod 1990; 43:1064-1069.

69. Izeradjene K, Douglas, L. Tillman, D.M.,Delaney, A.B., Houghton, J.A. Reactive Oxygen Species Regulate Caspase Activation in Tumor Necrosis Factor-Related Apoptosis-Inducing Ligand-Resistant Human Colon Carcinoma Cell Lines. Cancer Research 2005; 65:7436-7445.

70. Pascqualotto FF, Sharma, R.K., Nelson, D.R., Thomas, Jr., A.J., Agarwal, A. Relationship between oxidative stress, semen characteristics, and clinical diagnosis in men undergoing infertility investigation. Fertility and Sterility 2000; 73:459-464.

71. Dona G, Fiore, C., Tibaldi,E., Frezzato, F., Andrisani, A., Ambrosini, G. Fiorentin, D. Armanini, D., Bordin, L. and Clari, G. Endogenous reactive oxygen

species content and modulation of tyrosine phosphorylation during sperm capacitation. International Journal of Andrology 2010.

72. Griveau JF, Renard, P., and Le Lannou, D. An in vitro promoting role for hydrogen peroxide in human sperm capacitation. International Journal of Andrology 1994; 17:300-307.

73. Ecroyd H, Jones, R.C., Aitken, R.J. Endogenous redox activity in mouse spermatozoa and its role in regulating the tyrosine phosphorylation events associated with sperm capacitation. Biology of Reproduction 2003; 69:347-354.

74. Frenzel J, Richter, J., Eschrich, K. Fructose inhibits apoptosis induced by reoxygenation in rat hepatocytes by decreasing reactive oxygen species via stabilization of the glutathione pool. Biochimica et Biophysica Acta 2002; 1542:82-94.

75. Alvarez JGaS, B.T. Lipid peroxidation and the reactions of superoxide and hydrogen peroxide in mouse spermatozoa. Biology of Reproduction 1984; 30:833-841.

76. Mann T. Secretory function of the prostate, seminal vesicle and other male accessory organs of reproduction. J Reprod Fertil 1974; 37:179-188.

77. Marchlewska-Koj A. Fructose content of mouse ejaculates recovered from the uterus after mating. J Reprod Fertil 1971; 25:81-84.

78. Anderson RA, Jr., Oswald C, Willis BR, Zaneveld LJ. Relationship between semen characteristics and fertility in electroejaculated mice. J Reprod Fertil 1983; 68:1-7.

CHAPTER 4

SUMMARY AND FUTURE DIRECTIONS

Overview

The goals of the research presented were to investigate how the metabolism of various substrates affects functional parameters of sperm capacitation. Since the current methods available for analyzing sperm did not meet our needs in measuring patterns of motility, we first developed a tool for analyzing multiple sperm motility patterns in conjunction with CASA to allow for more comprehensive, quantitative analyses of sperm motion in response to genetic and biochemical perturbations. We then utilized this model to evaluate the effects of substrate utilization on sperm capacitation and hyperactivation. Our results indicate that CASAnova analysis of motility profiles will be a useful tool in future studies of sperm motility. Our studies of sperm metabolism and substrate-dependent effects on capacitation and hyperactivation reiterate the importance of glycolysis in supporting these processes, and also indicate that both sperm capacitation and hyperactivation depend on the type of glycolytic substrate being metabolized.

CASAnova: Modifications and Future Applications

CASAnova is based on the observation that sperm motility tracks plotted as a function of their CASA parameters, clustered in multidimensional space according to their visual classification. This software identifies five patterns of sperm motility, providing a more comprehensive analysis of sperm motion than previous methods. In addition, this automated approach completes the simultaneous analysis of all sperm recorded in a series of CASA fields. The analysis of greater numbers of sperm (typically 400-600 per sample) generates results that are more representative of the sperm population, unlike flagellar waveform analysis, which typically only characterizes 10-15 sperm per sample [1]. Furthermore, while CASA-associated hyperactivated gates do not consistently reflect visual assessment, CASAnova detects hyperactivation percentages in agreement with those determined visually. We demonstrated that CASAnova accurately identifies time-dependent changes in sperm motility profiles during capacitation and alterations in motility profiles that occur in some infertile phenotypes. We also showed that CASAnova is applicable to sperm from strains commonly used in generating transgenic mouse models. Application of CASAnova to these sperm revealed previously unreported differences in the levels of both slow and hyperactivated sperm between mouse strains.

We anticipate that CASAnova will be useful for reproductive phenotyping of other mouse models with defects in male fertility. For example, sperm deficient in angiotensin converting enzyme (ACE) display reduced male fertility due to an inability of sperm to migrate to the site of fertilization in the oviduct [2]. However, this defect is not associated with any reduction in overall sperm motility. Application of CASAnova to sperm from *Ace*$^{-/-}$ mice as well as mice with similar phenotypes [3, 4] would clarify

whether these sperm have defects in the timing or onset of hyperactivated motility. Similarly, we are currently using CASAnova to assess sperm motility in mice with a targeted deletion of *Coilin*. CASAnova analysis of motility profiles generated from wildtype and knockout sperm reveal that *Coilin*$^{-/-}$ sperm display lower levels of progressive sperm accompanied by higher proportions of weakly motile sperm at early time points. At later time points, these sperm display significant defects in hyperactivated motility (S. Goodson and I. Meier, unpublished results).

The inclusion of slow and weakly motile categories in CASAnova may be especially important in future characterization of sperm from knockout mice. For example, mice deficient in plasma membrane Ca^{2+} ATPase 4 (PMCA4) are infertile although there are no differences in total motility between wildtype and knockout sperm [5]. The authors propose that the infertility defect is due to an inability of these sperm to hyperactivate. However, analysis of the velocities of sperm from *Pmca*$^{-/-}$ mice reveals a dramatic decrease in both track speed (curvilinear velocity) and path velocity (average path velocity). Analysis of sperm motility profiles in these mice using CASAnova may indicate that, rather than a defect in hyperactivation, these mice are infertile due to an inability of sperm achieve any form of vigorous motility.

We also characterized sperm motility profiles from the C57BL/6J (BL6), 129S1/SvImJ (129) and PWK/PhJ (PWK) inbred mouse strains using CASAnova. We found that BL6 sperm consistently possessed higher levels of slow sperm at early time points. All three of these mouse strains are founder lines for the Collaborative Cross, a project creating a large number of recombinant inbred mouse lines that are genetically diverse [6]. We are currently utilizing CASAnova in analyses of male reproductive

phenotypes in Collaborative Cross parental strains and in lines that become extinct during inbreeding (F. Odet and D. O'Brien, unpublished results).

After further testing of CASAnova using other mouse strains and knockout models with motility defects, we envision that this tool could become a standardized approach for analyzing mouse sperm motility in conjunction with standard CASA practices. CASAnova is based on a combination of four SVM equations that were derived from visually classified motility tracks. While the current model classifies sperm into five different categories of motility, it could be easily be modified to detect additional motility patterns, if necessary. For example, CASAnova classifies two different motility patterns as hyperactivated. Both of these patterns have been previously identified as hyperactivated in the literature [7, 8]. Should the need arise for the model to differentiate between types of motility, the training set of hyperactivated sperm could be reexamined and reclassified, and a modified CASAnova could be created recognizing these motility patterns separately. This approach could then be utilized to train the model to recognize any pattern of motility that can be visually identified and differentiated from the rest of the populations.

CASAnova was developed for use with mouse sperm. However, its ease of use and rapid, detailed analysis of motile populations make it an attractive tool for use in the studies of sperm from other species including those used in basic and clinical research as well as for domestic livestock that commonly incorporate assisted reproduction into standard breeding schemes. In order to create species-specific CASAnova, training sets would need to be created by visually identifying sperm patterns in each species and then developing the model as described in Chapter 2. The ability to detect population of slow-

moving tracks in either fresh or cryopreserved sperm may be especially helpful in improving fertilization rates in large-scale breeding operations.

While a large portion of toxicology studies are performed in rat, the mouse also represents an excellent model in which to examine potential reproductive toxicants [9-11]. Use of CASAnova to investigate the effects of various toxicants would allow for more detailed analyses of the effects of these toxicants on specific patterns of motility that might not otherwise be detected in reports of average CASA parameters. In addition, CASAnova could be applied to early-stage screenings of potential contraceptives. Our lab is currently using CASAnova in a screen to identify potential inhibitors of GAPDHS in mouse sperm (P. Danshina, unpublished results).

CASAnova could also be beneficial to studies of human sperm motility. Infertility affects approximately 15 % of couples, and approximately half of these cases are due to male infertility [12, 13]. Currently, the criteria for sufficient sperm motility according to the World Health Organization is greater than 32 % progressive motility and total motility of $> 40\%$, with total motility comprising both progressive and non-progressive motility in the semen sample [14]. These values are not typically determined using CASA in the clinic, as the usefulness of CASA in this setting has been controversial [15-18]. CASAnova software adapted for human clinical studies could provide more detailed analyses of sperm motility in infertile patients, including the detection of specific defects in hyperactivation. Furthermore, human CASAnova would be beneficial in basic and translational research, such as studies investigating the efficacies of potential male contraceptives that affect sperm motility [19]. In particular, the use of CASAnova in these studies would be useful for assessing the efficacy of a contraceptive that selectively

inhibits hyperactivation. Taken together, CASAnova promises to be an invaluable tool in both basic and clinical studies of sperm motility and fertility.

Sperm metabolism, capacitation, and hyperactivation

Another goal of this work was to determine if substrates other than glucose fully support the functional transitions that mouse sperm must undergo during capacitation in order to achieve fertilization. Our results indicate that either glycolytic or non-glycolysable substrates maintain comparable percentages of motile sperm and steady-state ATP levels. However, only glycolysable substrates support both hyperactivation and the full pattern of tyrosine phosphorylation. We determined that different glycolytic substrates alter the timing and levels of hyperactivation. These findings underscore the importance of glycolysis and the requirement for specific glycolysable substrates, such as glucose or mannose, to accomplish the physiological changes associated with sperm capacitation.

Our studies demonstrate that the inability of substrates to support complete capacitation is not due to an overall decrease in energy production, since all substrates (except citrate) maintain comparable sperm ATP levels. While glycolysable substrates are required for sperm to undergo the full complement of capacitation-associated events, both lactate and pyruvate support a partial pattern of tyrosine phosphorylated proteins. Sperm incubated in either of these substrates consistently display a lack of tyrosine phosphorylation in a specific doublet with apparent molecular weights of 84,000 and 88,000. While some targets of sperm tyrosine phosphorylation have been described, the

proteins that are differentially phosphorylated in our experiments are not known. Identification of these proteins using a proteomics approach would improve our understanding of the intersection between sperm metabolism and capacitation. These studies may prove to be difficult, however, since many sperm proteins are insoluble, making proteomic analyses complicated [20].

Our studies also show that only two of the four glycolysable substrates tested (glucose and mannose) support changes in sperm comparable with HTF complete medium. Sorbitol induces a rapid increase in hyperactivation at early time points but does not maintain vigorous sperm motility over the capacitation period. Sperm incubated with sorbitol also do not undergo tyrosine phosphorylation. Fructose, in comparison, does not support hyperactivation even though tyrosine phosphorylation levels are comparable to those with HTF. Sorbitol is converted to fructose via sorbitol dehydrogenase, a reaction that requires NAD^+. The inability of sorbitol to support hyperactivation over the same time course as HTF complete medium may stem from its conversion to fructose in sperm. As glycolysis requires NAD^+ at the GAPDHS step, the conversion of sorbitol to fructose may deplete available NAD^+ stores in sperm, lowering glycolytic rates and leading to a greater proportion of non-vigorous sperm motility in the presence of sorbitol.

More detailed analyses of sperm incubated in glucose or fructose yielded insights into the metabolic consequences of the utilization of different glycolytic substrates. Our metabolomics studies revealed that sperm utilizing fructose possess higher levels of metabolites with antioxidant activities than sperm incubated with glucose. However, our studies did not use labeled substrates, and thus the exact mechanism by which this sugar increases antioxidants is not known. Fructose has been shown to stabilize pools of

glutathione in rat hepatocytes, possibly by increasing production of NADPH via the lower half of the pentose phosphate pathway [21]. ROS levels are reduced in mononuclear cells of subjects given fructose, whereas subjects given glucose display higher levels of ROS in these cells [22, 23]. The possibility exists that these results are due to higher antioxidant levels in cells metabolizing fructose. To determine the mechanism by which fructose induces antioxidant production, future studies should focus on analyzing sperm utilization of labeled glucose and fructose. In addition, NADPH levels could be measured in sperm metabolizing these substrates to determine if this mechanism could be responsible for the increased levels of antioxidants in fructose-metabolizing sperm.

The inability of fructose to support hyperactivated motility has been described previously [24, 25]. We discovered, however, that uncoupling mitochondria using CCCP restores the ability of sperm metabolizing fructose to undergo hyperactivation. The ability of CCCP to restore hyperactivation in the presence of fructose is not due to the inhibition of mitochondrial function, since mitochondrial activity is already lower in sperm incubated in fructose compared to glucose as indicated by reduced CO_2 production [26] and oxygen consumption (preliminary results). CCCP increases reactive oxygen species in human colon carcinoma cells with glucose in the medium, as well as in porcine oocytes incubated in medium containing glucose and pyruvate [27, 28]. Increased ROS production in the presence of CCCP may overcome the increased antioxidant levels produced in the presence of fructose, thus altering the redox state of these sperm in a manner that promotes hyperactivation. As previously discussed in Chapter 3, ROS levels have been shown to modulate sperm capacitation and hyperactivation. Whether increased

ROS levels are indeed responsible for these results can be further investigated using mitochondrial inhibitors that function differently than CCCP. We also performed experiments using the mitochondrial complex III inhibitor antimycin A [29] and found that it did not restore hyperactivated motility in the presence of fructose. Additional experiments with oligomycin, which inhibits mitochondria by blocking phosphorylation and does not impact respiration [30], could further ascertain whether CCCP-dependent ROS increases are responsible for these results. Conversely, the dependence of sperm hyperactivated in the presence of fructose and CCCP on ROS levels could also be determined by the addition of antioxidants, such as reduced glutathione, to the media. If increased ROS levels are responsible for hyperactivation in the presence of fructose, the addition of antioxidants should abrogate this effect.

Preincubation studies demonstrate that the maintenance of hyperactivation requires a suitable glycolytic substrate, as sperm preincubated in glucose-containing medium are not capable of maintaining hyperactivation after resuspension in fructose-containing medium. This result suggests that the signals promoting hyperactivation arise directly from the utilization of glucose. Early work on sperm hyperactivation demonstrated that sperm incubated in glucose in addition to 2-deoxyglucose, which inhibits glycolysis after phosphorylation by hexokinase, do not undergo hyperactivation [25]. These results further support the hypothesis that hyperactivation arises from the utilization of glucose through the glycolytic pathway.

Since glucose and fructose have different effects on sperm function, it is important to determine how these substrates are metabolized. While fructose can be metabolized via the top ATP-consuming half of glycolysis, it can also be metabolized via

the Hers pathway, entering glycolysis at the GAPDHS step [31] This pathway would avoid three glycolytic enzymes: HK-S, phosphoglucose isomerase, and phosphofructokinase . Aldolase and triose phosphate isomerase also precede GAPDHS but are involved in metabolism of alternative substrates by the Hers pathway. Studies using labeled substrates may yield information the potential use of the Hers pathway in sperm. Ketohexokinase phosphorylates fructose to generate fructose 1-phosphate in the Hers pathway, while glycolysis produces fructose 6-phosphate. A colorimetric ketohexokinase assay has been developed and used in archaebacteria [32], and could possibly be adapted for use with extracts of sperm incubated in fructose or glucose.

References

1. Carlson AE, Burnett LA, del Camino D, Quill TA, Hille B, Chong JA, Moran MM, Babcock DF. Pharmacological targeting of native CatSper channels reveals a required role in maintenance of sperm hyperactivation. PLoS One 2009; 4:e6844.

2. Hagaman JR, Moyer JS, Bachman ES, Sibony M, Magyar PL, Welch JE, Smithies O, Krege JH, O'Brien DA. Angiotensin-converting enzyme and male fertility. Proc Natl Acad Sci U S A 1998; 95:2552-2557.

3. Kim E, Yamashita M, Nakanishi T, Park KE, Kimura M, Kashiwabara S, Baba T. Mouse sperm lacking ADAM1b/ADAM2 fertilin can fuse with the egg plasma membrane and effect fertilization. J Biol Chem 2006; 281:5634-5639.

4. Nakanishi T, Isotani A, Yamaguchi R, Ikawa M, Baba T, Suarez SS, Okabe M. Selective passage through the uterotubal junction of sperm from a mixed population produced by chimeras of calmegin-knockout and wild-type male mice. Biol Reprod 2004; 71:959-965.

5. Okunade GW, Miller ML, Pyne GJ, Sutliff RL, O'Connor KT, Neumann JC, Andringa A, Miller DA, Prasad V, Doetschman T, Paul RJ, Shull GE. Targeted ablation of plasma membrane Ca2+-ATPase (PMCA) 1 and 4 indicates a major housekeeping function for PMCA1 and a critical role in hyperactivated sperm motility and male fertility for PMCA4. J Biol Chem 2004; 279:33742-33750.

6. Chesler EJ, Miller DR, Branstetter LR, Galloway LD, Jackson BL, Philip VM, Voy BH, Culiat CT, Threadgill DW, Williams RW, Churchill GA, Johnson DK, et al. The Collaborative Cross at Oak Ridge National Laboratory: developing a powerful resource for systems genetics. Mamm Genome 2008; 19:382-389.

7. Robertson L, Wolf DP, Tash JS. Temporal changes in motility parameters related to acrosomal status: identification and characterization of populations of hyperactivated human sperm. Biol Reprod 1988; 39:797-805.

8. Mortimer ST, Mortimer D. Kinematics of human spermatozoa incubated under capacitating conditions. J Androl 1990; 11:195-203.

9. Wang RS, Ohtani K, Suda M, Kitagawa K, Nakayama K, Kawamoto T, Nakajima T. Reproductive toxicity of ethylene glycol monoethyl ether in Aldh2 knockout mice. Ind Health 2007; 45:574-578.

10. Elangovan N, Chiou TJ, Tzeng WF, Chu ST. Cyclophosphamide treatment causes impairment of sperm and its fertilizing ability in mice. Toxicology 2006; 222:60-70.

11. Bone W, Jones AR, Morin C, Nieschlag E, Cooper TG. Susceptibility of glycolytic enzyme activity and motility of spermatozoa from rat, mouse, and human to inhibition by proven and putative chlorinated antifertility compounds in vitro. J Androl 2001; 22:464-470.

12. Sharlip ID, Jarow JP, Belker AM, Lipshultz LI, Sigman M, Thomas AJ, Schlegel PN, Howards SS, Nehra A, Damewood MD, Overstreet JW, Sadovsky R. Best practice policies for male infertility. Fertil Steril 2002; 77:873-882.

13. Nallella KP, Sharma RK, Aziz N, Agarwal A. Significance of sperm characteristics in the evaluation of male infertility. Fertil Steril 2006; 85:629-634.

14. Cooper TG, Noonan E, von Eckardstein S, Auger J, Baker HW, Behre HM, Haugen TB, Kruger T, Wang C, Mbizvo MT, Vogelsong KM. World Health Organization reference values for human semen characteristics. Hum Reprod Update 2010; 16:231-245.

15. Larsen L, Scheike T, Jensen TK, Bonde JP, Ernst E, Hjollund NH, Zhou Y, Skakkebaek NE, Giwercman A. Computer-assisted semen analysis parameters as predictors for fertility of men from the general population. The Danish First Pregnancy Planner Study Team. Hum Reprod 2000; 15:1562-1567.

16. De Geyter C, De Geyter M, Koppers B, Nieschlag E. Diagnostic accuracy of computer-assisted sperm motion analysis. Hum Reprod 1998; 13:2512-2520.

17. Amann RP, Katz DF. Reflections on CASA after 25 years. J Androl 2004; 25:317-325.

18. Krause W, Viethen G. Quality assessment of computer-assisted semen analysis (CASA) in the andrology laboratory. Andrologia 1999; 31:125-129.

19. O'Rand MG, Widgren EE, Beyler S, Richardson RT. Inhibition of human sperm motility by contraceptive anti-eppin antibodies from infertile male monkeys: effect on cyclic adenosine monophosphate. Biol Reprod 2009; 80:279-285.

20. Carrera A, Moos J, Ning XP, Gerton GL, Tesarik J, Kopf GS, Moss SB. Regulation of protein tyrosine phosphorylation in human sperm by a calcium/calmodulin-dependent mechanism: identification of A kinase anchor proteins as major substrates for tyrosine phosphorylation. Dev Biol 1996; 180:284-296.

21. Frenzel J, Richter, J., Eschrich, K. Fructose inhibits apoptosis induced by reoxygenation in rat hepatocytes by decreasing reactive oxygen species via stabilization of the glutathione pool. Biochimica et Biophysica Acta 2002; 1542:82-94.

22. Ghanim H, Mohanty P, Pathak R, Chaudhuri A, Sia CL, Dandona P. Orange juice or fructose intake does not induce oxidative and inflammatory response. Diabetes Care 2007; 30:1406-1411.

23. Mohanty P, Ghanim H, Hamouda W, Aljada A, Garg R, Dandona P. Both lipid and protein intakes stimulate increased generation of reactive oxygen species by polymorphonuclear leukocytes and mononuclear cells. Am J Clin Nutr 2002; 75:767-772.

24. Fraser LR, Quinn PJ. A glycolytic product is obligatory for initiation of the sperm acrosome reaction and whiplash motility required for fertilization in the mouse. J Reprod Fertil 1981; 61:25-35.

25. Cooper TG. The onset and maintenance of hyperactivated motility of spermatozoa in the mouse. Gamete Res 1984; 9:55-74.

26. Hoppe PC. Glucose requirement for mouse sperm capacitation in vitro. Biol Reprod 1976; 15:39-45.

27. Izeradjene K, Douglas L, Tillman DM, Delaney AB, Houghton JA. Reactive oxygen species regulate caspase activation in tumor necrosis factor-related apoptosis-inducing ligand-resistant human colon carcinoma cell lines. Cancer Res 2005; 65:7436-7445.

28. Cui MS, Wang XL, Tang DW, Zhang J, Liu Y, Zeng SM. Acetylation of H4K12 in porcine oocytes during in vitro aging: potential role of ooplasmic reactive oxygen species. Theriogenology 2011; 75:638-646.

29. Koppers AJ, De Iuliis GN, Finnie JM, McLaughlin EA, Aitken RJ. Significance of mitochondrial reactive oxygen species in the generation of oxidative stress in spermatozoa. J Clin Endocrinol Metab 2008; 93:3199-3207.

30. Penefsky HS. Mechanism of inhibition of mitochondrial adenosine triphosphatase by dicyclohexylcarbodiimide and oligomycin: relationship to ATP synthesis. Proc Natl Acad Sci U S A 1985; 82:1589-1593.

31. Hers HG. The conversion of fructose-1-C14 and sorbitol-1-C14 to liver and muscle glycogen in the rat. J Biol Chem 1955; 214:373-381.

32. Rangaswamy V, Altekar W. Ketohexokinase (ATP:D-fructose 1-phosphotransferase) from a halophilic archaebacterium, Haloarcula vallismortis: purification and properties. J Bacteriol 1994; 176:5505-5512.